Perturbations in loop quantum cosmology

Jakub Mielczarek

Thesis submitted to the Jagiellonian University
in partial fulfillment of the requirements
for the degree of Doctor of Philosophy in Physics

Thesis advisor:
Marek Szydłowski

Jagiellonian University, Kraków

May 8, 2012

Abstract

The search for the quantum theory of gravity is one of the main goals of theoretical physics. This goal will be never achieved unless a method of empirical verification of physics at the Planck scale is found. The aim of this dissertation is to construct such method, using observations of the cosmic microwave background radiation.

The main theoretical challenge of this dissertation is to construct theory of cosmological perturbations, taking into account modifications due to the holonomies of Ashtekar connection. These effects are expected due to discrete nature of space, resulting from loop quantum gravity (LQG). The discreteness is parametrized by a single quantity Δ, which can be related with the area gap of the area operator in LQG. As we show, this parameter may be the subject of observational constraints.

In the canonical formulation of general relativity, the Hamiltonian is a sum of constraints. The main obstacle in formulating theory of cosmological perturbations, in presence of the holonomy corrections, is the problem of anomalies. Because effective constraints are quantum-modified, the corresponding Poisson algebra might not be closed, leading to anomalies. In order to remove these anomalies we have introduced *counter-terms* into the Hamiltonian constraint. The counter-terms are vanishing in the classical limit while regularize anomalies in the quantum domain. We find a way to explicitly fulfill the conditions for anomaly freedom and we give explicit expressions for the counter-terms. The analysis is performed for all types of cosmological perturbations: scalar, vector and tensor (gravitational waves) modes. As we show, the requirement of anomaly freedom for the scalar perturbations naturally leads to the so-called $\bar{\mu}$−scheme ("new quantization scheme"). It was also shown that obtained algebra of constraints is deformed due to the effects of holonomies. The obtained deformation indicates that signature in changing from Lorentzian to Euclidean one while passing to the region of high energy densities. This unexpected result opens new possible directions for theoretical studies.

Gauge invariant variables were found for all types of perturbations. In case of the scalar perturbations they are holonomy-corrected analogues of the classical Bardeen potentials. Equations of motions for all the types or perturbations were derived. In case of the scalar perturbations, an analogue of the Mukhanov equation was also found. This new equation can be directly applied to study generation of scalar perturbations in the very early universe.

Based on the obtained equations, we have studied quantum generation of gravita-

tional waves during the Planck epoch described by loop quantum cosmology. We have studied realization of the phase of cosmic inflation in loop quantum cosmology. The phase of slow-roll inflation was shown to appear generically due to *cosmic bounce*, which is a consequence of quantum gravity effects in the Planck epoch. The spectrum of primordial gravitational waves was computed for this model and predictions regarding the B-type polarization of the cosmic microwave background radiation were performed. This allowed to put observational constraints on physical conditions in the Planck epoch. A possibility of testing the quantum gravity effects with use of cosmological observations was shown to be available.

Streszczenie

W pracy podjęto się skonstruowania teorii zaburzeń kosmologicznych w ramach pętlowej kosmologii kwantowej. Kluczowym zadaniem było wprowadzenie poprawek od holomomii, tak aby nie prowadziły one do anomalii w algebrze więzów. W celu rozwiązania problemu anomalii, zastosowano metodę bazującą na wprowadzeniu tak zwanych kontr-członów. Wymaganie zamykania się algebry więzów pozwoliło na wyznaczenie postaci kontr-członów oraz na usunięcie niejednoznaczności związanych z wprowadzaniem poprawek od holonomii.

Rozważania przeprowadzono dla zaburzeń skalarnych, wektorowych oraz tensorowych, na płaskiej przestrzeni Friedmana-Robertsona-Walkera (FRW). Jako materię wprowadzono pole skalarne. Dla wszystkich typów zaburzeń wyprowadzono równania ruchu oraz znaleziono zmienne niezależne od wyboru cechowania. W przypadku zaburzeń skalarnych, zmienne te są odpowiednikami potencjałów Bardeena. Wyprowadzono również odpowiednik równania Mukhanova, uwzględniający poprawki od holonomii. W przypadku zaburzeń skalarnych, analiza otrzymanej algebry więzów wykazała zmianę sygrantury metryki, z lorentzowskiej na euklidesową, w obszarze gęstości energii porównywalnych z gęstością energii Plancka.

W oparciu o otrzymane równania dla zaburzeń tensorowych, przeanalizowano generację pierwotnych fal grawitacyjnych podczas fazy tak zwanego odbicia, przewidywanego w ramach pętlowej kosmologii kwantowej. Pozwoliło to na wyprowadzenie widma pierwotnych fal grawitacyjnych i porównanie otrzymanych wyników z ograniczeniami pochodzącymi z obserwacji mikrofalowego promieniowania tła. Na tej podstawie, nałożono obserwacyjne ograniczenie na warunki fizyczne panujące podczas fazy odbicia. Przeprowadzono również analizę wpływu efektów holonomii na widmo zaburzeń skalarnych. Na tej podstawie, wyznaczono ograniczenia odnośnie możliwości testowania efektów kwantowej grawitacji z wykorzystaniem obserwacji mikrofalowego promieniowania tła. Otrzymane wyniki pokazują, że możliwość badania fizyki na skali Plancka staje się realna dzięki wykorzystaniu najnowszych obserwacji astronomicznych.

List of publications

This dissertation is partially based on results contained in the following publications and preprints.

List of publications:

1. J. Mielczarek and W. Piechocki, "Quantum of volume in de Sitter space," Phys. Rev. D **83** (2011) 104003.

2. J. Mielczarek, "Reheating temperature from the CMB," Phys. Rev. D **83** (2011) 023502.

3. J. Grain, A. Barrau, T. Cailleteau and J. Mielczarek, "Observing the Big Bounce with Tensor Modes in the Cosmic Microwave Background: Phenomenology and Fundamental LQC Parameters," Phys. Rev. D **82** (2010) 123520.

4. J. Mielczarek and W. Piechocki, "Observables for FRW model with cosmological constant in the framework of loop cosmology," Phys. Rev. D **82** (2010) 043529.

5. J. Mielczarek, T. Stachowiak and M. Szydłowski, "Vortex in axion condensate as a dark matter halo," Int. J. Mod. Phys. D **19** (2010) 1843.

6. J. Mielczarek, M. Kamionka, A. Kurek and M. Szydłowski, "Observational hints on the Big Bounce," JCAP **1007** (2010) 004.

7. J. Mielczarek, T. Cailleteau, J. Grain and A. Barrau, "Inflation in loop quantum cosmology: Dynamics and spectrum of gravitational waves," Phys. Rev. D **81** (2010) 104049.

8. J. Mielczarek, "Possible observational effects of loop quantum cosmology," Phys. Rev. D **81** (2010) 063503.

9. O. Hrycyna, J. Mielczarek and M. Szydłowski, "Asymmetric cyclic evolution in polymerised cosmology," JCAP **0912** (2009) 023.

10. J. Mielczarek, O. Hrycyna and M. Szydłowski, "Effective dynamics of the closed loop quantum cosmology," JCAP **0911** (2009) 014.

11. J. Mielczarek, "Tensor power spectrum with holonomy corrections in LQC," Phys. Rev. D **79** (2009) 123520.

12. J. Mielczarek, "Multi-fluid potential in the loop cosmology", Phys. Lett. B **675** (2009) 273.

13. O. Hrycyna, J. Mielczarek and M. Szydłowski, "Effects of the quantisation ambiguities on the Big Bounce dynamics," Gen. Rel. Grav. **41** (2009) 1025.

14. J. Mielczarek, "Gravitational waves from the Big Bounce", JCAP **0811** (2008) 011.

15. J. Mielczarek and M. Szydłowski, "Universe emerging from a vacuum in loop-string cosmology," JCAP **0808** (2008) 014.

16. J. Mielczarek and M. Szydłowski, "Emerging singularities in the bouncing loop cosmology," Phys. Rev. D **77** (2008) 124008.

17. J. Mielczarek, T. Stachowiak and M. Szydłowski, "Exact solutions for Big Bounce in loop quantum cosmology," Phys. Rev. D **77** (2008) 123506.

18. J. Mielczarek and M. Szydłowski, "Relic gravitons as the observable for Loop Quantum Cosmology," Phys. Lett. B **657** (2007) 20.

List of preprints:

1. T. Cailleteau, J. Mielczarek, A. Barrau, J. Grain, "Anomaly-free scalar perturbations with holonomy corrections in loop quantum cosmology," [arXiv:1111.3535 [gr-qc]].

2. J. Mielczarek and W. Piechocki, "Quantum memory of the Universe," arXiv:1108.0005 [gr-qc].

3. J. Mielczarek and W. Piechocki, "Evolution in bouncing quantum cosmology," arXiv:1107.4686 [gr-qc].

4. J. Mielczarek, T. Cailleteau, A. Barrau and J. Grain, "Anomaly-free vector perturbations with holonomy corrections in loop quantumcosmology," arXiv:1106.3744 [gr-qc].

5. J. Mielczarek and M. Kamionka, "Smoothed quantum fluctuations and CMB observations," arXiv:0909.4411 [hep-th].

6. J. Mielczarek, M. Szydłowski and P. Tambor, " Bayesian reasoning in cosmology", arXiv: 0901.4075

7. J. Mielczarek and M. Szydłowski, "Relic gravitons from super-inflation," arXiv:0710.2742 [gr-qc].

Contents

Chapter 1

Introduction

Modern physics has its roots in three traditions originating from the ancient Greece [1]. The first is the Platonic world view in which understanding of the Universe is built *a priori* with use of mathematics. In this approach, distinguishing the most symmetric structures leads to proper understanding of a given aspect of reality. Another tradition comes from Plato's student Aristotle. Aristotle world view was opposite to the Plato's one. In particular, he argued that the understanding of the Universe should be constructed *a posteriori* with respect to experiments and observations. The mathematical method played a secondary role here, and qualitative understanding of phenomenons was emphasized. The third tradition comes from Archimedes, which, in some sense, combines the both previous viewpoints. According to Archimedes, mathematics should be used *a posteriori* with respect to experiments and observations, in contrast to the Plato's view. The method aims to catch some aspects of reality by the mathematical model, allowing for its quantitative understanding.

Following only one of the discussed traditions would surely have not guided physics to its present position. Only skillful combination of the three ones may lead to deep and firm understanding of laws governing the Universe. However, it is not always possible to draw inspiration from the three traditions at the same time. Some ways, outlined by the ancient philosophers, may turn out to be unaccessible.

Such a situation takes place in search for the quantum theory of gravity, which aims to quantize gravitational degrees of freedom [2]. Present attempts to find such a theory follow mainly the Plato's approach. The theory is constructed *a priori*, guided by the concept of *mathematical beauty* and self-consistency. The situation looks like this not because scientists involved in the research are pure Platonists, but because there is a very limited possibility of *a posteriori* inferring here. In such a case, only very rigorous mathematical constructions may lead to some insight into the nature of quantum gravity. The reason why *a posteriori* inferring cannot be applied yet, is the lack of any observed effects of quantum gravity[1]. This comes from the fact that the quantum gravity effects are predicted to become significant at the so-called *Planck scale*. In particular, the quantum nature

[1]Or, we do not know whether they are due to the quantum gravity, *e.g.* cosmic acceleration.

of spacetime is expected to be manifested at distances of the order of the Planck length, $l_{Pl} \equiv \sqrt{\frac{\hbar G}{c^3}} \approx 1.62 \cdot 10^{-35}$ m [2]. This is incredibly small quantity, even if compared with sub-nuclear scales, currently under examination by particle accelerator experiments.

Despite this huge chasm in scales, there are some attempts to search for quantum gravity effects indirectly (see [3] for the recent discussion). One of the most extensively investigated approaches is based on a possible relation between the quantum gravity effects and violation of the Lorentz invariance [4]. Such an effect may lead to additional energy dependence in the dispersion relation of a photon. As a result of this, group velocity of high energy photons is a bit smaller than of low energy ones. Despite of the fact that this effect is very small, it may accumulate on cosmological distances leading to significant time lags of high energy photons. This effect is presently constrained with use of the Gamma Ray Bursts (GRB). In particular, the recent results from the FERMI satellite [5] indicate that, for the first order effects [3], the constraint on the energy scale of Lorentz symmetry violation is $E_{QG} > 1.2\ E_{Pl}$. Here, $E_{Pl} \equiv \sqrt{\frac{\hbar c^5}{G}} \approx 1.22 \cdot 10^{19}$GeV is the Planck energy. Therefore, indeed the Planck scale is approached with this method. However, if the second order effects are considered, the constraint is much weaker. Nevertheless, the method can be used to rule out (or confirm) some models of the Planck scale physics in the near future. This will require more statistics as well as better understanding of the GRB emission processes.

Another possible method of gaining empirical insight into the Planck scale physics is based on observations of the very early universe. In particular, observations of anisotropy and polarization of the Cosmic Microwave Background (CMB) radiation are employed. The CMB radiation is a rich source of information about high energy density state of the Universe. One of the greatest indications resulting from the CMB observations is the phase of *cosmic inflation* [6, 7]. This phase of nearly exponential expansion in the early universe is crucial for the explanation of the spectrum of primordial cosmological perturbations, determined from the CMB data. The CMB observations give us certain indications regarding the form of the primordial perturbations. One could naively suspect that the primordial perturbations have thermal origin, because the Universe was in thermal equilibrium at some early stages. However, this possibility is completely rejected by current observations. While thermal fluctuations lead to the spectrum of perturbations in the form $\mathcal{P} \sim 1/k$ (white-noise spectrum), the observations of the CMB indicate that the spectrum has a nearly *scale-invariant*[4] form $\mathcal{P} \sim k^{n_S-1}$, where $n_S \approx 1$ [8]. This is quite a problematic issue since it is not so easy to find a mechanism which produces spectrum in this form. But, there is also a good side. Namely, when we find a simple mechanism which leads to the observed spectrum, then we are more certain about its authenticity.

[2] Here $\hbar$ is reduced Planck constant, G is Newton's constant and c is a speed of light in vacuum.

[3] In this case, group velocity of photons is given by $v_g \simeq c\,(1 - E/E_{QG})$, where E_{QG} is the energy scale of quantum gravity.

[4] In cosmology, the "scale-invariance" means simply "constant". This definition is different from the standard mathematical notion where the scale-invariance is a scaling property of any power-law function.

The phase of cosmic inflation gives a simple mechanism generating primordial perturbations in agreement with the CMB data.

The phase of inflation is expected to proceed in consequence of the *Planck epoch*. The Planck epoch is a period in evolution of the Universe in which the quantum gravity effect played a significant role. In this epoch, the energy density of the matter content approached the Planck energy density $\rho_{Pl} \equiv E_{Pl}^4$. Extrapolation of the classical cosmology into this region leads to unphysical behavior in form of the so-called *Big Bang* singularity. A proper (quantum gravitational) description of the Planck epoch should resolve this problem as well as predict the phase of cosmic inflation. Therefore, observational studies of inflation as well generation of the primordial perturbations may be used as an indirect probe of the Planck scale physics. The analysis of the primordial perturbations generated during the phase of inflation can tell us something about initial conditions fixed in the Planck epoch. However, in order to obtain any reasonable predictions from the Planck era and confront them with available data, a theory of quantum gravity is needed.

At present, the research on quantum gravity focus mainly on four approaches: Causal Dynamical Triangulation (CDT) [9], Causal Set Theory (CST) [10], Loop Quantum Gravity (LQG) [11] and String Theory [12]. All of them have advantages and disadvantages of different nature. Therefore, it is difficult to favor any of them.

In this thesis we focus on LQG, which is a promising program to construct a quantum theory of gravity *a priori*. A symmetry of general covariance is employed here as a guiding principle for the applied method of quantization. A general covariance, called also invariance with respect to local diffeomorphisms, is a symmetry behind the classical theory of gravity, the General Relativity (GR). Predictions of GR were verified by many observational tests and no deviation from the general covariance was noticed [13]. The LQG program assumes that this symmetry is preserved also at the quantum level. Classically, the general covariance means background independence. No spacetime reference frame is distinguished by the theory. At the quantum level of LQG, this relativity is embedded in the mathematical structure of an abstract graph called *spin network* [14]. The spin network is a collection of links labeled by half-integer spin labels and joined by vertices. The vertices are additionally labeled by intertwiners. The links represent relations between different *atoms of space* located at the vertices, as presented in Fig. 1.1. The area of a given surface S can be computed, based on the spin network state, with use of the formula [15]

$$\mathrm{Ar}[S] = 8\pi l_{Pl}^2 \gamma \sum_i \sqrt{j_i(j_i+1)}, \tag{1.1}$$

where γ is a free parameter of LQG, known as the Barbero-Immirzi parameter. In Eq. 1.1, the summation runs over the links crossing the surface S. It is worth stressing that the area is a function of discrete parameters j_i, which reflects grainy nature of space. The minimal area is obtained when S is crossed by one link with the spin label $j = 1/2$. In that case we get expression for the *area gap*: $\Delta = 4\sqrt{3}\pi l_{Pl}^2 \gamma$.

The Loop Quantum Cosmology (LQC) [16, 17, 18] is a symmetry reduced model of LQG. In particular, by imposing symmetries of homogeneity and isotropy, the gravita-

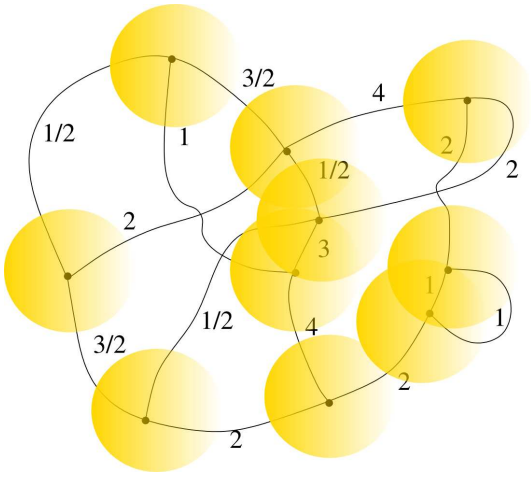

Figure 1.1: An abstract spin network with the corresponding *atoms of space*.

tional field is parametrized by a single quantity, the so-called scale factor. This, so-called Friedmann-Robertson-Walker (FRW) model, was extensively studied in LQC, leading to profound results. The first of them was avoidance of the cosmological singularity due to the *quantum repulsion* [19, 20]. The classical Big Bang singularity was replaced by the non-singular *Big Bounce* transition between contracting and expanding universe. The second was an indication that the phase of cosmic inflation may be due to the quantum gravity effects [21]. Both results were obtained for the model with a free scalar field.

The dynamics of LQC can be studied at the effective level by introducing quantum gravitational corrections into the gravity and matter Hamiltonians. In general, two types of corrections are considered: *inverse volume corrections* and *holonomy corrections*. The issues of singularity resolution and inflation were addressed in case of the both types of corrections. If was shown that, the singularity can be avoided either due to the first or the second type of corrections. In case of the inverse volume corrections, the singularity is avoided because the inverse volume operator $\widehat{1/V}$ is bounded [19]. In case of the holonomy corrections, the dynamics is nonsingular because the curvature operator is bounded [22]. Both effects are results of discreteness of space at the Planck scale. For the FRW model, this discreteness is embedded in the form of a regular cubic lattice with elementary lattice spacing λ. For such a model, energy density of matter cannot exceed the critical value [22]

$$\rho_c = \frac{3}{8\pi G\gamma^2\lambda^2}. \tag{1.2}$$

Usually, the value of λ is fixed from the value of area gap Δ of the area operator in LQG, then $\lambda = \sqrt{\Delta}$. However, in general, the parameter λ can be considered as a free parameter of the model.

Both types of quantum corrections in LQC led to the phase of *super-inflation* for the model with a free scalar field. However, the phases of super-inflation obtained are not

long enough to explain spectrum of primordial perturbations. However, the situation changes when potential of the scalar field is added. For a model with the holonomy corrections and the massive scalar field, realization of the inflationary phase was studied in [23]. It was shown there, that the phase of cosmic bounce leads to proper initial conditions for the inflationary phase. These results were later approved by exploring the whole parameter space and by calculating the probability of inflation [24, 25]. It was shown that the probability of inflation, with at least $N = 65$ e-folds, is very close to one. Therefore, the phase of inflation is generic in this model. It is in contrast with the classical case where the probability of inflation is suppressed by the factor e^{-3N} [26]. The appropriately long inflation obtained in LQC, with a massive scalar field, gives possibility to obtain a spectrum of primordial perturbations in agreement with the CMB data.

The generation of primordial fluctuations can be studied with use of the theory of cosmological perturbations [27]. In the classical theory of cosmological perturbations the spacetime metric $g_{\mu\nu}$ is used as a perturbative variable. The metric is decomposed for background and perturbation parts, $g_{\mu\nu} = \bar{g}_{\mu\nu} + \delta g_{\mu\nu}$, where consistency of the perturbative expansion is fulfilled by the requirement: $|\delta g_{\mu\nu}/\bar{g}_{\mu\nu}| \ll 1$. In case of the flat $(k = 0)$ FRW background, metric perturbations can be decomposed according to their spin as follows [28]:

$$\begin{aligned} g_{\mu\nu} &= \underbrace{a^2\begin{pmatrix} -1 & 0 \\ 0 & \delta_{ab} \end{pmatrix}}_{\text{FRW k=0 background}} + \underbrace{a^2\begin{pmatrix} -2\phi & \partial_a B \\ \partial_a B & -2\psi\delta_{ab} + \partial_a\partial_b E \end{pmatrix}}_{\text{scalar (s=0)}} \\ &+ \underbrace{a^2\begin{pmatrix} 0 & S_a \\ S_a & F_{a,b} + F_{b,a} \end{pmatrix}}_{\text{vector (s=1)}} + \underbrace{a^2\begin{pmatrix} 0 & 0 \\ 0 & h_{ab} \end{pmatrix}}_{\text{tensor (s=2)}}. \end{aligned}$$

Here, a is the scale factor. Furthermore, perturbation variables $(\phi, \psi, E, B, F_a, S_a, h_{ab})$ fulfill the following conditions:

$$\begin{aligned} \partial^a h_{ab} &= 0 \text{ (transverse) and } \delta^{ab} h_{ab} = 0 \text{ (traceless)}, \\ F^a{}_{,a} &= 0 \text{ (divergence free) and } S^a{}_{,a} = 0 \text{ (divergence free)}. \end{aligned}$$

Taking these conditions into account, there is in total 10 perturbative degrees of freedom, as expected for a symmetric 4×4 matrix.

In this thesis, we address the issue of cosmological perturbations in the canonical framework of LQC. In this approach the gravity sector is parametrized by the Ashtekar variables (E^a_i, A^i_a) [29]. Therefore, instead of perturbing metric $g_{\mu\nu}$, we will perturb the E^a_i and A^i_a variables as follows:

$$A^i_a = \bar{A}^i_a + \delta A^i_a, \tag{1.3}$$

$$E^a_i = \bar{E}^a_i + \delta E^a_i. \tag{1.4}$$

Moreover, conditions $|\delta A^i_a/\bar{A}^i_a| \ll 1$ and $|\delta E^a_i/\bar{E}^a_i| \ll 1$ ensure validity of the perturbative expansion. The theory of cosmological perturbation will be constructed at the level of

Hamiltonian. In this procedure, the matter Hamiltonian will be also a subject of perturbative expansion. In our considerations, we will focus on the model with a scalar field, which is relevant for description of the inflationary universe.

The main difficulty in formulating theory of cosmological perturbations in LQC is the problem of anomalies. In the canonical formulation, employed in LQC, the total Hamiltonian is a sum of constraints. At the classical level, these constraints form a closed algebra. However, the algebra of the quantum-modified effective constraints $\mathcal{C}_I^{\mathrm{eff}}$ might not be closed, leading to anomalies:

$$\{\mathcal{C}_I^{\mathrm{eff}}, \mathcal{C}_J^{\mathrm{eff}}\} = f^K{}_{IJ}(A_b^j, E_i^a)\mathcal{C}_K^{\mathrm{eff}} + \text{anomalies}, \tag{1.5}$$

where $f^K{}_{IJ}(A_b^j, E_i^a)$ are some structure functions. The necessary consistency condition is a requirement of vanishing of the anomaly terms. The possible quantum corrections must be therefore restricted to those which close the algebra. This issue, in case of perturbations with inverse volume corrections, was studied in numerous papers [30, 31, 32, 33, 34]. It was shown that the requirement of anomaly freedom can be fulfilled for the first order perturbation theory. This was derived for scalar [31, 32], vector [33] and tensor perturbations [34]. It is worth mentioning that, for the tensor perturbations, the anomaly freedom is automatically satisfied. In case of the vector and scalar perturbations, the conditions of anomaly freedom lead to certain restrictions on the form of the quantum corrections. Based on the obtained anomaly-free formulation of the scalar perturbations, predictions regarding the power spectrum of the cosmological perturbations were obtained [35]. These predictions were confronted with the CMB data, giving some constraints on the parameters of the model [36, 37].

The aim of this dissertation is to construct an anomaly-free theory of cosmological perturbations with holonomy corrections. Our approach will follow the method of *counterterms* developed in case of the inverse volume corrections [31]. In case of the tensor perturbations with holonomy corrections, the algebra of constraint is directly anomaly-free, as in case with the inverse volume corrections [34]. The cases of vector and scalar perturbations are however far from trivial. So far, it was shown in [33] that the holonomy-corrected vector perturbations can be anomaly-free up to the fourth order in the canonical variable $\bar{k}$. This, however, is not sufficient to perform the analysis of propagation of vector modes through the cosmic bounce. Vector perturbations with *higher order holonomy corrections* were also recently studied [38]. It was shown there that, in this case, an anomaly-free formulation can be found for the gravitational sector. In this thesis, we apply a different method, which is based on the introduction of the counter-terms in the Hamiltonian constraint. We show that conditions of anomaly freedom for the vector perturbations with holonomy corrections can be fulfilled. The scalar perturbations with holonomy corrections have been studied in [39]. However, the issue of anomaly freedom was not really addressed. Recently, a new possible way of introducing holonomy corrections to the scalar perturbations was proposed in [40]. Although it was interestingly shown that the formulation is anomaly-free, the approach is based on the choice of the longitudinal gauge and the extension of the method to the gauge-invariant case is not straightforward.

In contrast, the approach developed in this thesis does not rely on any particular choice of gauge and the gauge-invariant cosmological perturbations are constructed. The obtained anomaly-free theory of cosmological perturbations with holonomy corrections will allow us to perform predictions regarding the anisotropy and polarization of the CMB radiation. Based on this, observational insight into the Planck epoch will be reached.

The organization of this thesis is the following. In Chapter 2, the Hamiltonian formulation of General Relativity, in language of Ashtekar variables, is introduced. Then, the issues of holonomy corrections and the anomaly freedom are discussed. The equations of motion for the background part are derived. In Chapter 3, we use these equations to study dynamics of the universe in the Planck epoch. We focus on the model with a massive scalar field. This enables to study realization of the inflationary phase in the framework of LQC. Based on the obtained background dynamics, evolution of perturbations will be studied in the subsequent chapters. The classical theory of cosmological perturbations, in the Hamiltonian framework, is constructed in Chapter 4. Based on this, a theory of cosmological perturbations with the holonomy corrections will be constructed. In Chapter 5, quantum fluctuations of the scalar field are investigated for the background dynamics predicted in LQC. Some methods of the quantum field theory on curved backgrounds, used to describe quantum generation of the primordial perturbations, are introduced. In Chapters 6, 7 and 8, theory of cosmological perturbations with the holonomy corrections is studied in case of tensor, vector and scalar perturbations respectively. The obtained predictions are confronted with observational data in Chapter 9. The results obtained in this thesis are summarized in Chapter 10. Finally, Chapter 11 contains appendixes with detailed derivations of some useful formulas.

Chapter 2

Preliminaries

A great achievement of Einstein's theory of gravity (General Relativity) was to merge space and time into one dynamical object called *spacetime*. The concept of spacetime turned out to be very fruitful and gripped imaginations of the twenty century physicists. It was mainly because a geometrical picture of gravity, which emerged from the Einstein's theory, was very intuitive. The concept of spacetime have played invaluable role in the development of modern physics. Despite this, there are more and more indications that time and space are in fact quite different objects. In particular, such picture is emerging from loop quantum gravity [2, 11, 41], which is based on the Hamiltonian formulation of General Relativity.

In this chapter, the so-called ADM (Arnowitt-Deser-Misner) decomposition of spacetime is introduced. Based on this, the Hamiltonian formulation of the Einstein's theory of gravity, in the language of the Ashtekar variables, is constructed. The concept of holonomies, employed in LQG, is defined. Based on this, the so-called holonomy corrections are discussed. Taking into account these corrections, equations of motion for the FRW model are derived. A problem of anomalies in the algebra of effective constraints is formulated. The notation employed in the thesis is fixed in this chapter.

2.1 General Relativity

Classical theory of gravity, the General Relativity, describes gravitational interactions by a symmetric tensor field $g_{\mu\nu}$, the so-called *metric field*. The metric $g_{\mu\nu}$ field is defined on the manifold $\mathcal{M}$ of dimension $D = \dim \mathcal{M}$. The manifold $\mathcal{M}$ is called *spacetime* and the spacetime indices run over the range $\mu, \nu = 0, 1, 2, ..., D-1$. Due to the symmetricity, the field $g_{\mu\nu}$ has $D(D+1)/2$ independent components. In what follows, we consider only the four dimensional spacetime $D = 4$, in agreement with everyday experience. In this case, the gravitational field $g_{\mu\nu}$ has 10 degrees of freedom.

Metric is used to define line element between two space-time points:

$$ds^2 = g_{\mu\nu} dx^\mu dx^\nu. \tag{2.1}$$

In case of flat spacetime, the metric takes the following form $g_{\mu\nu} = \mathrm{diag}(-1, +1, +1, +1)$, which fixes convention employed in this thesis.

Equations of motion for the metric field, the so-called Einstein equations, can be derived by varying the action

$$S = \int dtL = \frac{1}{2\kappa}\int_{\mathcal{M}} d^4x\sqrt{\det g}R + \frac{1}{\kappa}\int_{\mathcal{M}} d^4x\sqrt{\det g}\Lambda + S_m \tag{2.2}$$

where $\kappa = 8\pi G$ and $G = 6,67257(85)\cdot 10^{-11}m^3kg^{-1}s^{-2}$ is the Newton's constant and Λ is the cosmological constant. The first contribution is Eq. 2.2 is the so-called Hilbert-Einstein action, where R is the Ricci scalar. The second contribution is the cosmological constant term and the last part is the matter action.

The symmetry underlying the action (2.2) is invariance with respect to the local diffeomorphisms, also called general covariance. It means that, action (2.2) remains unchanged under the infinitesimal transformation of coordinates

$$x^\mu \to x^\mu + \xi^\mu. \tag{2.3}$$

In order to pass from the Lagrangian formulation (2.2) to the Hamiltonian formulation, decomposition of $\mathcal{M}$ into space and time parts is required. Such step is necessary in order to define *velocities*. This can be achieved by virtue of the Arnowitt-Deser-Misner decomposition.

2.2 Arnowitt-Deser-Misner decomposition

The Arnowitt-Deser-Misner (ADM) decomposition is a split of the hyperbolic manifold $\mathcal{M}$ onto space and time parts. After decomposition, $\mathcal{M} = \mathbb{R}\times\Sigma$, where Σ is the spatial, three dimensional submanifold. The decomposition can be viewed as foliation of the spacetime $\mathcal{M}$ for the spatial slices Σ_t, where $t \in \mathbb{R}$.

In the ADM decomposition, the metric field is parametrized by three variables (N, N^a, q_{ab}) in the following way:

$$g_{\mu\nu} = \begin{pmatrix} -N^2 + q_{ab}N^aN^b & N_b \\ N_a & q_{ab} \end{pmatrix}, \tag{2.4}$$

therefore the line element

$$ds^2 = g_{\mu\nu}dx^\mu dx^\nu = -(Ndt)^2 + q_{ab}(N^a dt + dx^a)(N^b dt + dx^b). \tag{2.5}$$

The N is a scalar function called *lapse function*, so it has 1 degree of freedom. Th N^a is a vector called *shift vector*, having 3 degrees of freedom. The *spatial metric* q_{ab} is a symmetric field on Σ with 6 degrees of freedom. Adding the degrees of freedom we have $1 + 3 + 6 = 10$. Therefore, the initial number of metric degrees of freedom remain unchanged. One can also find the inverse of metric $g_{\mu\nu}$

$$g^{\mu\nu} = \begin{pmatrix} -1/N^2 & N^b/N^2 \\ N^a/N^2 & q^{ab} - N^aN^b/N^2 \end{pmatrix}, \tag{2.6}$$

such that $g_{\mu\alpha}g^{\alpha\nu} = \delta^{\nu}_{\mu}$.

In Fig. 2.1 we show graphical interpretation of the shift vector and the lapse function. The two spatial hypersurfaces Σ_t and Σ_{t+dt} are presented. Let n^μ be a unit vector normal

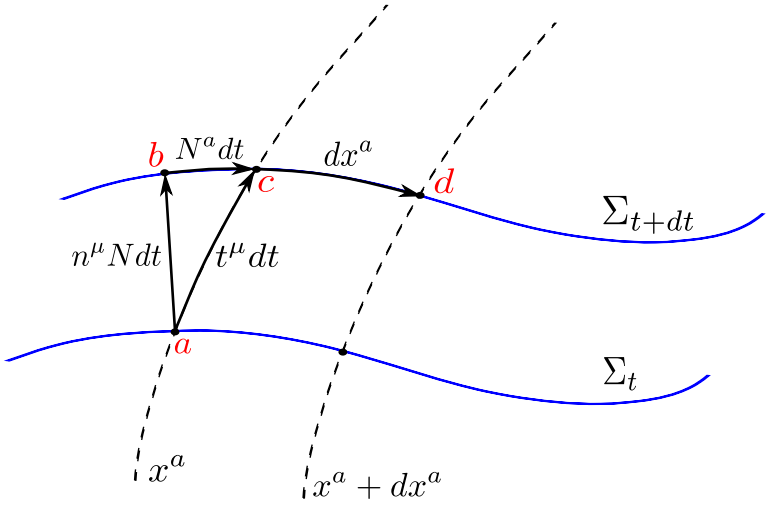

Figure 2.1: Graphical interpretation of the lapse function N and the shift vector N^a.

to the hypersurface Σ_t, so $g_{\mu\nu}n^\mu n^\nu = -1$. Let us consider this vector at the spacetime point $a = (t, x^a)$. By multiplying n^μ by the factor Ndt we get the vector which intersects Σ_{t+dt} in the point b. From this point one can move to the point $c = (t + dt, x^a)$ by performing the space shift $N^a dt$. Passing from c to $d = (t + dt, x^a + dx^a)$ is given by dx^a.

One can show that, with use of the vector n^μ, the spatial metric can be induced from $g_{\mu\nu}$ as follows:

$$q_{\mu\nu} = g_{\mu\nu} + n_\mu n_\nu. \tag{2.7}$$

Based on the normal vector n^μ and the induced metric $q_{\mu\nu}$ one can define the *extrinsic curvature* as follows:

$$K_{\mu\nu} = q^\rho{}_\mu q^\sigma{}_\nu \nabla_\rho n_\sigma. \tag{2.8}$$

In can be shown that, spatial part of extrinsic curvature (2.8) is expressed as follows:

$$K_{ab} = \frac{1}{2N}\left(\frac{\partial q_{ab}}{\partial t} - D_a N_b - D_b N_a\right), \tag{2.9}$$

where D_a is a spatial covariant derivative. The K_{ab} will be one of the building blocks in the construction of the Ashtekar variables.

2.3 Ashtekar variables

One of the main ideas leading to the Ashtekar variables is expressing the spatial metric q_{ab} as follows:

$$q_{ab} = e^i_a e^j_b \delta_{ij}, \tag{2.10}$$

where e^i_a are so-called co-triads, which are 3×3 matrices. One can also define triads e^a_i, such that the following relations between triads and co-triads are fulfilled: $e^a_j e^i_a = \delta^i_j$ and $e^a_i e^i_b = \delta^a_b$. An important property of expression (2.10) is the invariance under the three dimensional rotations in the $i, j, k, ... = 1, 2, 3$ indices. Namely, performing rotation $e^i_a \to R^i{}_j e^j_a$, we obtain

$$q_{ab} \to R^i{}_k e^k_a R^j{}_l e^l_b \delta_{ij} = e^k_a e^l_b \underbrace{R^i{}_k R^j{}_l \delta_{ij}}_{=\delta_{kl}} = q_{ab}, \tag{2.11}$$

because $R^i_j \in SO(3)$. This new internal symmetry, related with parametrizing a gravitational field by co-triads, is crucial for the construction of loop quantum gravity. In LQG the $SU(2)$ group, which is the double cover of $SO(3)$, is usually considered. This is because quantization of gauge theories with the compact Lie groups, as $SU(2)$, was much better understood so far. In the Hamiltonian formulation, the $SU(2)$ symmetry will be embedded in the Gauss constraint

Based on the co-triads field one can define the so-called *densitized triad* variable

$$E^a_i := \mathrm{sgn}(\det e) \frac{1}{2} \epsilon^{abc} \epsilon_{ijk} e^j_b e^k_c, \tag{2.12}$$

where for the sake of simplicity we call $\det e := \det(e^i_a)$, which is determinant of the co-triad field. By direct calculation (see Appendix 11.1.1) one can also show that equivalently

$$E^a_i = |\det e| e^a_i. \tag{2.13}$$

It will be also useful to introduce *densitized co-triad*, as follows

$$E^i_a := \frac{1}{|\det e|} e^i_a. \tag{2.14}$$

Based on the properties of triads and co-triads we find $E^a_j E^i_a = \delta^i_j$ and $E^a_i E^i_b = \delta^a_b$. With use of relation $\det E = |\det e|^3 \det(e^a_i) = |\det e|^2 \mathrm{sgn}(\det e)$, where $\det E = \det(E^a_i)$, the triad variable can be expressed in terms of densitized triad:

$$e^a_i = \frac{E^a_i}{\sqrt{|\det E|}}. \tag{2.15}$$

One can also prove (see Appendix 11.1.2) that

$$e^i_a = \frac{1}{2} \frac{\mathrm{sgn}(\det E) \epsilon_{abc} \epsilon^{ijk} E^b_j E^c_k}{\sqrt{|\det E|}}. \tag{2.16}$$

In the previous section we introduced an extrinsic curvature K_{ab} (2.9). Based on this quantity we define

$$K^i_a := \frac{K_{ab} E^b_j \delta^{ij}}{\sqrt{|\det E|}}. \tag{2.17}$$

With use of K_a^i we define the *Ashtekar connection*:

$$A_a^i := \Gamma_a^i + \gamma K_a^i, \tag{2.18}$$

where γ is the Barbero-Immirzi parameter and Γ_a^i is a spin connection

$$\Gamma_a^i = -\epsilon^{ijk} e_j^b \left(\partial_{[e} e_{b]}^k + \frac{1}{2} e_k^c e_a^l \partial_{[c} e_{b]}^l \right). \tag{2.19}$$

The connection A_a^i and densitized triad E_i^a are called *Ashtekar variables* and form a canonically conjugated pair

$$\left\{ E_j^a(\mathbf{x}), A_b^i(\mathbf{y}) \right\} = \kappa\gamma \delta_b^a \delta_j^i \delta(\mathbf{x} - \mathbf{y}), \tag{2.20}$$

where the Poisson bracket is defined as follows

$$\{\cdot, \cdot\} := \kappa\gamma \int_\Sigma d^3z \left[\frac{\delta \cdot}{\delta A_b^j(\mathbf{z})} \frac{\delta \cdot}{\delta E_j^b(\mathbf{z})} - \frac{\delta \cdot}{\delta E_j^b(\mathbf{z})} \frac{\delta \cdot}{\delta A_b^j(\mathbf{z})} \right]. \tag{2.21}$$

In terms of the Ashtekar variables (A_a^i, E_i^a), the theory of gravity can be viewed as a gauge theory with the $SU(2)$ symmetry group. In particular, comparing with electromagnetic U(1) gauge field, A_a^i is an analogue of the vector potential $\mathbf{A}$ and E_i^a is an analogue of the electric field $\mathbf{E}$. However, the Hamiltonian of the gravity is much different than in case of the Yang-Mills theory.

2.4 Hamiltonian

In the canonical formulation of General Relativity, the Hamiltonian is a sum of constraints. In particular, in the framework of Ashtekar variables, the Hamiltonian is a sum of three constraints [11, 41]:

$$H_G[N^i, N^a, N] = \frac{1}{2\kappa} \int_\Sigma d^3x \left(N^i C_i + N^a C_a + NC \right) \approx 0, \tag{2.22}$$

where (N^i, N^a, N) are Lagrange multipliers, C_i is called the Gauss constraint, C_a is a diffeomorphism constraint, and C is the Hamiltonian (scalar) constraint. The sign "$\approx$" means equality on the surface of constraints (*i.e.* weak equality). Functional expressions for the constraints are the following

$$C_i = \frac{2}{\gamma} \mathcal{D}_a E_i^a = \frac{2}{\gamma} \left(\partial_a E_i^a + \epsilon_{ijk} A_a^j E_k^a \right), \tag{2.23}$$

$$C_a = \frac{2}{\gamma} \left(E_i^b F_{ab}^i - A_a^i C_i \right), \tag{2.24}$$

$$C = \frac{E_i^a E_j^b}{\sqrt{|\det E|}} \left[\varepsilon^{ij}{}_k F_{ab}^k - 2(1+\gamma^2) K_{[a}^i K_{b]}^j \right], \tag{2.25}$$

where the curvature of the Ashtekar connection

$$F^i_{ab} = \partial_a A^i_b - \partial_b A^i_a + \epsilon^i{}_{jk} A^j_a A^k_b. \tag{2.26}$$

One can also define the corresponding smeared constraints as follows:

$$\mathcal{C}_1 = G[N^i] = \frac{1}{2\kappa}\int_\Sigma d^3x\, N^i C_i, \tag{2.27}$$

$$\mathcal{C}_2 = D[N^a] = \frac{1}{2\kappa}\int_\Sigma d^3x\, N^a C_a, \tag{2.28}$$

$$\mathcal{C}_3 = S[N] = \frac{1}{2\kappa}\int_\Sigma d^3x\, NC, \tag{2.29}$$

that is such that $H_G[N^i, N^a, N] = G[N^i] + D[N^a] + S[N]$. The Hamiltonian is a total constraint which is vanishing for all multiplier functions (N^i, N^a, N).

Because $H_G[N^i, N^a, N] \approx 0$ at all times, the time derivative of the Hamiltonian constraint is also weakly vanishing, $\dot{H}_G[N^i, N^a, N] \approx 0$. The Hamilton equation

$$\dot{f} = \{f, H_G[M^i, M^a, M]\} \tag{2.30}$$

therefore leads to

$$\left\{H_G[N^i, N^a, N], H_G[M^i, M^a, M]\right\} \approx 0, \tag{2.31}$$

which, when explicitly written, means:

$$\left\{G[N^i] + D[N^a] + S[N], G[M^i] + D[M^a] + S[M]\right\} \approx 0.$$

Due to the linearity of the Poisson bracket, one can straightforwardly find that the condition (2.31) is fulfilled if the smeared constraints belong to a first class algebra

$$\{\mathcal{C}_I, \mathcal{C}_J\} = f^K{}_{IJ}(A^j_b, E^a_i)\mathcal{C}_K. \tag{2.32}$$

In (2.32), the $f^K{}_{IJ}(A^j_b, E^a_i)$ are structure functions which, in general, depend on the phase space (Ashtekar) variables (A^j_b, E^a_i). The algebra of constraints is fulfilled at the classical level due to general covariance. To prevent the system from escaping the surface of constraints, leading to unphysical behavior, the algebra must also be closed at the quantum level. In addition, it was pointed out in [42] that the algebra of quantum constraints should be strongly closed (*off shell* closure). This means that the relation (2.32) should hold in the whole kinematical phase space, and not only on the surface of constraints (*on shell* closure). This should remain true after promoting the constraints to quantum operators.

2.5 Anomalies

At the effective level, the constraints $\mathcal{C}_I$ are subject of some quantum corrections. Because of this, the algebra of the effective constraints might not be closed

$$\{\mathcal{C}^{\text{eff}}_I, \mathcal{C}^{\text{eff}}_J\} = g^K{}_{IJ}(A^j_b, E^a_i)\mathcal{C}^{\text{eff}}_K + \mathcal{A}_{IJ}, \tag{2.33}$$

where ${g^K}_{IJ}(A^j_b, E^a_i)$ are structure functions, which can be different from those in the classical case (2.32). Such a difference would mean modification of the underlying general covariance. The $\mathcal{A}_{IJ}$ is the anomaly term.

In order to keep the system at the surface of constraints, the anomaly term $\mathcal{A}_{IJ}$ should vanish. The condition $\mathcal{A}_{IJ} = 0$ implies some restrictions on the form of the quantum corrections.

2.6 Holonomies

In LQG the gravitational degrees of freedom are parametrized by holonomies and fluxes (which are functionals of the Ashtekar variables). These are non-local functions used to construct background independent quantum theory of gravity. The holonomies and fluxes are non-trivial $SU(2)$ variables satisfying the holonomy-flux algebra. For the purpose of this thesis we need to focus only on holonomies of the Ashtekar connection.

The holonomy of the Ashtekar connection A^i_a along the curve $e \subset \Sigma$ is defined as follows

$$h_e = \mathcal{P} \exp \int_e A^i_a \tau_i dx^a, \tag{2.34}$$

where $\tau_i = -\frac{i}{2}\sigma_i$ (σ_i are the Pauli matrices) and $[\tau_i, \tau_j] = \epsilon_{ijk}\tau^k$. The $\mathcal{P}$ is a path-ordering operator.

In general, holonomies are complicated functions of the Ashtekar connections integrated along the curve e. However, in the highly symmetric spaces, like the FRW model, expression for the holonomies take a simple form.

2.7 Homogeneous cosmological model

In this section we will investigate homogenous and isotropic flat FRW model in the Hamiltonian formulation. This model will serve as a background while considering the perturbations. The line element for this model takes the following form

$$ds^2 = -N^2 dt^2 + q_{ab} dx^a dx^b \tag{2.35}$$

where

$$q_{ab} = a^2(t)\delta_{ab} = e^i_a e^j_b \delta_{ij} := a^2(t) {}^o e^i_a {}^o e^j_b \delta_{ij}. \tag{2.36}$$

The shift vector is vanishing. Based on (2.36), we find expression on the co-triads and triads:

$$e^i_a = a\delta^i_a, \tag{2.37}$$

$$e^a_i = \frac{1}{a}\delta^a_i. \tag{2.38}$$

With use of definition of the Ashtekar variables, we find

$$A_a^i = \gamma \bar{k} \delta_a^i, \tag{2.39}$$
$$E_i^a = \bar{p} \delta_i^a, \tag{2.40}$$

where we have defined $\bar{p} = a^2$ and $\bar{k} = \dot{a}$.

Volume of the flat $\mathbb{R}^3$ space is infinite. Therefore, all the expressions proportional to positive powers of volume diverge. In order to tackle with this problem we will restrict spatial integration into the so-called *fiducial volume* V_0. Physical volume of this subspace can be expressed as follows:

$$V = \int_{V_0} d^3y \sqrt{|\det E(\mathbf{y})|} = V_0 \bar{p}^{3/2}. \tag{2.41}$$

The Poisson bracket (2.21) for the considered FRW model simplifies to

$$\{\cdot, \cdot\} = \frac{\kappa}{3V_0} \left(\frac{\partial \cdot}{\partial \bar{k}} \frac{\partial \cdot}{\partial \bar{p}} - \frac{\partial \cdot}{\partial \bar{p}} \frac{\partial \cdot}{\partial \bar{k}} \right), \tag{2.42}$$

therefore

$$\left\{ \bar{k}, \bar{p} \right\} = \frac{\kappa}{3V_0}. \tag{2.43}$$

2.7.1 Elementary holonomy

Let us now consider a holonomy in a direction ${}^o e_k^a \partial_a$ and coordinate length $\bar{\mu} = \mu V_0^{1/3}$, where μ is a dimensionless parameter. With use of definition (2.34) and expression on the Ashtekar connection for the FRW model, we find

$$\begin{aligned} h_k &= e^{\bar{\mu}\gamma\bar{k}\tau_k} = e^{-i\bar{\mu}\gamma\bar{k}\frac{\sigma_k}{2}} = \sum_{n=0}^{\infty} \frac{1}{n!} \left(-i \frac{\bar{\mu}\gamma\bar{k}}{2} \sigma_k \right)^n \\ &= \sum_{n=0}^{\infty} \frac{(-1)^n}{(2n)!} \left(\frac{\bar{\mu}\gamma\bar{k}}{2} \right)^{2n} \sigma_k^{2n} - i \sum_{n=0}^{\infty} \frac{(-1)^n}{(2n+1)!} \left(\frac{\bar{\mu}\gamma\bar{k}}{2} \right)^{2n+1} \sigma_k^{2n+1} \\ &= \mathbb{I} \cos\left(\frac{\bar{\mu}\gamma\bar{k}}{2} \right) - i \sin\left(\frac{\bar{\mu}\gamma\bar{k}}{2} \right) \sigma_k \\ &= \mathbb{I} \cos\left(\frac{\bar{\mu}\gamma\bar{k}}{2} \right) + 2 \sin\left(\frac{\bar{\mu}\gamma\bar{k}}{2} \right) \tau_k. \end{aligned} \tag{2.44}$$

Inversion of the holonomy h_k can be easily found

$$(h_k)^{-1} = e^{-\bar{\mu}\gamma\bar{k}\tau_k} = \mathbb{I} \cos\left(\frac{\bar{\mu}\gamma\bar{k}}{2} \right) - 2 \sin\left(\frac{\bar{\mu}\gamma\bar{k}}{2} \right) \tau_k. \tag{2.45}$$

2.7.2 A loop

The elementary holonomy we investigated in the previous subsection can be now employed to compute holonomy along the closed curve $\alpha = \Box_{ij}$. This curve is schematically presented on the diagram below.

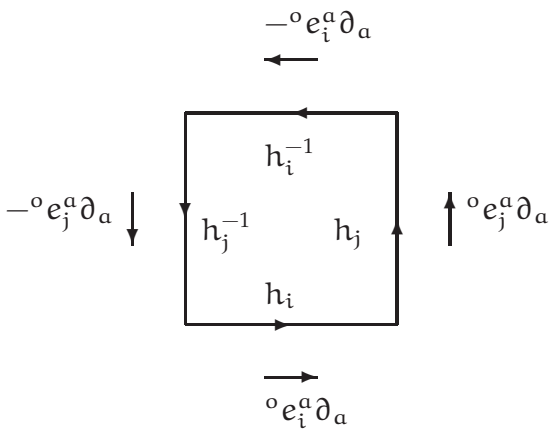

This holonomy can be written as

$$\begin{aligned} h_{\Box_{ij}} &= h_i h_j h_i^{-1} h_j^{-1} \\ &= e^{\mu V_0^{1/3} A_a {}^{o}e_i^a} e^{\mu V_0^{1/3} A_a {}^{o}e_j^a} e^{-\mu V_0^{1/3} A_a {}^{o}e_i^a} e^{-\mu V_0^{1/3} A_a {}^{o}e_j^a} \\ &= \exp\left[\mu^2 V_0^{2/3} A_a^l A_b^m {}^{o}e_i^a {}^{o}e_j^b [\tau_l, \tau_m] + \mathcal{O}(\mu^3)\right] \\ &= \mathbb{I} + \mu^2 V_0^{2/3} F_{ab}^k \tau_k {}^{o}e_i^a {}^{o}e_j^b + \mathcal{O}(\mu^3), \end{aligned} \tag{2.46}$$

where we have used Baker-Campbell-Hausdorff formula and the fact that, for the flat FRW model, the field strength simplifies to the form $F_{ab}^k = \epsilon_{ij}^k A_a^i A_b^j$. Now, the equation (2.46) can be simply rewritten to the form

$$F_{ab}^k = -2 \lim_{\mu \to 0} \frac{\mathrm{tr}\left[\tau_k \left(h_{\Box_{ij}} - \mathbb{I}\right)\right]}{\mu^2 V_0^{2/3}} {}^{o}e_a^i {}^{o}e_b^j. \tag{2.47}$$

The trace in this equation can be calculated with use of the definition (2.44) and properties of the τ_i matrices, one finds

$$\mathrm{tr}\left[\tau_k \left(h_{\Box_{ij}} - \mathbb{I}\right)\right] = -\frac{\epsilon_{kij}}{2} \sin^2\left(\bar{\mu}\gamma\bar{k}\right). \tag{2.48}$$

2.7.3 Hamiltonian

The LQG Hamiltonian is obtained by re-expressing Hamiltonian (2.22) in terms of fluxes and holonomies. Our purpose is to construct a symmetry reduced model, which will capture some features of LQG. Such treatment is phenomenological in its nature. However, this approach will enable us to study some possible consequences of LQG, which are technically hard to investigate in the full theory. This will be achieved by introducing the effect of holonomies.

Because for the homogeneous models $K_a^i = \frac{1}{\gamma}A_a^i$, the Hamiltonian (2.22) simplifies to

$$H_G[N] = -\frac{1}{\gamma^2}\frac{1}{16\pi G}\int_\Sigma d^3x \frac{N}{\sqrt{|\det E|}} E_i^a E_j^b \epsilon_k^{ij} F_{ab}^k. \tag{2.49}$$

Applying the classical identity (see Appendix 11.1.3)

$$\frac{1}{\sqrt{|\det E|}} E_i^a E_j^b \epsilon_k^{ij} F_{ab}^k = \frac{1}{4\pi G\gamma}\epsilon^{abc}\{A_c^i, V\}F_{abi}, \tag{2.50}$$

and the trace of a product of the $SU(2)$ variables we find

$$H_G[N] = \frac{1}{32\pi^2 G^2}\frac{1}{\gamma^3}\int_\Sigma d^3x N \epsilon^{abc} \mathrm{tr}\left[F_{ab}\{A_c, V\}\right]. \tag{2.51}$$

Regularization of this Hamiltonian can be performed with use of expressions

$${}^o e_k^a\{A_a, V\} \approx -\frac{1}{\mu V_0^{1/3}} h_k\{h_k^{-1}, V\} \tag{2.52}$$

and (2.46):

$$h_{\Box_{ij}} \approx \mathbb{I} + \mu^2 V_0^{2/3} F_{ab}^k \tau_k {}^o e_i^a {}^o e_j^b, \tag{2.53}$$

where the fiducial triad ${}^o e_i^a$ is dual to the fiducial co-triad ${}^o e_a^i$. Here $\mu V_0^{1/3}$ is the coordinate length of the path along which the elementary holonomy h_i is calculated. The μ is a dimensionless parameter which controls the length. In the limit $\mu \to 0$, Eqs. (2.52) and (2.53) become equalities. Combining Eq. (2.52) and Eq. (2.53) one can write

$$\epsilon^{ijk}\mathrm{tr}\left[h_{\Box_{ij}} h_k\{h_k^{-1}, V\}\right] = -\mu^3 V_0 \epsilon^{ijk o} e_i^{a o} e_j^{b o} e_k^c \mathrm{tr}\left[F_{ab}\{A_c, V\}\right]. \tag{2.54}$$

Based on this relation with $\epsilon^{ijk o} e_i^{a o} e_j^{b o} e_k^c = \epsilon^{abc}$ and restricting spatial integration to the fiducial volume V_0, one can regularize Eq. (2.51) into the form

$$H_G^{(\bar{\mu})} = -\frac{N V_0}{32\pi^2 G^2 \gamma^3 \bar{\mu}^3}\sum_{ijk}\epsilon^{ijk}\mathrm{tr}\left[h_{\Box_{ij}} h_k\{h_k^{-1}, V\}\right], \tag{2.55}$$

The classical unmodified Hamiltonian of the FRW model can be recovered from $\lim_{\bar{\mu}\to 0} H_G^{(\bar{\mu})} = H_G$.

Inserting the elementary holonomy and its inversion into the Hamiltonian [Eq. (2.55)]. Next, we find that

$$h_k \left\{ (h_k)^{-1}, V \right\} = h_k 4\pi G \sqrt{\bar{p}} \frac{\partial}{\partial \bar{k}} (h_k)^{-1} = -4\pi G \gamma \bar{\mu} \sqrt{\bar{p}} \tau_k. \tag{2.56}$$

To get this relation we have used the definition of the Poisson bracket and the equality $\tau_k^2 = -\frac{1}{4}\mathbb{I}$. Then, making use of Eq. (2.56) turns the Hamiltonian, Eq. (2.55), into

$$H_g^{(\lambda)} = \frac{N V_0 \sqrt{\bar{p}}}{8\pi G \gamma^2 \bar{\mu}^2} \sum_{ijk} \epsilon^{ijk} \mathrm{tr}\left[h_{\square_{ij}} \tau_k \right]. \tag{2.57}$$

At this stage, the relation

$$\mathrm{tr}\left[h_{\square_{ij}} \tau_k \right] = -\frac{\epsilon_{ijk}}{2} \sin^2(\bar{\mu}\gamma\bar{k}) \tag{2.58}$$

can be applied to get

$$\begin{aligned} \sum_{ijk} \epsilon^{ijk} \mathrm{tr}\left[h_{\square_{ij}} \tau_k \right] &= -\frac{1}{2} \sin^2(\bar{\mu}\gamma\bar{k}) \sum_{ijk} \epsilon^{ijk} \epsilon_{ijk} \\ &= -3 \sin^2(\bar{\mu}\gamma\bar{k}). \end{aligned} \tag{2.59}$$

Finally, inserting Eq. (2.59) into Eq. (2.57) gives

$$H_G^{(\bar{\mu})} = -\frac{3 N V_0}{8\pi G} \sqrt{\bar{p}} \left(\frac{\sin(\bar{\mu}\gamma\bar{k})}{\bar{\mu}\gamma} \right)^2 = -\frac{3 N V_0}{8\pi G} \sqrt{\bar{p}} \mathbb{K}[1]^2, \tag{2.60}$$

where, for the sake of simplicity, we introduced the notation

$$\mathbb{K}[n] := \begin{cases} \frac{\sin(n\bar{\mu}\gamma\bar{k})}{n\bar{\mu}\gamma} & \text{for} \quad n \in \mathbb{Z}/\{0\}, \\ \\ \bar{k} & \text{for} \quad n = 0, \end{cases} \tag{2.61}$$

for the holonomy correction function.

The (2.60) is holonomy-corrected gravity Hamiltonian of the FRW model. The classical limit is recovered by shrinking the length $\bar{\mu}$ to zero.

2.7.4 Equations of motion

The total Hamiltonian is the sum of gravity and matter Hamiltonians:

$$H_{tot} = H_G^{(\bar{\mu})} + H_m. \tag{2.62}$$

The corresponding equations of motion for the conjugated $\bar{p}$ and $\bar{k}$ variables are

$$\dot{\bar{p}} = \{\bar{p}, H_{tot}\} = N2\sqrt{\bar{p}}(\mathbb{K}[2]), \tag{2.63}$$

$$\dot{\bar{k}} = \{\bar{p}, H_{tot}\} = -\frac{N}{\sqrt{\bar{p}}}\left[\frac{1}{2}(\mathbb{K}[1])^2 + \bar{p}\frac{\partial}{\partial\bar{p}}(\mathbb{K}[1])^2\right] + \frac{\kappa}{3V_0}\left(\frac{\partial H_m}{\partial\bar{p}}\right). \tag{2.64}$$

By choosing $N = 1$, the dot "$\cdot$" sign corresponds to the differentiation with respect to the coordinate time t.

Energy density of the matter field is given by

$$\rho := \frac{1}{V_0\bar{p}^{3/2}}\frac{\partial H_m}{\partial N}. \tag{2.65}$$

By combining the Hamiltonian constraint $H_{tot} \approx 0$ and equation (2.63) we find the modified Friedmann equation

$$H^2 = \frac{\kappa}{3}\rho\left(1 - \frac{\rho}{\rho_c}\right), \tag{2.66}$$

where the Hubble factor H is defined as follows

$$H := \frac{1}{2\bar{p}}\frac{d\bar{p}}{dt} = \frac{\dot{a}}{a} \tag{2.67}$$

and

$$\rho_c = \frac{3}{\kappa\bar{\mu}^2\gamma^2\bar{p}} \tag{2.68}$$

is the critical energy density.

As it is clear from the form of equation (2.66), there is no physical evolution for $\rho > \rho_c$, because that would mean $H^2 < 0$. Therefore, due to the effects of holonomies, dynamics is non-singular. The classical Big Bang singularity is replaced by the nonsingular Big Bounce. The maximal energy density ρ_c is reached at the bounce. At this point, the value of the Hubble parameter is equal zero, $H = 0$. Therefore, the bounce is a transition point between the contracting ($H < 0$) and expanding ($H > 0$) periods.

2.8 Holonomy corrections

In LQC, quantum gravity effects are introduced by the holonomies of Ashtekar connection. This replacement is necessary because connection operators do not exist in LQG. The holonomy corrections arise while regularizing classical constraints, by expressing the Ashtekar connection in terms of holonomies. In particular, the regularization of the curvature of the Ashtekar connection F^i_{ab} leads to the factor $\left(\frac{\sin(\bar{\mu}\gamma\bar{k})}{\bar{\mu}\gamma}\right)^2$, which simplifies to $\bar{k}^2$ in the classical limit $\bar{\mu} \to 0$. However, the Ashtekar connection does not appear only

because of F^i_{ab}: in the classical perturbed constraints, terms linear in $\bar{k}$ are also involved. In principle, such terms should be holonomy-corrected. However, there is no direct expression for them, analogous to the regularization of the F^i_{ab} factor. Nevertheless, one can naturally expect that $\bar{k}$ factors are corrected by the replacement

$$\bar{k} \to \frac{\sin(n\bar{\mu}\gamma\bar{k})}{n\bar{\mu}\gamma}, \tag{2.69}$$

where n is some unknown integer. It should be an integer because, when quantizing the theory, the $e^{i\gamma\bar{k}}$ factor is promoted to be a shift operator acting on the lattice states. If n was not an integer, the action of the operator corresponding to $e^{in\gamma\bar{k}}$ would be defined in a different basis. Another issue is related with the choice of $\bar{\mu}$, which corresponds to the so-called *lattice refinement*. Models with a power-law parametrization $\bar{\mu} \propto \bar{p}^{\beta}$ were discussed in details in the literature. While, in general, $\beta \in [-1/2, 0]$, it was pointed out that the choice $\beta = -1/2$ is favored [43]. This particular choice is called the $\bar{\mu}-$scheme (new quantization scheme). In this thesis, we will find additional support for this quantization scheme.

Motivation of the domain of the parameter β comes from the investigation of the lattice states in LQC. A number of the lattice blocks is expressed as $\mathcal{N} = V_0/l_0^3$ where l_0 is the average coordinate length of the lattice edge. This value is connected to the earlier introduced length $\bar{\mu}$, namely $\mathcal{N} = \bar{\mu}^{-3}(\bar{p})$. During the evolution an increase of the total volume is due to the increase of spin labels on the graph edges or due to the increase of the number of vortices. In this former case the number of lattice blocks is constant during the evolution, $\mathcal{N} = \text{const}$. Otherwise, when the spin labels do not change, the number of vortices scales with the volume, $\mathcal{N} \propto \bar{p}^{3/2}$. Therefore, for the physical evolution the power index lies in the range $[0, 3/2]$. Applying the definition of $\mathcal{N}$ we see that the considered boundary values translate to the domain of β introduced earlier, $\beta \in [-1/2, 0]$.

A proportionality factor in the relation $\bar{\mu} \propto \bar{p}^{\beta}$ is an another issue to be fixed. In order to do so, let us consider physical area of the loop around which the holonomy was derived. The physical area is $\text{Ar}_{\square} = (\bar{\mu}a)^2 = \bar{p}\bar{\mu}^2$. For the $\bar{\mu}-$scheme $\bar{\mu} \propto \bar{p}^{-1/2}$, so $\text{Ar}_{\square} = \text{const}$. Therefore, in the $\bar{\mu}-$scheme, a physical area of the elementary lattice cell is constant. This area can be related with the physical lattice spacing λ, then $\bar{\mu} = \lambda/\sqrt{\bar{p}}$ and $\text{Ar}_{\square} = \lambda^2$. It is expected that $\lambda \sim l_{Pl}$, because of the quantum gravitational origin of discretization. The lattice spacing λ can be fixed by assuming that $\lambda^2 = \Delta$, where Δ is the area gap in LQG. However, in general, the value of λ should be considered as a free parameter to be fixed observationally.

In what follows, introduction of holonomy corrections is performed by replacing $\bar{k} \to \mathbb{K}[n]$. However, factors $\bar{k}^2$ are simply replaced by $\mathbb{K}[1]^2$, because they arise from the curvature of the Ashtehar connection. For the linear terms, the integers are parameters to be fixed.

Chapter 3

Planck epoch and cosmic inflation

The phase of cosmic inflation was historically introduced in order to explain the horizon of flatness problems in cosmology [6]. At present, the main motivation for the phase of inflation comes from observations of the cosmic microwave background radiation. The CMB data indicate that the power spectrum of primordial perturbations was nearly flat, in agreement with what is predicted from the phase of inflation. In this chapter, we study the realization of the phase of inflation in the framework of LQC with the holonomy corrections.

3.1 Inflation in loop quantum cosmology

In general, many different evolutionary scenarios are possible within the framework of LQC. However, all of them have a fundamental common feature, namely the cosmic bounce. As we will show, the implementation of a suitable matter content also generically leads to a phase of inflation. This phase is nearly mandatory in any meaningful cosmological scenario since our current understanding of the growth of cosmic structures requires inflation in the early universe. It is therefore important to study the links between the inflationary paradigm and the LQC framework, as emphasized, *e.g.*, in [24].

The demonstration that a phase of super-inflation can occur due to quantum gravity effects was one of the first great achievements of LQC [21]. This result was based on the so-called inverse volume corrections. It has however been understood that such corrections exhibit fiducial cell dependence, making the physical meaning of the associated results harder to understand. As discussed earlier, other corrections also arise in LQC, due to the so-called holonomy terms, which do not depend on the fiducial cell volume. Those corrections lead to a dramatic modification of the Friedmann equation which becomes (2.66):

$$H^2 = \frac{\kappa}{3}\rho\left(1 - \frac{\rho}{\rho_c}\right), \tag{3.1}$$

where ρ is the energy density, ρ_c is the critical energy density, H is the Hubble parameter,

and $\kappa = 8\pi G$. In principle, ρ_c can be viewed as a free parameter of theory. However, its value is usually determined thanks to the results of area quantization in LQG. For the $\bar{\mu} - scheme$ we have $\bar{\mu} = \sqrt{\Delta/\bar{p}}$ and by taking $\Delta = 2\sqrt{3}\pi\gamma l_{Pl}^2$ [15] the expression (2.68) is:

$$\rho_c = \frac{\sqrt{3}}{16\pi^2\gamma^3} m_{Pl}^4 \simeq 0.82 m_{Pl}^4, \tag{3.2}$$

where value $\gamma \simeq 0.239$ has been used, as obtained from the computation of the entropy of black holes [44]. The Planck mass $m_{Pl} \approx 1.22 \cdot 10^{19}$GeV.

As it can easily be seen from (Eq. 3.1), a general prediction associated with models including holonomy corrections is a bounce which occurs for $\rho = \rho_c$. The appearance of this ρ^2 term with the correct negative sign is a highly non-trivial and appealing feature of this framework which shows that repulsive quantum geometrical effects become dominant in the Planck region. The very quantum nature of spacetime is capable of overwhelming the huge gravitational attraction. The dynamics of models with holonomy corrections was studied in several articles [23, 24, 45, 46].

In this thesis we further perform a detailed and consistent study of a universe filled with a massive scalar field in this framework. In that case, potential has the following form

$$V(\varphi) = \frac{1}{2} m^2 \varphi^2, \tag{3.3}$$

where m is a mass of the inflaton field. The global dynamics of such models was firstly studied in Ref. [45]. Recently, it was pointed out in Ref. [23] that the "standard" slow-roll inflation is triggered by the preceding phase of the quantum bounce. This general effect is due to the fact that the universe undergoes contraction before the bounce, resulting in a negative value of the Hubble factor H. Since the equation governing the evolution of a massive scalar field in a FRW universe is

$$\ddot{\varphi} + 3H\dot{\varphi} + m^2\varphi = 0, \tag{3.4}$$

the negative value of H during the pre-bounce phase acts as an *anti-friction* term leading to amplification of the oscillations of field φ. In particular, when the scalar field is initially at the bottom of the potential well with some small non-vanishing derivative $\dot{\varphi}$, then it is driven up the potential well as a result of the contraction of the universe. This situation is presented in Fig. 3.1

To some extent, it is therefore reasonable to say that the LQC framework solves both the main "problems" of the Big Bang theory: the singularity (which is regularized and replaced by a bounce) and the initial conditions for inflation (which are naturally set by the anti-friction term).

However, this *shark fin* evolution (see caption of Fig. 3.1) is not the only possible one. In particular, a nearly *symmetric* evolution can also take place, as studied in Ref. [46]. Those different scenarios can be distinguished by the fraction of potential energy at the

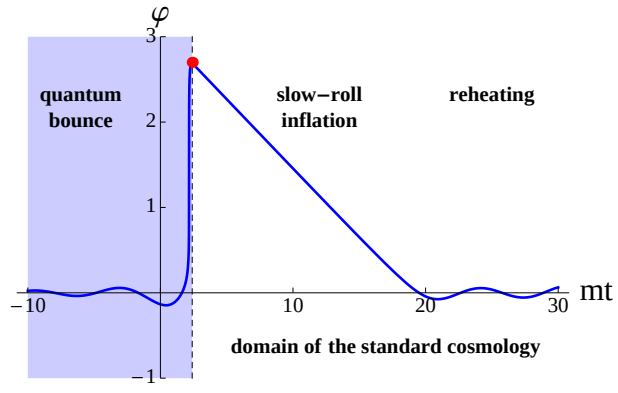

Figure 3.1: The *shark fin* type evolution of a scalar field for $m = 10^{-3} m_{Pl}$. The (red) dot represents the point where the initial conditions in classical cosmology are usually set.

bounce, described by the parameter

$$F_B := \frac{V(\varphi_B)}{\rho_c} \in [0, 1], \tag{3.5}$$

where $V(\varphi)$ is potential of the scalar field and φ_B is value of the scalar field at the bounce. When $F_B = 0$, the evolution of the field is symmetric. When a small fraction of potential energy is introduced, which is the general case, the symmetry is broken and the field behaves as in the *shark fin* case. It is however important to underline that we consider only scenarios where the contribution from the potential is sub-dominant at the bounce, as it would otherwise be necessary to include quantum backreaction effects [47, 48] expected for $F_B \sim 1$. Effective dynamics would then be more complicated and could not be anymore described by equation (3.1).

In order to perform qualitative studies of the dynamics of the model, it is useful to introduce the variables

$$x := \frac{m\varphi}{\sqrt{2\rho_c}} \text{ and } y := \frac{\dot{\varphi}}{\sqrt{2\rho_c}}. \tag{3.6}$$

Since the energy density of the field is constrained ($\rho \leqslant \rho_c$), the inequality

$$x^2 + y^2 \leqslant 1 \tag{3.7}$$

has to be fulfilled. The x^2 term corresponds to the potential part while the y^2 corresponds to the kinetic term. The case $x^2 + y^2 = 1$ corresponds to the bounce, when the energy density reaches its maximum.

In Fig. 3.2, exemplary evolutionary paths in the $x - y$ phase plane are shown. For all the presented cases, the evolution begins at the origin (in the limit $t \to -\infty$), and then evolves (dashed line) to the point on the circle $x^2 + y^2 = 1$. Finally, the field moves back to the origin for $t \to +\infty$ (solid line). However, the shapes of the intermediate paths are different. The $x = 0$ case corresponds to the *symmetric* evolution which was studied in

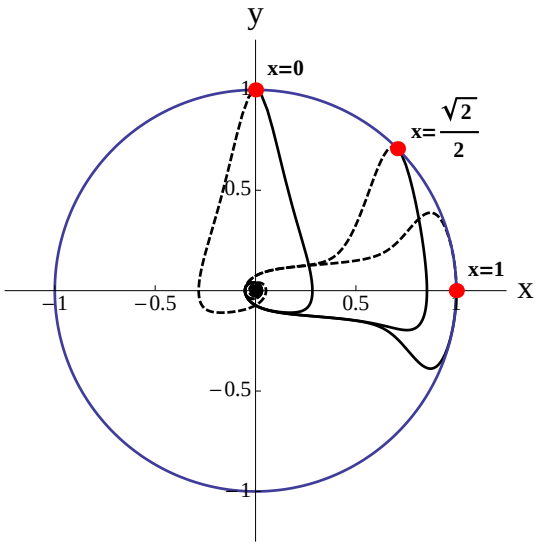

Figure 3.2: Exemplary phase trajectories of the scalar field with $m = m_{Pl}$.

Ref. [46] (if the bounce is set at $t = 0$, the scale factor is an even function of time and the scalar field is an odd function). In this case, the field is at the bottom of the potential well exactly at the bounce ($H = 0$). This is however a very special choice of initial conditions. In the case $x = \sqrt{2}/2$, the potential term and kinetic term contribute equally at the bounce. In this case, both deflation and inflation occur. However one observes differences in their duration. The third case, $x = 1$, corresponds to the domination of the potential part at the bounce. In this case, symmetric phases of deflation and inflation also occur (both the scale factor and the field being this time even functions). However in this situation, as well as in $x = \sqrt{2}/2$ case, the effect of quantum backreaction should be taken into account. The dynamics can therefore significantly differ from the one computed with (Eq. 3.1).

In Fig. 3.3 we show some exemplary evolutions of the scalar field for different contributions from the potential part at the bounce. It can be easily seen that the maximal value of the field (φ_{max}) increases with the fraction of potential energy at the bounce. This monotonic relation can be determined based on the numerical computations. In particular, for $m = 10^{-6} m_{Pl}$ we found the formula

$$\varphi_{max} = (2.33 + 1.28 \cdot 10^6 \sqrt{F_B}) m_{Pl}. \tag{3.8}$$

This formula was plotted in Fig. 3.4 The minimal value of φ_{max} is equal to $2.33 m_{Pl}$ and corresponds to $F_B = 0$. Because the total energy density is constrained, φ_{max} is bounded from above by

$$|\varphi_{max}| \leqslant \frac{\sqrt{2\rho_c}}{m}. \tag{3.9}$$

The values of φ_{max} associated with different evolutionary scenarios were computed in [24, 23, 46]. The conclusion of those studies is that necessary conditions for inflation

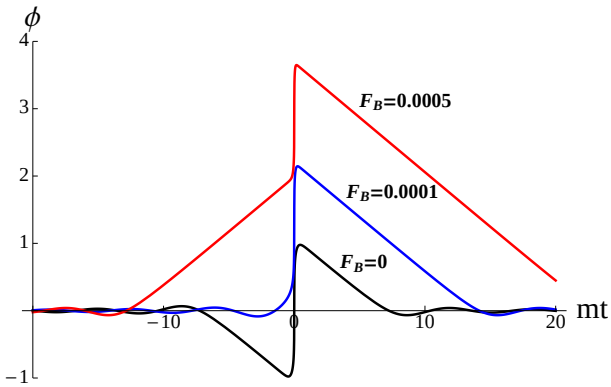

Figure 3.3: Time evolution of the scalar field. Different evolutionary scenarios leading to a slow-roll inflation phase are displayed. The bottom (black) line represents the *symmetric* case. The middle (blue) line represents the *shark fin* type evolution mostly investigated in this thesis. The top (red) line corresponds to a larger fraction of potential energy. For all curves $m = 0.01 m_{Pl}$.

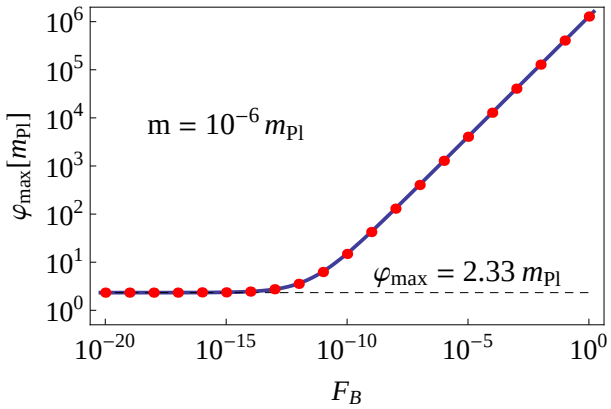

Figure 3.4: Relation between φ_{max} and F_B for $m = 10^{-6} m_{Pl}$ given by equation (3.8). The (red) dots correspond to numerically determined data points.

are generically met. Only in case of a *symmetric* evolution, does the value of φ_{max} become too small in some cases. In particular, for $m = 10^{-6} m_{Pl}$ one obtains $\varphi_{max} = 2.33 m_{Pl}$ for *symmetric* evolution. The corresponding number of $e-$folds can be computed with $N \simeq 2\pi \frac{\varphi^2}{m_{Pl}^2}$, which gives $N \simeq 34$. By introducing a small fraction of potential energy (as in the *shark fin* case), the number of $e-$folds can be appropriately increased. Relation between the number of $e-$folds and F_B, obtained based on equation (3.8), was shown in Fig. 3.5.

The argument that inflation requires sufficient number of $e-$folds comes from the CMB observations. In particular, based the WMAP observations [8], the value of the scalar spectral index was measured to be $n_S = 0.963 \pm 0.012$. As, for a massive slow-roll

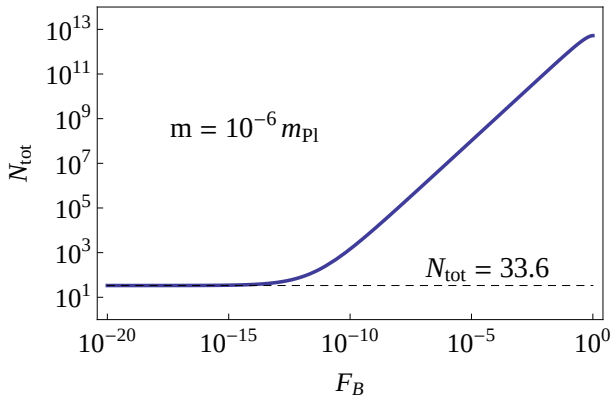

Figure 3.5: Relation between the total number of inflationary $e-$ folds N_{tot} and parameter F_B for $m = 10^{-6} m_{Pl}$.

inflation the relation

$$n_S = 1 - \frac{1}{\pi}\frac{m_{Pl}^2}{\varphi^2} \tag{3.10}$$

holds, one obtains $\varphi_{obs} = 2.9 \pm 0.5 m_{Pl}$. Since the consistency relation $\varphi_{max} > \varphi_{obs}$ must be fulfilled, the *symmetric* evolution with $m = 10^{-6} m_{Pl}$ (for which $\varphi_{max} = 2.33 m_{Pl} < \varphi_{obs}$) is not favored by the WMAP 7-Years observations. As already mentioned, higher values of φ can be easily reached if some contribution from the potential term is introduced (this supports the *shark fin* scenario). The number of $e-$folds will therefore be naturally increased in this way. However it remains bounded by above: since $N \simeq 2\pi\frac{\varphi^2}{m_{Pl}^2}$, (Eq. 9.5) leads to the constrain:

$$N \leqslant \frac{4\pi\rho_c}{m^2 m_{Pl}^2}. \tag{3.11}$$

The value of the parameter ρ_c can be fixed by (Eq. 3.2). However, this expression is based on the computation of the area gap as performed in LQG. This, in general, can be questioned. Moreover, a particular value of the Barbero-Immirzi parameter (imposed by black hole entropy considerations) has been used. Therefore, the value of ρ_c can, in general, differ and it is worth investigating how the variation of ρ_c can alter the dynamics of the model. In particular, we have studied how the *shark fin* scenario can be modified by different choices of ρ_c. In Fig. 3.6, the evolution of the field is displayed as a function of the value of the critical energy density. As expected, the larger ρ_c, the higher the maximum value reached by the field. It can be seen that φ_{max} approaches the usually required value $\sim 3 m_{Pl}$ for $\rho_c \sim m_{Pl}^4$, making the whole scenario quite natural.

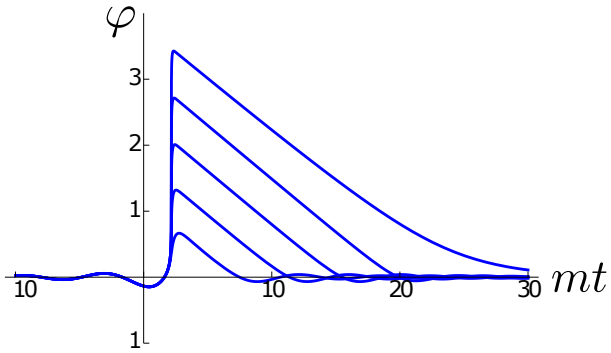

Figure 3.6: The *shark fin* type evolution of the scalar field for $m = 10^{-3} m_{Pl}$. Curves from bottom to top were computed for $\rho_c = 10^{-6}, 10^{-4}, 10^{-2}, 1, 100\ [m_{Pl}^4]$ respectively.

Chapter 4

Cosmological perturbations in the Hamiltonian formulation

In the previous chapter, we studied dynamics of the flat FRW model with holonomy corrections. The assumption of homogeneity made in those considerations is valid at the large (cosmological) scales only. In that case, local inhomogeneities are averaged and universe is modeled by homogeneous distribution of matter. The observed Universe is however not homogeneous but contains a variety of gravitational structures at the different length scales. Such a system is enormously complex to describe in general, due to its nonlinearity. However, at some early stages, inhomogeneity of the universe can be treated at perturbative level[1]. This allows to linearize the equations of motion, which simplifies considerations in the significant way. In particular, the three types of perturbations (scalar, vector and tensor) are decoupled from one another in the linear regime.

In this chapter, we derive a classical theory of cosmological perturbations in the Hamiltonian formulation. We perform perturbative expansion of the classical constraints up to the second order. This will lead to equations of motion in the first order in perturbations. In the subsequent chapters, we will modify the expression derived here by introducing the quantum holonomy corrections.

4.1 Perturbation of the canonical variables

The Ashtekar variables can be decomposed for the background and perturbation parts as follows:

$$E^a_i = \bar{E}^a_i + \delta E^a_i, \tag{4.1}$$

$$A^i_a = \bar{A}^i_a + \delta A^i_a. \tag{4.2}$$

[1]This can be seen, *e.g.*, by considering temperature anisotropy of the CMB, which is $\delta T/T \sim 10^{-5}$. The observed fluctuations of temperature are of the same order of magnitude as inhomogeneities in matter distribution. Therefore, early universe was very homogeneous, allowing for a perturbative description of inhomogeneities.

Validity of the perturbative expansion based on the above decomposition requires that $|\delta E^a_i/\bar{E}^a_i| \ll 1$ as well as $|\delta A^i_a/\bar{A}^i_a| \ll 1$. Because we consider a model with a scalar field, we also decompose the canonical variables:

$$\varphi = \bar{\varphi} + \delta\varphi, \tag{4.3}$$
$$\pi = \bar{\pi} + \delta\pi. \tag{4.4}$$

Here also, validity of the perturbative expansion requires that $|\delta\varphi/\bar{\varphi}| \ll 1$ and $|\delta\pi/\bar{\pi}| \ll 1$

In this thesis we consider perturbations on the flat FRW cosmological background. In this case $\bar{\Gamma}^i_a = 0$ and the background part of the Ashtekar variable is given by $\bar{A}^i_a = \gamma\bar{k}\delta^i_a$. The homogeneous part of the densitized triad variable is given by $\bar{E}^a_i = \bar{p}\delta^a_i$. Therefore, for the flat FRW background

$$E^a_i = \bar{p}\delta^a_i + \delta E^a_i, \tag{4.5}$$
$$A^i_a = \gamma\bar{k}\delta^i_a + \delta A^i_a. \tag{4.6}$$

In the following consideration we will work mainly with perturbations of K^i_a instead of A^i_a. The, perturbation of the K^i_a is given by

$$K^i_a = \frac{1}{\gamma}\left(A^i_a - \Gamma^i_a\right) = \bar{K}^i_a + \delta K^i_a, \tag{4.7}$$

where $\bar{K}^i_a = \bar{k}\delta^i_a$. In such case, the background variables for the system under consideration are $(\bar{k}, \bar{p}, \bar{\varphi}, \bar{\pi})$, while the perturbed variables are $(\delta K^i_a, \delta E^a_i, \delta\varphi, \delta\pi)$. It can be shown that the Poisson bracket for this system can be decomposed as follows [31, 32]:

$$\{\cdot,\cdot\} = \{\cdot,\cdot\}_{\bar{k},\bar{p}} + \{\cdot,\cdot\}_{\delta K,\delta E} + \{\cdot,\cdot\}_{\bar{\varphi},\bar{\pi}} + \{\cdot,\cdot\}_{\delta\varphi,\delta\pi} \tag{4.8}$$

where

$$\{\cdot,\cdot\}_{\bar{k},\bar{p}} := \frac{\kappa}{3V_0}\left[\frac{\partial\cdot}{\partial\bar{k}}\frac{\partial\cdot}{\partial\bar{p}} - \frac{\partial\cdot}{\partial\bar{p}}\frac{\partial\cdot}{\partial\bar{k}}\right], \tag{4.9}$$
$$\{\cdot,\cdot\}_{\delta K,\delta E} := \kappa\int_\Sigma d^3x\left[\frac{\delta\cdot}{\delta\delta K^i_a}\frac{\delta\cdot}{\delta\delta E^a_i} - \frac{\delta\cdot}{\delta\delta E^a_i}\frac{\delta\cdot}{\delta\delta K^i_a}\right], \tag{4.10}$$
$$\{\cdot,\cdot\}_{\bar{\varphi},\bar{\pi}} := \frac{1}{V_0}\left[\frac{\partial\cdot}{\partial\bar{\varphi}}\frac{\partial\cdot}{\partial\bar{\pi}} - \frac{\partial\cdot}{\partial\bar{\pi}}\frac{\partial\cdot}{\partial\bar{\varphi}}\right], \tag{4.11}$$
$$\{\cdot,\cdot\}_{\delta\varphi,\delta\pi} := \int_\Sigma d^3x\left[\frac{\delta\cdot}{\delta\delta\varphi}\frac{\delta\cdot}{\delta\delta\pi} - \frac{\delta\cdot}{\delta\delta\pi}\frac{\delta\cdot}{\delta\delta\varphi}\right]. \tag{4.12}$$

In the Einstein formulation of gravity the space-time metric $g_{\mu\nu}$ is used as a perturbative variable. The metric is decomposed for the background and perturbation parts, $g_{\mu\nu} = \bar{g}_{\mu\nu} + \delta g_{\mu\nu}$, where the consistency of the perturbative expansion is fulfilled by the

requirement $|\delta g_{\mu\nu}/\bar{g}_{\mu\nu}| \ll 1$. In case of the flat FRW background, the metric perturbations can be decomposed according to their spin as follows

$$\begin{aligned} g_{\mu\nu} &= \underbrace{a^2\begin{pmatrix} -1 & 0 \\ 0 & \delta_{ab} \end{pmatrix}}_{\text{FRW k=0 background}} + \underbrace{a^2\begin{pmatrix} -2\phi & \partial_a B \\ \partial_a B & -2\psi\delta_{ab} + \partial_a\partial_b E \end{pmatrix}}_{\text{scalar (s=0)}} \\ &+ \underbrace{a^2\begin{pmatrix} 0 & S_a \\ S_a & F_{a,b} + F_{b,a} \end{pmatrix}}_{\text{vector (s=1)}} + \underbrace{a^2\begin{pmatrix} 0 & 0 \\ 0 & h_{ab} \end{pmatrix}}_{\text{tensor (s=2)}}. \end{aligned} \tag{4.13}$$

The $\phi, \psi, B, E, S_a, F_a$ and h_{ab} are perturbative variables. Furthermore, the following conditions are fulfilled:

$$\begin{aligned} \partial^a h_{ab} &= 0 \text{ (transverse) and } \delta^{ab} h_{ab} = 0 \text{ (traceless)}, \\ F^a{}_{,a} &= 0 \text{ (divergence free) and } S^a{}_{,a} = 0 \text{ (divergence free)}. \end{aligned}$$

In this chapter, we decompose perturbations of the Ashtekar variables for the tensor, vector and scalar parts and relate them with the functions $\phi, \psi, B, E, S_a, F_a$ and h_{ab}. This way we will have a relation with the standard (metric) theory of cosmological perturbations.

4.2 Matter field

The scalar field Hamiltonian is a sum of the scalar constraint $S_\varphi[N]$ and diffeomorphism constraint $D_\varphi[N^a]$:

$$H_\varphi[N, N^a] = S_\varphi[N] + D_\varphi[N^a], \tag{4.14}$$

where

$$S_\varphi[N] = \int_\Sigma d^3x N \left(\frac{1}{2}\frac{\pi^2}{\sqrt{|\det E|}} + \frac{1}{2}\frac{E^a_i E^b_i \partial_a\varphi\partial_b\varphi}{\sqrt{|\det E|}} + \sqrt{|\det E|}V(\varphi) \right), \tag{4.15}$$

$$D_\varphi[N^a] = \int_\Sigma d^3x N^a \pi(\partial_a\varphi). \tag{4.16}$$

The scalar constraint can be expanded as follows

$$S_\varphi[N] = S_\varphi[\bar{N}] + S_\varphi[\delta N],$$

where

$$\begin{aligned} S_\varphi[\bar{N}] &= \int_\Sigma d^3x \bar{N} \left[\left(C^{(0)}_\pi + C^{(0)}_\varphi\right) + \left(C^{(2)}_\pi + C^{(2)}_\nabla + C^{(2)}_\varphi\right) \right], \\ S_\varphi[\delta N] &= \int_\Sigma d^3\delta N \left[C^{(1)}_\pi + C^{(1)}_\varphi \right]. \end{aligned}$$

Here

$$
\begin{aligned}
C_\pi^{(0)} &= \frac{\bar\pi^2}{2\bar p^{3/2}},\\
C_\varphi^{(0)} &= \bar p^{3/2} V(\bar\varphi),\\
C_\pi^{(1)} &= \frac{\bar\pi\delta\pi}{\bar p^{3/2}} - \frac{\bar\pi^2}{2\bar p^{3/2}}\frac{\delta_c^j\delta E_j^c}{2\bar p},\\
C_\varphi^{(1)} &= \bar p^{3/2}\left[V_{,\varphi}(\bar\varphi)\delta\varphi + V(\bar\varphi)\frac{\delta_c^j\delta E_j^c}{2\bar p}\right],\\
C_\pi^{(2)} &= \frac{1}{2}\frac{\delta\pi^2}{\bar p^{3/2}} - \frac{\bar\pi\delta\pi}{\bar p^{3/2}}\frac{\delta_c^j\delta E_j^c}{2\bar p} + \frac{1}{2}\frac{\bar\pi^2}{\bar p^{3/2}}\left[\frac{(\delta_c^j\delta E_j^c)^2}{8\bar p^2} + \frac{\delta_c^k\delta_d^j\delta E_j^c\delta E_k^d}{4\bar p^2}\right],\\
C_\nabla^{(2)} &= \frac{1}{2}\sqrt{\bar p}\delta^{ab}\partial_a\delta\varphi\partial_b\delta\varphi,\\
C_\varphi^{(2)} &= \frac{1}{2}\bar p^{3/2}V_{,\varphi\varphi}(\bar\varphi)\delta\varphi^2 + \bar p^{3/2}V_{,\varphi}(\bar\varphi)\delta\varphi\frac{\delta_c^j\delta E_j^c}{2\bar p}\\
&+ \bar p^{3/2}V(\bar\varphi)\left[\frac{(\delta_c^j\delta E_j^c)^2}{8\bar p^2} - \frac{\delta_c^k\delta_d^j\delta E_j^c\delta E_k^d}{4\bar p^2}\right].
\end{aligned}
$$

The perturbed diffeomorphism constraint is given by

$$
D_\varphi[N^a] = \int_\Sigma d^3x\delta N^a\bar\pi(\partial_a\delta\varphi), \tag{4.17}
$$

where we used the fact that for the flat FRW background $\bar N^a = 0$.

4.3 Scalar constraint

We start considerations of the gravity sector we from the scalar constraint:

$$
S[N] = \frac{1}{16\pi G}\int_\Sigma d^3x NC = \frac{1}{16\pi G}\int_\Sigma d^3x N\frac{E_i^aE_j^b}{\sqrt{|\det E|}}\left[\varepsilon^{ij}{}_kF_{ab}^k - 2(1+\gamma^2)K_{[a}^iK_{b]}^j\right]. \tag{4.18}
$$

Before we perturbatively expand this constraint, we firstly decompose C for two parts, where one is independent on the parameter γ. For this purpose, let us express curvature of the Ashtekar connection as follows

$$
\begin{aligned}
F_{ab}^i &= \partial_aA_b^i - \partial_bA_a^i + \varepsilon^i{}_{jk}A_a^jA_b^k\\
&= \gamma(\partial_aK_b^i - \partial_bK_a^i) + \partial_a\Gamma_b^i - \partial_b\Gamma_a^i + \varepsilon^i{}_{jk}(\Gamma_a^j + \gamma K_a^j)(\Gamma_b^k + \gamma K_b^k)\\
&= \gamma(\partial_aK_b^i - \partial_bK_a^i) + (\partial_a\Gamma_b^i - \partial_b\Gamma_a^i) + \varepsilon^i{}_{jk}\Gamma_a^j\Gamma_b^k + \gamma^2\varepsilon^i{}_{jk}K_a^jK_b^k\\
&+ \gamma\left(\varepsilon^i{}_{jk}\Gamma_a^jK_b^k + \varepsilon^i{}_{jk}K_a^j\Gamma_b^k\right).
\end{aligned} \tag{4.19}
$$

Applying this expression to (4.18) and using

$$E^a_i E^b_j \varepsilon^{ij}{}_k \gamma(\partial_a K^k_b - \partial_b K^k_a) = 2\gamma E^a_i E^b_j \varepsilon^{ij}{}_k \partial_a K^k_b, \tag{4.20}$$

$$E^a_i E^b_j \varepsilon^{ij}{}_k (\partial_a \Gamma^k_b - \partial_b \Gamma^k_a) = 2E^a_i E^b_j \varepsilon^{ij}{}_k \partial_a \Gamma^k_b, \tag{4.21}$$

$$E^a_i E^b_j \varepsilon^{ij}{}_k \gamma \left(\varepsilon^k{}_{lm} \Gamma^l_a K^m_b + \varepsilon^k{}_{lm} K^j_a l \Gamma^m_b\right) = 2\gamma E^a_i E^b_j \varepsilon^{ij}{}_k \varepsilon^k{}_{lm} \Gamma^l_a K^m_b, \tag{4.22}$$

together with

$$2K^i_{[a} K^j_{b]} = \varepsilon^{ij}{}_k \varepsilon^k{}_{lm} K^l_a K^m_b, \tag{4.23}$$

we obtain

$$C = \frac{E^a_i E^b_j}{\sqrt{|\det E|}} \varepsilon^{ij}{}_k \left[2\partial_a \Gamma^k_b + \varepsilon^k{}_{lm} \left(\Gamma^l_a \Gamma^m_b - K^l_a K^m_b\right)\right] + C_\gamma \tag{4.24}$$

where

$$C_\gamma = 2\gamma \frac{E^a_i E^b_j}{\sqrt{|\det E|}} \varepsilon^{ij}{}_k \left(\partial_a K^k_b + \varepsilon^k{}_{lm} \Gamma^l_a K^m_b\right). \tag{4.25}$$

We will now show that the C_γ contribution is vanishing. The covariant derivative D_a is defined as follows $D_a X^k_b := \partial_a X^k_b + \varepsilon^k{}_{lm} \Gamma^l_a X^m_b$. Therefore, the S_γ term can be written in the form

$$C_\gamma = 2\gamma \frac{E^a_i E^b_j}{\sqrt{|\det E|}} \varepsilon^{ij}{}_k D_a K^k_b = 2\gamma \frac{E^a_i}{\sqrt{|\det E|}} D_a G^i, \tag{4.26}$$

$G^i = \varepsilon^{ij}{}_k E^b_j K^k_b \approx 0$ is the Gauss constraint. Therefore, by fulfilling the Gauss constraint we get $C_\gamma = 0$, so only the first part of equation (4.24) remains.

4.3.1 Perturbations of C

In order to simplify the calculations, it is useful to decompose the remaining part of the scalar constraint into three parts:

$$C = C_A + C_B + C_C, \tag{4.27}$$

where

$$C_A = 2\varepsilon^{ij}{}_k \frac{E^a_i E^b_j}{\sqrt{|\det E|}} \partial_a \Gamma^k_b, \tag{4.28}$$

$$C_B = \varepsilon^{ij}{}_k \frac{E^a_i E^b_j}{\sqrt{|\det E|}} \varepsilon^k{}_{lm} \Gamma^l_a \Gamma^m_b, \tag{4.29}$$

$$C_C = -\varepsilon^{ij}{}_k \frac{E^a_i E^b_j}{\sqrt{|\det E|}} \varepsilon^k{}_{lm} K^l_a K^m_b. \tag{4.30}$$

$$\tag{4.31}$$

By applying results of Appendix 11.2 we have

$$\frac{1}{\sqrt{|\det E|}} = X^{(0)} + X^{(1)} + X^{(2)} + \ldots, \tag{4.32}$$

where

$$\begin{aligned} X^{(0)} &= \frac{1}{\bar{p}^{3/2}}, & (4.33)\\ X^{(1)} &= -\frac{1}{2\bar{p}^{5/2}}\delta^i_a \delta E^a_i, & (4.34)\\ X^{(2)} &= \frac{1}{4\bar{p}^{7/2}}\delta^i_a \delta E^a_j \delta^j_b \delta E^b_i + \frac{1}{8\bar{p}^{7/2}}\delta^i_a \delta E^a_i \delta^j_b \delta E^b_j. & (4.35) \end{aligned}$$

In turn, the $E^a_i E^b_j$ term can be expanded as follows

$$\begin{aligned} E^a_i E^b_j &= (\bar{E}^a_i + \delta E^a_i)(\bar{E}^b_j + \delta E^b_j)\\ &= \bar{E}^a_i \bar{E}^b_j + \bar{E}^a_i \delta E^b_j + \bar{E}^b_j \delta E^a_i + \delta E^a_i \delta E^b_j\\ &= \bar{p}^2 \delta^a_i \delta^b_j + \bar{p}\left(\delta^a_i \delta E^b_j + \delta^b_j \delta E^a_i\right) + \delta E^a_i \delta E^b_j. \end{aligned} \tag{4.36}$$

Based on the above expansions, we find that:

$$\begin{aligned} C^{(0)}_A &= 0, & (4.37)\\ C^{(1)}_A &= 2\varepsilon^{ij}{}_k X^{(0)} \bar{E}^a_i \bar{E}^b_j \partial_a \delta\Gamma^k_b = 2\varepsilon^{ij}{}_k \frac{1}{\bar{p}^{3/2}} \bar{p}^2 \delta^a_i \delta^b_j \partial_a \delta\Gamma^k_b\\ &= 2\sqrt{\bar{p}}\varepsilon^{ab}{}_k \partial_a \delta\Gamma^k_b, & (4.38)\\ C^{(2)}_A &= 2\varepsilon^{ij}{}_k X^{(1)} \bar{E}^a_i \bar{E}^b_j \partial_a \delta\Gamma^k_b + 2\varepsilon^{ij}{}_k X^{(0)} (\bar{E}^a_i \delta E^b_j + \bar{E}^b_j \delta E^a_i)\partial_a \delta\Gamma^k_b\\ &= 2\varepsilon^{ij}{}_k \left(-\frac{1}{2\bar{p}^{5/2}}\delta^l_c \delta E^c_l\right) \bar{p}^2 \delta^a_i \delta^b_j \partial_a \delta\Gamma^k_b + 2\varepsilon^{ij}{}_k \frac{1}{\bar{p}^{3/2}} \bar{p}(\delta^a_i \delta E^b_j + \delta^b_j \delta E^a_i)\partial_a \delta\Gamma^k_b\\ &= -\frac{1}{\sqrt{\bar{p}}}\varepsilon^{ij}{}_k \delta^l_c \delta E^c_l \delta^a_i \delta^b_j \partial_a \delta\Gamma^k_b + \frac{1}{\sqrt{\bar{p}}}\varepsilon^{ij}{}_k (\delta^a_i \delta E^b_j + \delta^b_j \delta E^a_i)\partial_a \delta\Gamma^k_b. & (4.39) \end{aligned}$$

Analogously, for the C_B term:

$$\begin{aligned} C^{(0)}_B &= 0, & (4.40)\\ C^{(1)}_B &= 0, & (4.41)\\ C^{(2)}_B &= \varepsilon^{ij}{}_k X^{(0)} \bar{E}^a_i \bar{E}^b_j \varepsilon^k{}_{lm} \delta\Gamma^l_a \delta\Gamma^m_b\\ &= \varepsilon^{ij}{}_k \frac{1}{\bar{p}^{3/2}} \bar{p}^2 \delta^a_i \delta^b_j \varepsilon^k{}_{lm} \delta\Gamma^l_a \delta\Gamma^m_b\\ &= \sqrt{\bar{p}}\varepsilon^{ab}{}_k \varepsilon^k{}_{lm} \delta\Gamma^l_a \delta\Gamma^m_b. & (4.42) \end{aligned}$$

The C_C contribution is the most complicated one. In order to simplify the calculations we define

$$C_C = -\varepsilon^{ij}{}_k \varepsilon^k{}_{lm} \underbrace{\frac{1}{\sqrt{|\det E|}}}_{:=X} \underbrace{E^a_i E^b_j}_{:=Y} \underbrace{K^l_a K^m_b}_{:=Z}. \tag{4.43}$$

The lowest order term can be therefore written as

$$\begin{aligned} C_C^{(0)} &= -\varepsilon^{ij}{}_k \varepsilon^k{}_{lm} X^{(0)} Y^{(0)} Z^{(0)} \\ &= -\varepsilon^{ij}{}_k \varepsilon^k{}_{lm} \frac{1}{\bar{p}^{3/2}} \bar{p}^2 \delta^a_i \delta^b_j \bar{k}^2 \delta^l_a \delta^m_b \\ &= -\varepsilon^{ab}{}_k \varepsilon^k{}_{ab} \sqrt{\bar{p}} \bar{k}^2 \\ &= -(\delta^a_a \delta^b_b - \delta^a_b \delta^b_a) \sqrt{\bar{p}} \bar{k}^2 \\ &= -6\sqrt{\bar{p}} \bar{k}^2. \end{aligned} \tag{4.44}$$

The first order term is given by

$$\begin{aligned} C_C^{(1)} &= -\varepsilon^{ij}{}_k \varepsilon^k{}_{lm} \left(X^{(1)} Y^{(0)} Z^{(0)} + X^{(0)} Y^{(1)} Z^{(0)} + X^{(0)} Y^{(0)} Z^{(1)} \right) \\ &= -\frac{\bar{k}^2}{\sqrt{\bar{p}}} \delta^i_a \delta E^a_i - 4\sqrt{\bar{p}} \bar{k} \delta^a_i \delta K^i_a. \end{aligned} \tag{4.45}$$

The second order term corresponds to

$$\begin{aligned} C_C^{(2)} &= -\varepsilon^{ij}{}_k \varepsilon^k{}_{lm} \left(X^{(1)} Y^{(1)} Z^{(0)} + X^{(1)} Y^{(0)} Z^{(1)} + X^{(0)} Y^{(1)} Z^{(1)} \right. \\ &+ \left. X^{(2)} Y^{(0)} Z^{(0)} + X^{(0)} Y^{(2)} Z^{(0)} + X^{(0)} Y^{(0)} Z^{(2)} \right) \\ &= \frac{\bar{k}^2}{4\bar{p}^{3/2}} (\delta^i_a \delta E^a_i)^2 - \frac{2\bar{k}}{\sqrt{\bar{p}}} \delta E^a_i \delta K^i_a - \frac{\bar{k}^2}{2\bar{p}^{3/2}} \delta^i_a \delta E^a_j \delta^j_b \delta E^b_i \\ &- \sqrt{\bar{p}} (\delta^a_i \delta K^i_a)^2 + \sqrt{\bar{p}} \delta K^i_a \delta^b_i \delta K^j_b \delta^a_j. \end{aligned} \tag{4.46}$$

4.3.2 Collecting all together

Right now one can collect together all terms in the perturbative expansion

$$C = C^{(0)} + C^{(1)} + C^{(2)}, \tag{4.47}$$

where

$$C^{(0)} = C_A^{(0)} + C_B^{(0)} + C_C^{(0)}, \tag{4.48}$$

$$C^{(1)} = C_A^{(1)} + C_B^{(1)} + C_C^{(1)}, \tag{4.49}$$

$$C^{(2)} = C_A^{(2)} + C_B^{(2)} + C_C^{(2)}. \tag{4.50}$$

$$\tag{4.51}$$

Combining all terms we find

$$C^{(0)} = -6\sqrt{\bar{p}}\bar{k}^2, \tag{4.52}$$

$$C^{(1)} = -4\sqrt{\bar{p}}\bar{k}\delta^a_i\delta K^i_a - \frac{\bar{k}^2}{\sqrt{\bar{p}}}\delta^i_a\delta E^a_i + 2\sqrt{\bar{p}}\varepsilon^{ab}{}_k\partial_a\delta\Gamma^k_b, \tag{4.53}$$

$$\begin{aligned} C^{(2)} &= -\frac{1}{\sqrt{\bar{p}}}\varepsilon^{ij}{}_k\delta^l_c\delta E^c_l\delta^a_i\delta^b_j\partial_a\delta\Gamma^k_b + \frac{1}{\sqrt{\bar{p}}}\varepsilon^{ij}{}_k(\delta^a_i\delta E^b_j + \delta^b_j\delta E^a_i)\partial_a\delta\Gamma^k_b \\ &+ \sqrt{\bar{p}}\varepsilon^{ab}{}_k\varepsilon^k{}_{lm}\delta\Gamma^l_a\delta\Gamma^m_b + \frac{\bar{k}^2}{4\bar{p}^{3/2}}(\delta^i_a\delta E^a_i)^2 - \frac{2\bar{k}}{\sqrt{\bar{p}}}\delta E^a_i\delta K^i_a - \frac{\bar{k}^2}{2\bar{p}^{3/2}}\delta^i_a\delta E^a_j\delta^j_b\delta E^b_i \\ &- \sqrt{\bar{p}}(\delta^a_i\delta K^i_a)^2 + \sqrt{\bar{p}}\delta K^i_a\delta^b_i\delta K^j_b\delta^a_j. \end{aligned} \tag{4.54}$$

The $\delta\Gamma^i_a$ can be expressed in terms of δE^a_i based on relation [32]

$$\Gamma^i_a = -\frac{1}{2}\epsilon^{ijk}E^b_j\left(\partial_a E^k_b - \partial_b E^k_a + E^c_k E^l_a\partial_c E^l_b - E^k_a\frac{\partial_b \det E}{\det E}\right). \tag{4.55}$$

However, the functional form is depended on a particular type of perturbations. Therefore, we derive it separately for the three considered types of perturbations.

4.4 Diffeomorphism constraint

The gravitational diffeomorphism constraint is defined as follows

$$D_G[N^a] = \frac{1}{8\pi G\gamma}\int_\Sigma d^3x N^a\left[F^i_{ab}E^b_i - A^i_a G_i\right], \tag{4.56}$$

where $G_i = \partial_a E^a_i + \epsilon_{ij}{}^k A^j_a E^a_k$ is a Gauss constraint. If the Gauss constraint is fulfilled, the diffeomorphism constraint can be expanded as follows

$$D_G[N^a] = \frac{1}{8\pi G\gamma}\int_\Sigma d^3x\delta N^a\left[\delta F^i_{ab}\bar{E}^b_i + \bar{F}^i_{ab}\delta E^b_i\right]. \tag{4.57}$$

4.5 Tensor perturbations

For the tensor perturbations, the ADM variables are expressed as follows:

$$N = a = \sqrt{\bar{p}}, \tag{4.58}$$

$$N^a = 0, \tag{4.59}$$

$$q_{ab} = a^2(\delta_{ab} + h_{ab}), \tag{4.60}$$

where $\partial^a h_{ab} = 0 = \delta^{ab}h_{ab}$. Moreover, the perturbative expansion of the tensor modes is valid only if $|h_{ab}| \ll 1$. The h_{ab} is a symmetric tensor, where $a, b = 1, 2, 3$. Therefore, h_{ab}

has 6 independent components. Furthermore, three constraints are imposed by $\partial^a h_{ab} = 0$ and one by $\delta^{ab} h_{ab} = 0$. Taking this into account only two degrees of freedom of the perturbation h_{ab} remain. They correspond to the two possible polarization states of the gravitational waves. The tensor modes are vacuum perturbations of the gravitational field.

Based on the expression (4.60), applied to the definition (2.12), one can find an expression for the perturbation of the densitized triad

$$\delta E^a_i = -\frac{1}{2}\bar{p} h^a_i, \tag{4.61}$$

where we defined $h^a_i := \delta^{ac}\delta^b_i h_{cb}$. Taking into account the fact that for the tensor perturbations $\delta^i_a \delta E = 0$, one can show that [34]

$$\delta\Gamma^i_a = \frac{1}{\bar{p}} \epsilon^{ije}\delta_{ac}\partial_e \delta E^c_j. \tag{4.62}$$

With use of this relation, the scalar constraint for the tensor modes is

$$S[N] = \frac{1}{2\kappa}\int_\Sigma d^3x \left[\bar{N}(C^{(0)} + C^{(2)})\right], \tag{4.63}$$

where

$$C^{(0)} = -6\bar{k}^2\sqrt{\bar{p}}, \tag{4.64}$$

$$C^{(2)} = -\frac{1}{2\bar{p}^{3/2}}\bar{k}^2(\delta E^c_j \delta E^d_k \delta^k_c \delta^j_d) + \sqrt{\bar{p}}(\delta K^j_c \delta K^k_d \delta^c_k \delta^d_j) - \frac{2\bar{k}}{\sqrt{\bar{p}}}(\delta E^c_j \delta K^j_c) + \frac{1}{\bar{p}^{3/2}}(\delta_{cd}\delta^{jk}\delta^{ef}\partial_e E^c_j \partial_f E^d_k). \tag{4.65}$$

Because for the tensor modes the shift vector N^a is vanishing, the diffeomorphism constraint is identically equal zero.

4.6 Vector perturbations

For the vector perturbations the ADM variables are expressed as follows:

$$N = a, \tag{4.66}$$

$$N^a = S^a, \tag{4.67}$$

$$q_{ab} = a^2(\delta_{ab} + F_{a,b} + F_{b,a}), \tag{4.68}$$

where $F^a{}_{,a} = 0$ and $S^a{}_{,a} = 0$. Taking into account these conditions, there are 4 degrees of freedom for the vector perturbations. It is worth stressing that vector modes are not vacuum perturbations of the gravitational field. They may propagate only in presence of

vector matter. In the case where such matter is absent, the vector perturbations are pure gauge fields.

Based on the formula (4.55) one can show that, for the vector perturbations [33]

$$\delta\Gamma^i_a = \frac{1}{\bar{p}}\epsilon^{ije}\delta_{ac}\partial_e\delta E^c_j. \tag{4.69}$$

Taking this into account, the perturbed scalar constraint for the vector modes takes the following form

$$S[N] = \frac{1}{2\kappa}\int_\Sigma d^3x\left[\bar{N}(C^{(0)} + C^{(2)})\right], \tag{4.70}$$

where

$$C^{(0)} = -6\bar{k}^2\sqrt{\bar{p}}, \tag{4.71}$$

$$C^{(2)} = -\frac{1}{2\bar{p}^{3/2}}\bar{k}^2(\delta E^c_j\delta E^d_k\delta^k_c\delta^j_d) + \sqrt{\bar{p}}(\delta K^j_c\delta K^k_d\delta^c_k\delta^d_j) - \frac{2\bar{k}}{\sqrt{\bar{p}}}(\delta E^c_j\delta K^j_c). \tag{4.72}$$

Perturbed diffeomorphism constraint for the vector modes is given by

$$D_G[N^a] = \frac{1}{8\pi G}\int_\Sigma d^3x\delta N^c\left[-\bar{p}(\partial_k\delta K^k_c) - \bar{k}\delta^k_c(\partial_d\delta E^d_k)\right] \tag{4.73}$$

4.7 Scalar perturbations

For the tensor perturbations the ADM variables are expressed as follows:

$$N = a\sqrt{1+2\phi}, \tag{4.74}$$

$$N^a = \partial^a B, \tag{4.75}$$

$$q_{ab} = a^2(\delta_{ab} - 2\psi\delta_{ab} + \partial_a\partial_b E). \tag{4.76}$$

So, there are four perturbative variables (ϕ, ψ, E, B). These variables, as in case of the vector perturbations, are pure gauge fields in absence of matter.

For the scalar modes, the lapse function is a subject of perturbation. Performing the perturbative expansion of (4.74) we find

$$N = \bar{N} + \delta N = a(1+\phi), \tag{4.77}$$

where we have neglected the higher order terms in ϕ.

Based on the formula (4.55) one can show that, for the scalar perturbations [32]

$$\delta\Gamma^i_a = \frac{1}{2\bar{p}}\epsilon^{ij}{}_a\partial_b\delta E^b_j. \tag{4.78}$$

Taking this into account, the perturbed scalar constraint for the scalar modes takes the following form

$$S[N] = \frac{1}{2\kappa}\int_\Sigma d^3x \left[\bar{N}(C^{(0)} + C^{(2)}) + \delta N C^{(1)}\right], \tag{4.79}$$

where

$$C^{(0)} = -6\bar{k}^2\sqrt{\bar{p}}, \tag{4.80}$$

$$C^{(1)} = -4\bar{k}\sqrt{\bar{p}}\delta^c_j\delta K^j_c - \frac{\bar{k}^2}{\sqrt{\bar{p}}}\delta^j_c\delta E^c_j + \frac{2}{\sqrt{\bar{p}}}\partial_c\partial^j\delta E^c_j, \tag{4.81}$$

$$\begin{aligned} C^{(2)} &= \sqrt{\bar{p}}\delta K^j_c\delta K^k_d\delta^c_k\delta^d_j - \sqrt{\bar{p}}(\delta K^j_c\delta^c_j)^2 - \frac{2\bar{k}}{\sqrt{\bar{p}}}\delta E^c_j\delta K^j_c \\ &- \frac{\bar{k}^2}{2\bar{p}^{3/2}}\delta E^c_j\delta E^d_k\delta^k_c\delta^j_d + \frac{\bar{k}^2}{4\bar{p}^{3/2}}(\delta E^c_j\delta^j_c)^2 - \frac{1}{2\bar{p}^{3/2}}\delta^{jk}(\partial_c\delta E^c_j)(\partial_d\delta E^d_k). \end{aligned} \tag{4.82}$$

Perturbed diffeomorphism constraint for the scalar modes is given by

$$D_G[N^a] = \frac{1}{\kappa}\int_\Sigma d^3x\delta N^c\left[\bar{p}\partial_c(\delta^k_d\delta K^k_d) - \bar{p}(\partial_k\delta^k_c) - \bar{k}\delta^k_c\delta^k_c(\partial_d\delta E^d_k)\right]. \tag{4.83}$$

Chapter 5

Quantum origin of cosmic structures

Gravitation and matter form a coupled system. Therefore, any change in distribution of matter modifies gravitational field and vice versa. Under some conditions, this mutual interaction of matter and gravity can be studied perturbatively. This interaction takes, in general, very complex form. In particular, while the scalar perturbations are considered.

Before we face the challenge to describe this interaction in details, let us gain some experience by considering a bit simpler case. This will also be an occasion to introduce all necessary tools to study quantum generation of cosmic structures and understand the idea behind this mechanism.

The simplification we assume is that the gravitational part is homogeneous. Only perturbations of the matter sector are considered. We focus on scalar field matter. Investigation of the systems of this kind (fields on the gravitational backgrounds) is a domain of the field theory on curved spaces [49]. In this chapter, we will perform quantization of the scalar field on the FRW background. We will introduce a concept of the power spectrum, which is crucial from the perspective of further consideration. We will compute power spectra of the scalar field for some cosmological evolutions appearing LQC.

5.1 The model

Hamiltonian of the model is the following sum

$$H_{tot} = \bar{H}_G^{(\bar{\mu})}[N] + H_\varphi[N], \tag{5.1}$$

where the homogeneous gravity Hamiltonian

$$\bar{H}_G^{(\bar{\mu})}[N] = -\frac{3NV_0}{\kappa}\sqrt{\bar{p}}\left(\frac{\sin(\bar{\mu}\gamma\bar{k})}{\bar{\mu}\gamma}\right)^2, \tag{5.2}$$

and the scalar field Hamiltonian

$$\begin{aligned} H_\varphi[N] &= \int_{V_0} d^3x N \left(\frac{1}{2}\frac{\pi^2}{\sqrt{|\det E|}} + \frac{1}{2}\frac{E_i^a E_i^b \partial_a\varphi\partial_b\varphi}{\sqrt{|\det E|}} + \sqrt{|\det E|}V(\varphi) \right) \\ &= \int_{V_0} d^3x N \left(\frac{1}{2}\frac{\pi^2}{\bar{p}^{3/2}} + \frac{1}{2}\bar{p}^{1/2}\delta^{ab}\partial_a\varphi\partial_b\varphi + \bar{p}^{3/2}V(\varphi) \right). \end{aligned} \tag{5.3}$$

The scalar field can be decomposed for homogeneous and perturbation parts

$$\varphi = \bar{\varphi} + \delta\varphi \;\; \pi = \bar{\pi} + \delta\pi, \tag{5.4}$$

where the homogeneous parts are

$$\bar{\varphi}(t) = \frac{1}{V_0}\int_{V_0} d^3x\varphi(\mathbf{x}, t), \tag{5.5}$$

$$\bar{\pi}(t) = \frac{1}{V_0}\int_{V_0} d^3x\pi(\mathbf{x}, t). \tag{5.6}$$

Equations of motion for the background and perturbation parts are given by

$$\dot{\bar{\varphi}} = \{\bar{\varphi}, H_{tot}\} = \bar{N}\bar{p}^{-3/2}\bar{\pi}, \tag{5.7}$$

$$\dot{\bar{\pi}} = \{\bar{\pi}, H_{tot}\} = -\bar{N}\bar{p}^{3/2}\frac{dV(\bar{\varphi})}{d\bar{\varphi}}, \tag{5.8}$$

$$\delta\dot{\varphi} = \{\delta\varphi, H_{tot}\} = \bar{N}\bar{p}^{-3/2}\delta\pi_\varphi, \tag{5.9}$$

$$\delta\dot{\pi}_\varphi = \{\delta\pi_\varphi, H_{tot}\} = \bar{N}\left(\sqrt{\bar{p}}\nabla^2\delta\varphi - \bar{p}^{3/2}\frac{d^2V(\bar{\varphi})}{d\bar{\varphi}^2}\delta\varphi \right). \tag{5.10}$$

It is convenient work in the conformal time η, so we set $\bar{N} = \sqrt{\bar{p}}$. Combining equations (5.7) and (5.8) we obtain equation

$$\ddot{\bar{\varphi}} + \frac{\dot{\bar{p}}}{\bar{p}}\dot{\bar{\varphi}} + \bar{p}\frac{dV(\bar{\varphi})}{d\bar{\varphi}} = 0. \tag{5.11}$$

The variable $\delta\varphi$ can be decomposed for the Fourier modes

$$\delta\varphi(\eta, \mathbf{x}) \equiv \frac{u(\eta, \mathbf{x})}{\sqrt{\bar{p}}} = \int \frac{d^3k}{(2\pi)^{3/2}}\frac{u_{\mathbf{k}}(\eta)}{\sqrt{\bar{p}}}e^{i\mathbf{k}\cdot\mathbf{x}}. \tag{5.12}$$

Based on this decomposition and on the equations (5.9) and (5.10) we obtain equation

$$\frac{d^2}{d\eta^2}u_{\mathbf{k}}(\eta) + [k^2 + m_{eff}^2]u_{\mathbf{k}}(\eta) = 0, \tag{5.13}$$

where $k^2 = \mathbf{k}\cdot\mathbf{k}$ and

$$m_{eff}^2 = \bar{p}\frac{d^2V(\bar{\varphi})}{d\bar{\varphi}^2} - \frac{1}{\sqrt{\bar{p}}}\frac{d^2\sqrt{\bar{p}}}{d\eta^2}. \tag{5.14}$$

5.2 Quantization

In our considerations, quantization of the scalar field $u(\eta, \mathbf{x})$ follows the canonical procedure. The Fourier components $u_{\mathbf{k}}(\eta)$ are promoted to be operators, and are decomposed for the creation and annihilation operators as follows:

$$\hat{u}_{\mathbf{k}}(\eta) = f_k(\eta)\hat{b}_{\mathbf{k}} + f_k^*(\eta)\hat{b}^\dagger_{-\mathbf{k}}, \tag{5.15}$$

where $f_k(\eta)$ is the so-called mode function which satisfies the same equation as $u_{\mathbf{k}}(\eta)$. The creation ($\hat{b}^\dagger_{\mathbf{k}}$) and annihilation ($\hat{b}_{\mathbf{k}}$) operators fulfill the commutation relations $[\hat{b}_{\mathbf{k}}, \hat{b}^\dagger_{\mathbf{q}}] = \delta^{(3)}(\mathbf{k} - \mathbf{q})$ and $[\hat{b}_{\mathbf{k}}, \hat{b}_{\mathbf{q}}] = 0 = [\hat{b}^\dagger_{\mathbf{k}}, \hat{b}^\dagger_{\mathbf{q}}]$.

By applying decomposition (5.15), the field operator $\hat{u}(\eta, \mathbf{x})$ takes the form

$$\hat{u}(\eta, \mathbf{x}) = \int \frac{d^3k}{(2\pi)^{3/2}} \left[f_k(\eta)\hat{b}_{\mathbf{k}} e^{i\mathbf{k}\cdot\mathbf{x}} + f_k^*(\eta)\hat{b}^\dagger_{\mathbf{k}} e^{-i\mathbf{k}\cdot\mathbf{x}} \right]. \tag{5.16}$$

5.3 Power spectrum

Quantum fluctuations of the field $\hat{u}(\mathbf{x}, \eta)$ in some state $|\Psi\rangle$ can be characterized by n-point correlation function

$$\langle\Psi|\hat{u}(\mathbf{x}_1, \eta)\hat{u}(\mathbf{x}_2, \eta)\ldots\hat{u}(\mathbf{x}_n, \eta)|\Psi\rangle. \tag{5.17}$$

In the special case of Gaussian fields, all the statistical properties of the quantum fluctuations are contained in a two-point function

$$\langle\Psi|\hat{u}(\mathbf{x}_1, \eta)\hat{u}(\mathbf{x}_2, \eta)|\Psi\rangle, \tag{5.18}$$

and the odd n-point correlation functions are vanishing. This is an analogue of the result known from statistics where, for the Gaussian distribution, all higher moments can be expressed in terms of variance.

The Gaussian fields are of great importance in cosmology. The Gaussianity is a feature resulting from the lack of self-interaction of a given field. However, when different modes of perturbations are interacting one another then the field becomes non-Gaussian. This interaction can be produced by the potential of the scalar field, higher order corrections in the perturbative expansion or possibly by some quantum gravitational effects. In order to describe the non-Gaussian effects it is necessary to consider higher order correlation functions. The first contribution of non-linearity comes in tree-point function

$$\langle\Psi|u_{\mathbf{k}_1}u_{\mathbf{k}_2}u_{\mathbf{k}_3}|\Psi\rangle = \delta^{(3)}(\mathbf{k_1} + \mathbf{k_2} + \mathbf{k_3})P_3(\mathbf{k_1}, \mathbf{k_2}, \mathbf{k_3}), \tag{5.19}$$

where $P_3(\mathbf{k_1}, \mathbf{k_2}, \mathbf{k_3})$ is called bispectrum. In case of the Gaussian field, this spectrum is equal to zero.

The primordial non-Gaussianity, if present, could affect also the spectrum of the CMB anisotropies leading to its non-Gaussianity. However, present observations have not indicated any deviation from Gaussianity of the CMB [8]. This supports the inflationary

model with the massive potential studied in Chapter 3. This is the only possible potential for which there is no self-interaction. It is worth noticing, that the current constraints on the non-Gaussianity of the CMB may serve as a possible method of constraining some quantum cosmological models. However, all the models considered in this thesis do not lead to non-Gaussianity. This is because of two reasons. Firstly, we consider only models with free or massive scalar field. Secondly, we consider theory of cosmological perturbations only at the the linear level. Taking into considerations the higher order terms in the perturbative expansion would lead to some non-Gaussian features. Investigation of this interesting subject is behind the scope of this thesis.

According to our current understanding, the primordial seeds of all structures in the Universe were quantum vacuum fluctuations of the inflationary scalar field. Therefore, since we are going to study the vacuum fluctuations, we choose the sate $|\Psi\rangle$ to be a vacuum sate $|0\rangle$. Moreover, since our field is Gaussian at the considered perturbative level, we will focus only at the two-point function (correlator) $\langle 0|\hat{u}(\mathbf{x},\eta)\hat{u}(\mathbf{y},\eta)|0\rangle$. By applying the Fourier decomposition (5.16) of the field $\hat{u}(\mathbf{x},\eta)$ we find

$$\begin{aligned}
\langle 0|\hat{u}(\mathbf{x},\eta)\hat{u}(\mathbf{y},\eta)|0\rangle &= \langle 0|\int \frac{d^3k d^3q}{(2\pi)^3}\left[f_k(\eta)\hat{b}_{\mathbf{k}}e^{i\mathbf{k}\cdot\mathbf{x}} + f_k^*(\eta)\hat{b}_{\mathbf{k}}^\dagger e^{-i\mathbf{k}\cdot\mathbf{x}}\right]\times \\
&\times \left[f_q(\eta)\hat{b}_{\mathbf{q}}e^{i\mathbf{q}\cdot\mathbf{y}} + f_q^*(\eta)\hat{b}_{\mathbf{q}}^\dagger e^{-i\mathbf{q}\cdot\mathbf{y}}\right]|0\rangle \\
&= \int \frac{d^3k d^3q}{(2\pi)^3} f_k(\eta)f_q^*(\eta)e^{i\mathbf{k}\cdot\mathbf{x}}e^{-i\mathbf{q}\cdot\mathbf{y}}\underbrace{\langle 0|\hat{b}_{\mathbf{k}}\hat{b}_{\mathbf{q}}^\dagger|0\rangle}_{=\delta^{(3)}(\mathbf{k}-\mathbf{q})} \\
&= \int \frac{d^3k}{(2\pi)^3}|f_k(\eta)|^2 e^{i\mathbf{k}\cdot(\mathbf{x}-\mathbf{y})} \\
&= \int_0^\infty \frac{dk}{k}\mathcal{P}_u(k,\eta)\frac{\sin kr}{kr},
\end{aligned} \tag{5.20}$$

where $r = |\mathbf{x}-\mathbf{y}|$ and the *power spectrum* $\mathcal{P}_u(k,\eta)$ is defined as follows

$$\mathcal{P}_u(k,\eta) \equiv \frac{k^3}{2\pi^2}|f_k(\eta)|^2. \tag{5.21}$$

The power spectrum (5.21) is the most important quantity describing primordial perturbations. Much of the subsequent considerations will be focused on determination of this function.

As an example, let us compute the power spectrum (5.21) for the case of a free field in Minkowski space. In this case, the mode functions are $f_k = e^{-i\eta k}/\sqrt{2k}$, therefore

$$\mathcal{P}_u(k) = \left(\frac{k}{2\pi}\right)^2. \tag{5.22}$$

This spectrum is of great importance because it serves as a reference while considering more sophisticated examples. For any considered case, at sufficiently short distances,

the Minkowski space should serve as a good approximation. Therefore, the spectrum (5.22) should be, in general, recovered in the limit $k \to \infty$. Of course, only if the Lorentz symmetry is conserved at the very short distances.

The two-point corresponding correlation function corresponding to spectrum (5.22) is

$$\langle 0|\hat{u}(\mathbf{x},\eta)\hat{u}(\mathbf{y},\eta)|0\rangle = \frac{1}{4\pi^2}\frac{1}{r}\int_0^\infty dk \sin(kr) = \frac{1}{4\pi^2}\frac{1}{|\mathbf{x}-\mathbf{y}|}, \tag{5.23}$$

where the integration was performed by introducing regularizator $e^{-\epsilon k r}$ and performing the limit $\epsilon \to 0$. This correlation function diverges while $|\mathbf{x}-\mathbf{y}| \to 0$. It is however expected that the correlation function is modified at the Planck scale due to the quantum gravity effects. Such effects may remove singularity from the correlation function [50].

5.4 Bogoliubov transformation

In the Schrödinger picture of a field theory one usually consider transition between some $|\text{in}\rangle$ and $|\text{out}\rangle$ states. In the Heisenberg picture the state remains unchanged (in our case the vacuum state $|0\rangle$) however the field operators evolve. In particular, evolution of $\hat{u}(\mathbf{x},\eta)$ is given by the time dependent mode functions $f_k(\eta)$.

Let our system evolve from the initial time η_{in} to the the final time η_{out}. At the time η_{in} the field operator can be decomposed as follows

$$\hat{u}_{\mathbf{k}}(\eta) = g_k(\eta)\hat{a}_{\mathbf{k}} + g_k^*(\eta)\hat{a}^\dagger_{-\mathbf{k}}. \tag{5.24}$$

Where $g_k(\eta)$ are the mode functions and the creation ($\hat{a}^\dagger_{\mathbf{k}}$) and annihilation ($\hat{a}_{\mathbf{k}}$) operators fulfill the commutation relation $[\hat{a}_{\mathbf{k}}, \hat{a}^\dagger_{\mathbf{q}}] = \delta^{(3)}(\mathbf{k}-\mathbf{q})$ and $[\hat{a}_{\mathbf{k}}, \hat{a}_{\mathbf{q}}] = 0 = [\hat{a}^\dagger_{\mathbf{k}}, \hat{a}^\dagger_{\mathbf{q}}]$. The operator $\hat{a}_{\mathbf{k}}$ defines our initial vacuum state $|0_{\text{in}}\rangle$ such that $\hat{a}_{\mathbf{k}}|0_{\text{in}}\rangle = 0$. This state remains unchanged during the evolution and we call it simply $|0\rangle = |0_{\text{in}}\rangle$. At the final time η_{out} one can perform mode decomposition

$$\hat{u}_{\mathbf{k}}(\eta) = f_k(\eta)\hat{b}_{\mathbf{k}} + f_k^*(\eta)\hat{b}^\dagger_{-\mathbf{k}}, \tag{5.25}$$

where $f_k(\eta)$ is a new mode function. The creation ($\hat{b}^\dagger_{\mathbf{k}}$) and annihilation ($\hat{b}_{\mathbf{k}}$) operators fulfill the commutation relations $[\hat{b}_{\mathbf{k}}, \hat{b}^\dagger_{\mathbf{q}}] = \delta^{(3)}(\mathbf{k}-\mathbf{q})$ and $[\hat{b}_{\mathbf{k}}, \hat{b}_{\mathbf{q}}] = 0 = [\hat{b}^\dagger_{\mathbf{k}}, \hat{b}^\dagger_{\mathbf{q}}]$. The new annihilation operator $\hat{b}_{\mathbf{k}}$ can be used to define the final (true) vacuum state $|0_{\text{out}}\rangle$ such that $\hat{b}_{\mathbf{k}}|0_{\text{out}}\rangle = 0$. However, since we are working in the Heisenberg picture, the $|0_{\text{out}}\rangle$ is not the actual state of the system which is $|0_{\text{in}}\rangle$.

The mode functions at η_{out} can be related with those at η_{in} by the relation

$$f_k(\eta) = \alpha_k g_k(\eta) + \beta_k g_k^*(\eta). \tag{5.26}$$

Because decompositions (5.25) and (5.24) are equivalent, based on (Eq. 5.26) and on the Wronskian conditions for the mode functions f_k and g_k, one obtains:

$$\begin{bmatrix} \hat{b}_{\mathbf{k}} \\ \hat{b}^\dagger_{-\mathbf{k}} \end{bmatrix} = \begin{bmatrix} \alpha_k & \beta_k^* \\ \beta_k & \alpha_k^* \end{bmatrix} \begin{bmatrix} \hat{a}_{\mathbf{k}} \\ \hat{a}^\dagger_{-\mathbf{k}} \end{bmatrix}, \tag{5.27}$$

which corresponds to the Bogoliubov transformation with coefficients α_k and β_k. Due to the commutation relation of the creation and annihilation operators we have $|\alpha_k|^2 - |\beta_k|^2 = 1$. It is clear from (Eq. 5.27) that if $\beta_k \neq 0$ particles are created from the vacuum, just because $\hat{b}_{\mathbf{k}}|0\rangle = \beta_k^* \hat{a}^\dagger_{-\mathbf{k}}|0\rangle \neq 0$.

5.4.1 Symmetric bounce

As the first case we consider scalar field perturbations at the symmetric bounce. In the considered case a field is free, $V(\varphi) = 0$. We set initial conditions to be the Minkowski vacuum

$$u_{in} = \frac{e^{-ik\eta}}{\sqrt{2k}}. \tag{5.28}$$

This approximation works however only for sub-horizontal modes. With these initial conditions we solve the equation (5.13) numerically. Based on these computations we obtain the power spectrum of the field u in the post-bounce phase. We show the results in Fig. 5.1. In this figure, black straight line represents analytical approximation of the

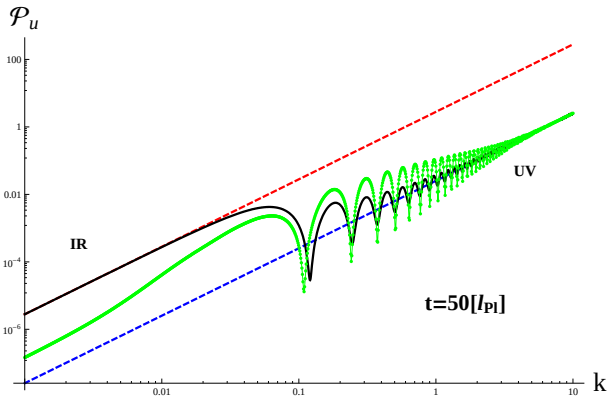

Figure 5.1: Numerical power spectrum of the field u with $\bar{\pi} = 0.1 m_{Pl}^2$ (green points). Black line represents the analytical spectrum given by Eq. 5.35 with $U_0 = 2m_{Pl}^2$ and $\eta_0 = 0.1 l_{Pl}$. Dashed lines represent UV and IR limits given by Eq. 5.36 and Eq. 5.37.

spectrum. In order to derive this approximation we assume

$$u_{out} = \frac{\alpha_k}{\sqrt{2k}} e^{-ik\eta} + \frac{\beta_k}{\sqrt{2k}} e^{ik\eta}. \tag{5.29}$$

Here the relation $|\alpha_k|^2 - |\beta_k|^2 = 1$ holds, as a consequence of the normalisation condition. Now we base on integral representation

$$u(\eta, \mathbf{k}) = u_{in}(\eta, \mathbf{k}) + \frac{1}{k} \int_{-\infty}^{\eta} d\eta' U(\eta') \sin k(\eta - \eta') u(\eta, \mathbf{k}) \tag{5.30}$$

of the Eq. 5.13 where $U(\eta) = -m_{\rm eff}^2(\eta)$. Solving this equation in the first order of perturbative expansion we compute values of α_k and β_k. We approximate the $U(\eta)$ function by the step function $U(\eta) = U_0\Theta(\eta+\eta_0)\Theta(\eta_0-\eta)$ of the width $2\eta_0$. The values of parameters U_0 and η_0 can be fixed from the numerical computation of the full model. However we expect that

$$U_0 \sim -m_{\rm eff}^2(t=0) = \frac{\kappa}{3}\left(2\bar{\pi}_\varphi \rho_c\right)^{2/3} \tag{5.31}$$

where the equality comes from the analytical expression for the $m_{\rm eff}^2$ function (See Ref. [51]). Moreover, it was shown in Ref. [51] that η_0 can be related with the value of conformal time at $H_{\rm max}$, then

$$\eta_0 = \eta(t_0) = \frac{{}_2F_1\left[\frac{1}{2},\frac{1}{6},\frac{3}{2};-1\right]}{\sqrt{3\kappa}\rho_c^{1/3}(\bar{\pi}_\varphi^2/2)^{1/6}}. \tag{5.32}$$

The value of a parameter η_0 do not have to be however precisely equal to $\eta(t_0)$. We expect rather $\eta_0 \sim \eta(t_0)$. Namely, its value can not be much bigger or much lower than $\eta(t_0)$. In Fig. 5.1 we showed the case $\bar{\pi}_\varphi = 0.1m_{\rm Pl}^2$ which was approximated by the model above with $U_0 = 2m_{\rm Pl}^2$ and $\eta_0 = 0.1l_{\rm Pl}$. Based on the values of $\eta(t_0)$ and $-m_{\rm eff}^2(t=0)$ we obtain $\eta_0 = 0.3l_{\rm Pl}$ and $U_0 = 2.5m_{\rm Pl}^2$. Better fit to numerical data is obtained when a step function is more narrow than $2\eta(t_0)$ and a bit lower than $-m_{\rm eff}^2(t=0)$.

Based on the performed step function approximation, we find

$$\alpha_k \approx 1 + \frac{i}{2k}\int_{-\infty}^{\infty} d\eta U(\eta) = 1 + i\frac{U_0\eta_0}{k}, \tag{5.33}$$

$$\beta_k \approx -\frac{i}{2k}\int_{-\infty}^{\infty} d\eta U(\eta)e^{-2ik\eta} = -i\frac{U_0}{2k^2}\sin(2k\eta_0). \tag{5.34}$$

Now with use of definition of the power spectrum we obtain analytical expression

$$\mathcal{P}_u = \left(\frac{k}{2\pi}\right)^2 + \frac{U_0\left(\sin\left[2k\eta_0\right]{}^2U_0 + 4k^2U_0\eta_0^2 + 4k\sin\left[2k\eta_0\right]\left(k\sin[2\eta k] - \cos[2\eta k]U_0\eta_0\right)\right)}{16\pi k^2} \tag{5.35}$$

which was shown in Fig. 5.1. In the UV and IR limits, the power spectrum given by Eq. 5.35 behaves like

$$\mathcal{P}_u^{\rm UV} \rightarrow \left(\frac{k}{2\pi}\right)^2, \tag{5.36}$$

$$\mathcal{P}_u^{\rm IR} \rightarrow \left(\frac{k}{2\pi}\right)^2\left(1 + 4U_0\eta_0\eta + 4U_0^2\eta_0^2\eta^2\right). \tag{5.37}$$

The term in the second bracket in Eq. 5.37 is the difference between the UV and IR slopes in Fig. 5.1.

The analytical model correctly reproduces the structure of oscillations obtained from the numerical simulations. However, the relative amplitudes of the modes are not exactly recovered. In particular, the analytical model predicts more power for the low values of k.

5.5 Bounce and inflation

Phase of symmetric bounce is a very idealized situation. More physically relevant is the joined bounce with an inflation phase. Such model was studied in Chapter 3. In this section, we will construct a simple analytical model of perturbations in this phase.

In the contracting phase, the sub-horizontal modes are given by Eq. 5.28, as previously. The subsequent phase of inflation can be approximated by de Sitter phase where evolution of the scale factor is given by $a = -\frac{1}{H_0\eta}$. In this phase, the fluctuation modes are given by superposition of Bunch-Davies modes

$$u_{out} = \frac{\alpha_k}{\sqrt{2k}} e^{-ik\eta}\left(1 - \frac{i}{k\eta}\right) + \frac{\beta_k}{\sqrt{2k}} e^{ik\eta}\left(1 + \frac{i}{k\eta}\right), \tag{5.38}$$

where a relation $|\alpha_k|^2 - |\beta_k|^2 = 1$ holds. Performing matching conditions $u_{in}(\eta_i) = u_{out}(\eta_i)$ and $u'_{in}(\eta_i) = u'_{out}(\eta_i)$ we determinate coefficients

$$\alpha_k = -\frac{1 - 2ik\eta_i - 2k^2\eta_i^2}{2k^2\eta_i^2}, \tag{5.39}$$

$$\beta_k = -\frac{e^{-2ik\eta_i}}{2k^2\eta_i^2}. \tag{5.40}$$

Based on this, we can derive the power spectrum. At the time $\eta \to 0^-$, it takes a form

$$\mathcal{P}_{\delta\varphi} = \left(\frac{H_0}{2\pi}\right)^2 + \left(\frac{H_0}{2\pi}\right)^2 \frac{k_*^4}{2k^4}\left[1 + \cos\left(\frac{2k}{k_*}\right)\left(-1 + \frac{2k^2}{k_*^2}\right) - \frac{2k}{k_*}\sin\left(\frac{2k}{k_*}\right)\right], \tag{5.41}$$

where we have defined $k_* = -1/\eta_i$. We show plot of this spectrum in Fig. 5.2.

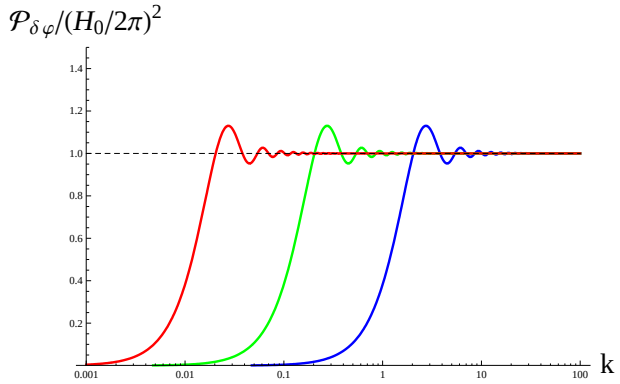

Figure 5.2: Power spectrum of the field $\delta\varphi$. Here $\eta_i = -1, -10, -100$ (from right to left).

The obtained spectrum is characterized by the suppression for the low values of k. For the large k the spectrum holds the inflationary form. Other important features are

oscillations, which are residue of the bouncing phase. We see that damping begins when $-\eta_i k \sim 1$. This corresponds to the k on the horizon scale at the time η_i. At the time η_i value of the scale factor is given by $a_i = -\frac{1}{H_0 \eta_i}$, therefore $k_* = a_i H_0$. Defining the length scale $\lambda_* = a_i/k_*$ we obtain $\lambda_* = \frac{1}{H_0}$. Today, the value of λ_* is given by $\lambda_* a_0/a_i$ where a_0 is the present value of a scale factor.

Chapter 6

Tensor perturbations

In this chapter, we study tensor perturbations (gravitational waves) with holonomy corrections. We determine power spectrum of gravitational waves for the background dynamics investigated in Chapter 3.

Tensor modes, are the most explored type of perturbations in LQC. The effects of quantum gravitational effects on propagation of gravitational waves were studied for both inverse volume and holonomy corrections. In case of the inverse volume corrections the investigations were performed in [34, 52, 53]. The case with the holonomy corrections was studied in [34, 51, 54]. In particular, in Ref. [51], generation of the gravitational waves in the symmetric bounce model was studied. In Ref. [54] holonomy corrections to the inflationary spectrum of gravitational waves were derived.

Although quite a lot of work has already been devoted to gravitational waves in LQC, this study aims at treating, for the first time, the problem in a fully self-consistent way with explicit emphasize on the investigation of the spectrum that can be used as an input to study possible experimental signatures.

6.1 Holonomy-corrected constraints

The holonomy-corrected scalar constraint for the tensor modes can be obtained based on the classical expression (4.63). The corrections are introduced by replacing $\bar{k}$ by the function $\mathbb{K}[n]$, as discussed on Chapter 2. Based on this, we define the holonomy-corrected Hamiltonian constraint as follows [34]

$$S^{Q}[N] = \frac{1}{2\kappa}\int_{\Sigma} d^{3}x\bar{N}(C^{(0)} + C^{(2)}), \tag{6.1}$$

where

$$C^{(0)} = -6\sqrt{\bar{p}}\,(\mathbb{K}[1])^2 \tag{6.2}$$

$$C^{(2)} = -\frac{1}{2\bar{p}^{3/2}}\,(\mathbb{K}[1])^2\,(\delta E^c_j \delta E^d_k \delta^k_c \delta^j_d) + \sqrt{\bar{p}}(\delta K^j_c \delta K^k_d \delta^c_k \delta^d_j) - \frac{2}{\sqrt{\bar{p}}}\,(\mathbb{K}[t_1])\,(\delta E^c_j \delta K^j_c) + \frac{1}{\bar{p}^{3/2}}(\delta_{cd}\delta^{jk}\delta^{ef}\partial_e E^c_j \partial_f E^d_k). \tag{6.3}$$

Here, the factors $\bar{k}^2$ were replaced by $\mathbb{K}[1]^2$ as in case of the homogeneous model studied in Chapter 2. The last holonomy correction $\mathbb{K}[t_1]$ is parametrized by some unknown parameter $t_1 \in \mathbb{N}$. In this chapter, we assume that $t_1 = 2$. Motivation for this particular choice may be derived from considerations of the vector modes [34] (see also Chapter 7). However, the value of this parameter cannot be fixed by considering the tensor modes only. This is because the Poisson bracket

$$\left\{S^Q[N_1], S^Q[N_2]\right\} = 0 \tag{6.4}$$

is anomaly-free, independently on the value of t_1. Moreover, the diffeomorphism constraint is equal to zero, because for the tensor modes $N^a = 0$. Therefore, other possible Poisson brackets are vanishing.

Because the requirement of the anomaly freedom is trivially fulfilled for the tensor modes, presence of additional holonomy corrections to equation (6.1) is not excluded. Such corrections can originate from the counter-terms, as studied in case of the vector and scalar modes. In particular, the most restrictive conditions were obtained for the case of scalar perturbations in Chapter 8. If we extrapolated those results into the case of the tensor modes, the holonomy-corrected scalar constraint would take a form different from (6.1). While the $C^{(0)}$ factor would hold its form, the $C^{(2)}$ term, given by equation (6.3), should be replaced by

$$C^{(2)}_{\rm new} = -\frac{1}{2\bar{p}^{3/2}}\left(6\bar{k}\mathbb{K}[2] - 3\mathbb{K}[1]^2 - 2\bar{k}^2\cos(2\bar{\mu}\gamma\bar{k})\right)(\delta E^c_j \delta E^d_k \delta^k_c \delta^j_d) + \cos(2\bar{\mu}\gamma\bar{k})\sqrt{\bar{p}}(\delta K^j_c \delta K^k_d \delta^c_k \delta^d_j) - \frac{2}{\sqrt{\bar{p}}}\left(2\mathbb{K}[2] - \bar{k}\cos(2\bar{\mu}\gamma\bar{k})\right)(\delta E^c_j \delta K^j_c) + \frac{1}{\bar{p}^{3/2}}(\delta_{cd}\delta^{jk}\delta^{ef}\partial_e E^c_j \partial_f E^d_k). \tag{6.5}$$

It is clear that in the limit $\bar{\mu} \to 0$, the classical expression is correctly recovered. However, quantum modifications are strictly different from those in equation (6.3).

In this Chapter we will focus on investigating the model defined by the Hamiltonian constraint (6.1). The case with $C^{(2)}_{\rm new}$ will be studied elsewhere.

6.2 Evolution of tensor modes

The equation of motion for tensor modes, resulting from the Hamiltonian constraint (6.1), is given by [51]

$$\frac{d^2}{d\eta^2}h_a^i + 2aH\frac{d}{d\eta}h_a^i - \nabla^2 h_a^i + m_Q^2 h_a^i = 0, \tag{6.6}$$

where h_a^i are gravitational perturbations, η is the conformal time and the factor due to the holonomy corrections is given by

$$m_Q^2 := 16\pi G a^2 \frac{\rho}{\rho_c}\left(\frac{2}{3}\rho - V\right). \tag{6.7}$$

This factor acts as an effective mass term. For convenience we introduce the variable

$$u = \frac{ah_\oplus}{\sqrt{16\pi G}} = \frac{ah_\otimes}{\sqrt{16\pi G}}, \tag{6.8}$$

where $h_1^1 = -h_2^2 = h_\oplus$, $h_2^1 = h_1^2 = h_\otimes$. Then, performing the Fourier transform

$$u(\mathbf{x},\eta) = \int \frac{d^3k}{(2\pi)^3} u_{\mathbf{k}}(\eta) e^{i\mathbf{k}\cdot\mathbf{x}}, \tag{6.9}$$

one can rewrite the equation as

$$\frac{d^2}{d\eta^2}u_{\mathbf{k}}(\eta) + \left[k^2 + m_{\text{eff}}^2\right] u_{\mathbf{k}}(\eta) = 0, \tag{6.10}$$

where $k^2 = \mathbf{k}\cdot\mathbf{k}$ and

$$m_{\text{eff}}^2 := m_Q^2 - \frac{a''}{a} = a^2\frac{\kappa}{2}\left[P - \frac{1}{3}\rho\right], \tag{6.11}$$

where the P is the pressure of the scalar field. It is worth underlining that the final expression of m_{eff} has no explicit dependence upon the critical energy density ρ_c. In (Eq.6.1), both m_Q^2 and a''/a depend on ρ_c. However, because

$$\frac{a''}{a} = a^2\left[\frac{2\kappa}{3}\rho\left(1 - \frac{\rho}{\rho_c}\right) - \frac{\kappa}{2}(\rho + P)\left(1 - \frac{2\rho}{\rho_c}\right)\right], \tag{6.12}$$

factors depending on ρ_c cancel out precisely. This is perhaps not a coincidence and this could exhibit the conservation of classical symmetries while introducing the quantum corrections.

Next step consists in quantizing the Fourier modes $u_{\mathbf{k}}(\eta)$. This follows the standard canonical procedure. Promoting this quantity to be an operator, one performs the decomposition

$$\hat{u}_{\mathbf{k}}(\eta) = f_k(\eta)\hat{b}_{\mathbf{k}} + f_k^*(\eta)\hat{b}_{-\mathbf{k}}^\dagger, \tag{6.13}$$

where $f_k(\eta)$ is the so-called mode function which satisfies the same equation as $u_{\mathbf{k}}(\eta)$, namely (Eq. 6.10). The creation ($\hat{b}^\dagger_{\mathbf{k}}$) and annihilation ($\hat{b}_{\mathbf{k}}$) operators fulfill the commutation relation $[\hat{b}_{\mathbf{k}}, \hat{b}^\dagger_{\mathbf{q}}] = \delta^{(3)}(\mathbf{k}-\mathbf{q})$.

The problem is now shifted to the resolution of a Schrödinger-like equation (6.10) which can be used to compute observationally relevant quantities. In particular, the correlation function for tensor modes is given by

$$\langle 0|\hat{h}^a_b(\mathbf{x},\eta)\hat{h}^b_a(\mathbf{y},\eta)|0\rangle = \int_0^\infty \frac{dk}{k}\mathcal{P}_T(k,\eta)\frac{\sin kr}{kr}, \tag{6.14}$$

where $\mathcal{P}_T$ is the tensor power spectrum and $|0\rangle$ is the vacuum state. In our case, $\mathcal{P}_T$ can be written as

$$\mathcal{P}_T(k,\eta) = \frac{64\pi G}{a^2(\eta)}\frac{k^3}{2\pi^2}|f_k(\eta)|^2. \tag{6.15}$$

This spectrum is a fundamental observable associated with gravitational wave production. As will be shown in the next sections, very substantial deviations from the usual shape are to be expected within the LQC framework.

6.3 Analytical investigation of the power spectrum

In this section we perform analytical studies of gravitational wave creation in the scenario previously described. In particular, we derive approximate formulas for the tensor power spectrum at the end of inflation. In next section we will compare this result with numerical computations.

In the considered model, the evolution is split into three parts: contraction, bounce and slow-roll inflation. For this model, the effective mass square is defined as follows

$$m^2_{\text{eff}}(\eta) = \begin{cases} 0 & \text{for} \quad \eta < \eta_i - \Delta\eta. \\ k_0^2 & \text{for} \quad \eta_i - \Delta\eta < \eta < \eta_i. \\ -\left(\nu^2 - \frac{1}{4}\right)\frac{1}{\eta^2} & \text{for} \quad \eta > \eta_i. \end{cases} \tag{6.16}$$

Basically, the phenomenological parameters entering the model are therefore:

- η_i - the beginning of the inflation.
- $\Delta\eta$ - the width of the bounce.
- k_0 - which is approximately equal to the value of m_{eff} at the bounce (when $H = 0$). It can therefore be related to energy scale of the bounce.
- ν - which is related to slow-roll parameter

$$\epsilon := \frac{1}{16\pi G}\left(\frac{V_{,\varphi}}{V}\right)^2 \tag{6.17}$$

by $\nu = \sqrt{\frac{9}{4}+3\epsilon} = \frac{3}{2}+\epsilon+\mathcal{O}(\epsilon^2)$, where $\epsilon \ll 1$.

For the considered model, we have $k_0^2 \geqslant 0$. This comes from the fact that we consider a particular *shark fin* type of evolution where the bounce is dominated by the kinetic energy term.

Matching should be performed between the three considered phases. It can be done, as displayed in Fig. 6.1, with transition matrices defined as follows:

$$\mathbf{M} := \begin{bmatrix} f_k(\eta) & f_k^*(\eta) \\ \partial_\eta f_k(\eta) & \partial_\eta f_k^*(\eta) \end{bmatrix}, \tag{6.18}$$

where the Wronskian condition implies

$$W(f_k(\eta), f_k^*(\eta)) := \det \mathbf{M} = i. \tag{6.19}$$

The inverse of the transition matrix is then given by:

$$\mathbf{M}^{-1} := -i \begin{bmatrix} \partial_\eta f_k^*(\eta) & -f_k^*(\eta) \\ -\partial_\eta f_k(\eta) & f_k(\eta) \end{bmatrix}. \tag{6.20}$$

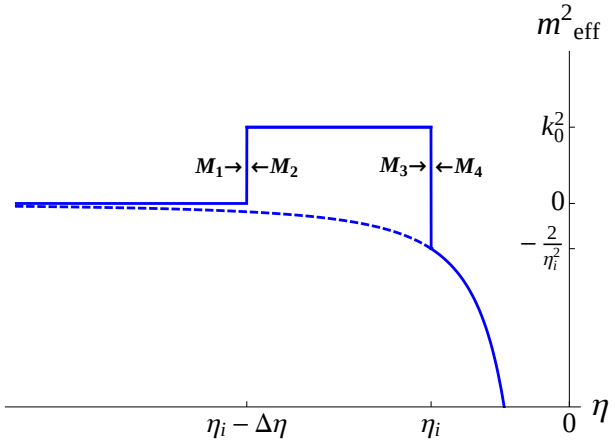

Figure 6.1: Evolution of the effective mass used in the analytical approximation (Eq. 6.16). On this plot, ϵ is set to zero as an example. The dashed line represents the case without a bounce. The points where the transfer matrices are computed in our model are also indicated.

The three first transition matrices are:

$$\mathbf{M_1} = \begin{bmatrix} \frac{e^{-ik(\eta_i-\Delta\eta)}}{\sqrt{2k}} & \frac{e^{ik(\eta_i-\Delta\eta)}}{\sqrt{2k}} \\ -i\sqrt{\frac{k}{2}}e^{-ik(\eta_i-\Delta\eta)} & i\sqrt{\frac{k}{2}}e^{ik(\eta_i-\Delta\eta)} \end{bmatrix}, \tag{6.21}$$

$$\mathbf{M_2} = \begin{bmatrix} \frac{e^{-i\Omega(\eta_i-\Delta\eta)}}{\sqrt{2\Omega}} & \frac{e^{i\Omega(\eta_i-\Delta\eta)}}{\sqrt{2\Omega}} \\ -i\sqrt{\frac{\Omega}{2}}e^{-i\Omega(\eta_i-\Delta\eta)} & i\sqrt{\frac{\Omega}{2}}e^{i\Omega(\eta_i-\Delta\eta)} \end{bmatrix}, \tag{6.22}$$

$$\mathbf{M_3} = \begin{bmatrix} \frac{e^{-i\Omega\eta_i}}{\sqrt{2\Omega}} & \frac{e^{i\Omega\eta_i}}{\sqrt{2\Omega}} \\ -i\sqrt{\frac{\Omega}{2}}e^{-i\Omega\eta_i} & i\sqrt{\frac{\Omega}{2}}e^{i\Omega\eta_i} \end{bmatrix}, \tag{6.23}$$

where

$$\Omega = \sqrt{k^2 + k_0^2}. \tag{6.24}$$

In the last region, mode functions can be written as

$$f_k(\eta) = \alpha_k g_k(\eta) + \beta_k g_k^*(\eta), \tag{6.25}$$

where

$$g_k(\eta) = \sqrt{-\eta}\sqrt{\frac{\pi}{4}} e^{i\pi(2\nu+1)/4} H_\nu^{(1)}(-k\eta), \tag{6.26}$$

$H_\nu(x)$ being a Hankel function of the first kind. The mode functions $g_k(\eta)$ correspond to another decomposition of the field $\hat{u}_{\mathbf{k}}(\eta)$ in the form:

$$\hat{u}_{\mathbf{k}}(\eta) = g_k(\eta)\hat{a}_{\mathbf{k}} + g_k^*(\eta)\hat{a}^\dagger_{-\mathbf{k}}. \tag{6.27}$$

The creation ($\hat{a}^\dagger_{\mathbf{k}}$) and annihilation ($\hat{a}_{\mathbf{k}}$) operators fulfill the commutation relation $[\hat{a}_{\mathbf{k}}, \hat{a}^\dagger_{\mathbf{q}}] = \delta^{(3)}(\mathbf{k}-\mathbf{q})$. Because decompositions (6.13) and (6.27) are equivalent, based on (Eq. 6.25) and on the Wronskian conditions for the mode functions f_k and g_k, one obtains:

$$\begin{bmatrix} \hat{b}_{\mathbf{k}} \\ \hat{b}^\dagger_{-\mathbf{k}} \end{bmatrix} = \begin{bmatrix} \alpha_k & \beta_k^* \\ \beta_k & \alpha_k^* \end{bmatrix} \begin{bmatrix} \hat{a}_{\mathbf{k}} \\ \hat{a}^\dagger_{-\mathbf{k}} \end{bmatrix}, \tag{6.28}$$

which corresponds to the Bogoliubov transformation with coefficients α_k and β_k. Due to the commutation relation of the creation and annihilation operators we have $|\alpha_k|^2 - |\beta_k|^2 = 1$. It is clear from (Eq. 6.28) that if $\beta_k \neq 0$ particles are created from the vacuum, just because $\hat{b}_{\mathbf{k}}|0\rangle = \beta_k^* \hat{a}^\dagger_{-\mathbf{k}}|0\rangle$. By matching the three regions, the unknown coefficients α_k and β_k can be determined:

$$\begin{aligned} \begin{bmatrix} \alpha_k \\ \beta_k \end{bmatrix} &= \mathbf{M_4}^{-1}\mathbf{M_3}\mathbf{M_2}^{-1}\mathbf{M_1}\begin{bmatrix} 1 \\ 0 \end{bmatrix} \\ &= \mathbf{M_4}^{-1}\begin{bmatrix} \frac{e^{ik(\Delta\eta-\eta_i)}(\Omega\cos[\Delta\eta\Omega] - ik\sin[\Delta\eta\Omega])}{\sqrt{2k}\Omega} \\ \frac{e^{ik(\Delta\eta-\eta_i)}(-ik\cos[\Delta\eta\Omega] - \Omega\sin[\Delta\eta\Omega])}{\sqrt{2k}} \end{bmatrix}, \end{aligned} \tag{6.29}$$

where $\mathbf{M_4}$ is given by

$$\mathbf{M_4} = \begin{bmatrix} g_k(\eta) & g_k^*(\eta) \\ \partial_\eta g_k(\eta) & \partial_\eta g_k^*(\eta) \end{bmatrix}_{\eta=\eta_i}, \tag{6.30}$$

the mode function g_k being given by (Eq. 6.26). In a special case corresponding to a de Sitter inflation ($\epsilon = 0$ and $\nu = \frac{3}{2}$), the mode functions given by (Eq. 6.26) simplify to the Bunch-Davies vacuum

$$g_k(\eta)|_{\nu=\frac{3}{2}} = g_k^{\text{B-D}}(\eta) = \frac{e^{-ik\eta}}{\sqrt{2k}}\left(1 - \frac{i}{k\eta}\right). \tag{6.31}$$

In general, the amplitude of the mode function during inflation can be written as

$$|f_k|^2 = |g_k|^2|\alpha_k - \beta_k|^2 + 4\mathfrak{R}(\alpha_k^*\beta_k g_k^*)\mathfrak{R}g_k. \tag{6.32}$$

As we are interested in the spectrum at the end of inflation ($\eta \to 0^-$), the approximation

$$H_\nu^{(1)}(x) \simeq -\frac{i}{\pi}\Gamma(\nu)\left(\frac{x}{2}\right)^{-\nu} \tag{6.33}$$

holds and, based on this, one can easily see that for a slow-roll inflation ($\epsilon \ll 1$):

$$\lim_{\eta\to 0^-} \frac{\mathfrak{R}g_k(\eta)}{\mathfrak{I}g_k(\eta)} = \mathcal{O}(\epsilon). \tag{6.34}$$

Therefore, the leading order contribution from (Eq. 6.32) becomes

$$\lim_{\eta\to 0^-} |f_k|^2 = |g_k|^2|\alpha_k - \beta_k|^2. \tag{6.35}$$

With this approximation, the tensor power spectrum at the end of inflation takes the form

$$\mathcal{P}_T(k) = \frac{16}{\pi}\left(\frac{H}{m_{Pl}}\right)^2\left(\frac{k}{aH}\right)^{-2\epsilon}|\alpha_k - \beta_k|^2. \tag{6.36}$$

The coefficients α_k and β_k are computed from (Eq. 6.29). Since the resulting expression for $|\alpha_k - \beta_k|^2$ is very long, it is not explicitly given here. It exhibits the correct ultra-violet (UV) behavior, namely $\lim_{k\to\infty}|\alpha_k - \beta_k|^2 = 1$. Therefore, the UV spectrum simplifies to

$$\mathcal{P}_T(k \to \infty) = \frac{16}{\pi}\left(\frac{H}{m_{Pl}}\right)^2\left(\frac{k}{aH}\right)^{-2\epsilon}. \tag{6.37}$$

In Fig. 6.2, spectra, as obtained from (Eq. 6.36), are displayed for different values of k_0 and normalized to the usual non-LQC corrected spectrum. In Fig. 6.3, the width of the bounce $\Delta\eta$ is varied. In both cases, ϵ is vanishing.

Main features that can be drawn from those plots are the following:

- Power is suppressed in the infra-red (IR) regime. This is a characteristic feature associated with the bounce.
- UV behavior agrees with the standard general relativistic picture.
- Damped oscillations are superimposed with the spectrum around the "transition" momentum k_* between the suppressed regime and the standard regime.
- The first oscillation behaves like a "bump" that can substantially exceed the UV asymptotic value.
- The parameter k_0 basically controls the amplitude of the oscillations whereas $\Delta\eta$ controls their frequency.

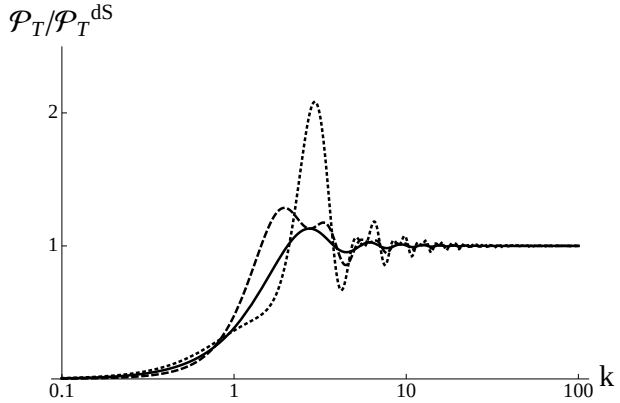

Figure 6.2: Analytical tensor power spectra, normalized to the non-LQC-corrected spectrum, for three different values of k_0 in the $\epsilon = 0$ case. The parameters are: $k_0 = 0$ (solid line), $k_0 = 1.5$ (dashed line), $k_0 = 3$ (dotted line), $\eta_i = -1$, and $\Delta\eta = 1$.

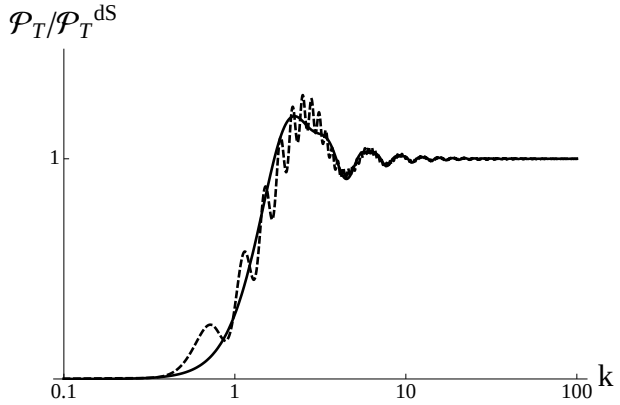

Figure 6.3: Analytical tensor power spectra, normalized to the non-LQC-corrected spectrum, for two different values of $\Delta\eta$ in the $\epsilon = 0$ case. The parameters are: $\Delta\eta = 0$ (solid line), $\Delta\eta = 10$ (dashed line), $k_0 = 1$, and $\eta_i = -1$.

6.4 Numerical investigation of the power spectrum

To perform a more detailed analysis, we have also fully numerically solved the system of coupled differential equations which leads to both the evolution of the modes and of the

background:

$$\frac{d^2 f_k}{dt^2} = -H\frac{df_k}{dt} - \left[\frac{k^2}{a^2} + \frac{\kappa}{6}(3P-\rho)\right] f_k, \tag{6.38}$$

$$\frac{dH}{dt} = \frac{1}{2}\kappa(\rho+P)\left(2\frac{\rho}{\rho_c}-1\right), \tag{6.39}$$

$$\frac{da}{dt} = Ha, \tag{6.40}$$

$$\frac{d\varphi}{dt} = \frac{\pi}{a^3}, \tag{6.41}$$

$$\frac{d\pi}{dt} = -a^3 m^2 \varphi, \tag{6.42}$$

where

$$\rho = \frac{\pi^2}{2a^6} + \frac{m^2}{2}\varphi^2 \text{ and } P = \frac{\pi^2}{2a^6} - \frac{m^2}{2}\varphi^2 \tag{6.43}$$

are respectively the energy density and pressure of the scalar field whereas π is the momentum.

To compute the evolution of the modes, the initial condition was assumed to be the Minkowski vacuum

$$f_k = \frac{e^{-ik\eta}}{\sqrt{2k}}. \tag{6.44}$$

This approximation is valid for the sub-horizontal modes. Therefore, in the numerical computations we have evolved only modes that were sub-horizontal at the initial time.

In Fig. 6.4, the analytical spectrum (Eq. 6.36) evaluated as explained in the previous section is compared with the full numerical computation. The overall agreement is very good with slight deviations due to subtle dynamical effects. The UV tilt associated with the slow-roll parameter is perfectly recovered. The values of parameters H, k_0 and ϵ were determined from the evolution of the background. In turn, the parameters η_i and $\Delta\eta$ were fixed to fit the numerical data.

The mass of the scalar field is, of course, the key physical parameter of this model. The canonically chosen value (around $10^{-6} m_{Pl}$) may not be especially meaningful in this approach as the standard requirements of inflation are substantially modified by the specific history of the Hubble radius. This value is nonetheless still the mostly preferred one.

In Fig. 6.5, the spectra computed for three different mass values are displayed. As expected, the UV value of the spectrum scales as m^2, since during inflation $\mathcal{P}_T \sim H^2 \sim m^2$. It is also clear that the region of oscillations becomes broader while lowering the value of m.

In Fig. 6.6, we show how the spectrum is modified by different choices of ρ_c. It is clear that increasing ρ_c leads to amplification of the spectrum. The dependence is however not very strong. The increase of ρ_c leads to the increase of the field displacement φ_{max}. This dependence was shown to be rather weak. Since $\mathcal{P}_T \sim H^2 \sim m^2\varphi^2$, the increase of φ due

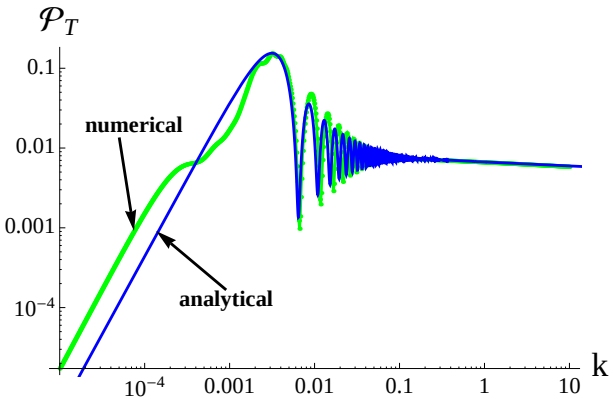

Figure 6.4: Comparison of numerical and analytical spectra (Eq. 6.36) for $m = 10^{-2} m_{Pl}$. In the IR region the spectra behave as $\mathcal{P}_T \propto k^2$ while in the UV region they behave as $\mathcal{P}_T \propto k^{-2\epsilon}$, where $\epsilon \ll 1$ is the slow-roll parameter. Here: $H = 0.037 m_{Pl}$, $\epsilon = 0.0246$, $k_0 = 0.037 m_{Pl}$, $\eta_i = -750$, $\Delta\eta = 10$.

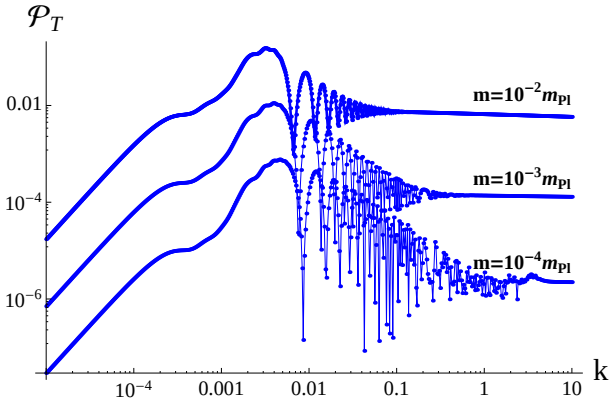

Figure 6.5: Numerically computed power spectra for $m = 10^{-4}, 10^{-3}, 10^{-2}\ m_{Pl}$ (from bottom to top in the UV range).

to the dependence upon ρ_c will result in amplification of the power spectrum. This is in agreement with numerical results. From Fig. 6.6, it can also be noticed that increasing ρ_c amplifies the oscillatory structure.

Numerical investigations performed for this work have shown that the quantity R defined as

$$R := \frac{\mathcal{P}_T(k = k_*)}{\mathcal{P}_T^{\text{standard}}(k = k_*)}, \tag{6.45}$$

basically evolves as

$$R \simeq \left(\frac{m_{Pl}}{m}\right)^{0.64}, \tag{6.46}$$

where k_* is the position of the highest peak in the power spectrum and $\mathcal{P}_T^{\text{standard}}(k)$ is

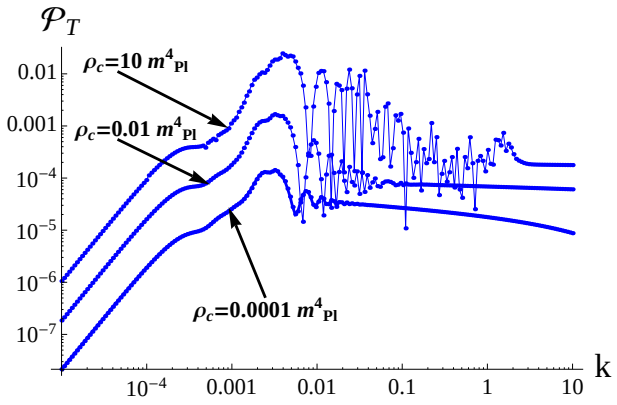

Figure 6.6: Numerically computed power spectra for $\rho_c = 10^{-4}, 10^{-2}, 10\ m_{Pl}^4$ (from bottom to top in the UV range) with $m = 10^{-3} m_{Pl}$.

a standard inflationary power spectrum (See e.g. Eq. 6.37) which overlaps with $\mathcal{P}_T(k)$ for $k \to \infty$. The function (6.46) was obtained by fitting the numerical data in the mass range $m = 5 \cdot 10^{-5} m_{Pl}$ ... $10^{-1} m_{Pl}$. Due to numerical instabilities, it was not possible to perform computations for lower values of the inflaton mass. The numerically obtained values of R together with the approximation given by (Eq. 6.46) are given in Fig. 6.7. This

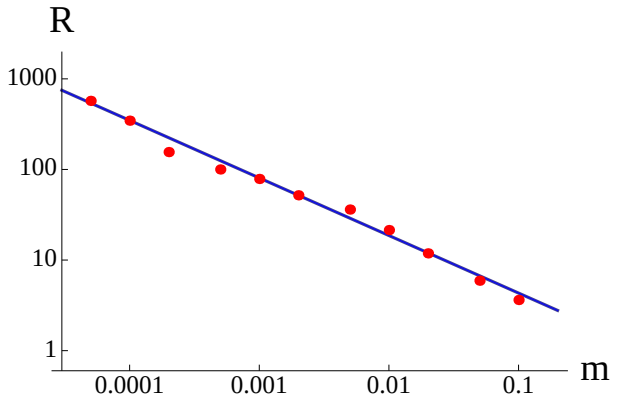

Figure 6.7: Ratio defined by (Eq. 6.45) as a function of inflaton mass in Planck units. Dots are values obtained from the numerical computations. The straight line is the fit given by (Eq. 6.46).

parametrization is useful for phenomenological purposes. Interestingly, R can become very high for low values of the mass of the field. This partially compensates for the lower overall normalization of the spectrum and can become a very specific feature of the model. In particular, for the mass $m \approx 10^{-6} m_{Pl}$ (which is the value preferred by some estimations), extrapolating the relation (6.46) leads to $R \approx 8000$. If the relation still holds in this range, the effect is very significant, and could have important observational consequences.

Finally, to make basic studies easier, we performed rough parametrization of the full spectrum:

$$\mathcal{P}_T = \frac{16}{\pi}\left(\frac{H}{m_{Pl}}\right)^2 \frac{\left(\frac{k}{aH}\right)^{-2\epsilon}}{1+(k_*/k)^2}\left[1+\frac{4R-2}{1+(k/k_*)^2}\right], \tag{6.47}$$

leading to

$$\mathcal{P}_T^{dS} = \frac{16}{\pi}\left(\frac{H}{m_{Pl}}\right)^2 \frac{1}{1+(k_*/k)^2}\left[1+\frac{4R-2}{1+(k/k_*)^2}\right], \tag{6.48}$$

in the specific case of de Sitter inflation. In both cases, the classical behavior is recovered in the limit $k \to \infty$. The point for introducing the R factor the way it was done becomes clear when calculating the value of the spectra at $k = k_*$. For a modified de Sitter spectrum (Eq 6.48), we get

$$\mathcal{P}_T^{dS}(k = k_*) = R\frac{16}{\pi}\left(\frac{H}{m_{Pl}}\right)^2. \tag{6.49}$$

Thanks to the relation (6.46), the number of free parameters can be decreased in a phenomenological analysis.

As shown on Fig. 6.8, this formula correctly reproduces the main features, namely the IR power suppression, the bump and the UV limit. Oscillations are missed but due to momentum integration there is little hope that they can observationally be seen on a cosmological microwave background (CMB) spectrum.

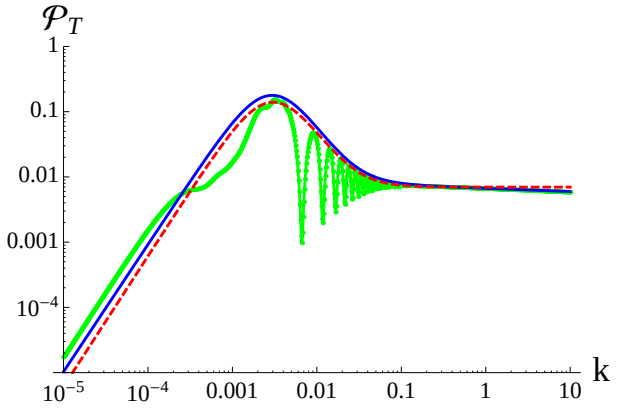

Figure 6.8: Comparison of the numerical spectrum for $m = 10^{-2}m_{Pl}$ with formulas (6.47) and (6.48). The solid (blue) line corresponds to (6.47) while the dashed (red) line corresponds to (6.48).

To conclude this section, we have schematically represented the evolution of the Hubble radius ($R_H := 1/|H|$), together with exemplary physical modes, in Fig. 6.9. This helps to understand the shape of the obtained spectra.

We consider the modes that are initially (at time t_1) shorter than the Hubble radius. For those modes, the normalized solution is given by the Minkowski vacuum $f_k = e^{-ik\eta}/\sqrt{2k}$.

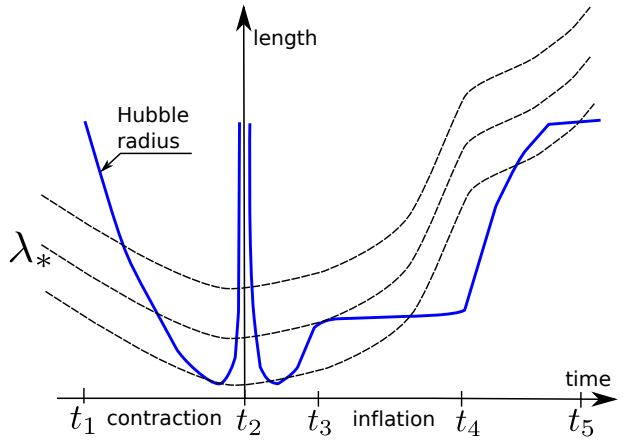

Figure 6.9: Schematic picture of the evolution of the Hubble radius (solid line) and of the different length scales (dashed lines) for the considered model of the universe. Different times are distinguished: t_1—time when the initial conditions are set; t_2—bounce ($H = 0$); t_3—beginning of inflation; t_4—end of inflation; t_5—present epoch of dark energy domination.

Therefore, the initial power spectrum takes the form $\mathcal{P}_T \sim k^3|f_k|^2 \sim k^2$. Starting from the largest scales, the modes cross the Hubble radius. This is possible since the Hubble radius undergoes contraction faster than any particular length scale. While crossing the horizon, the shape of the spectrum becomes *frozen* in the initial $\mathcal{P}_T \sim k^2$ form. Then, the modes evolve through the bounce (at time t_2) until the beginning of inflation (at time t_3). The main consequence of the transition of modes through the bounce is the appearance of additional oscillations in the spectrum. This issue was studied in details in Ref. [51], where the spectrum at time t_3 was calculated for the symmetric bounce model. After the bounce, modes with wavelengths shorter than λ_* start to re-enter the Hubble radius. The super-horizon modes $\lambda > \lambda_*$ ($k < k_*$) hold the k^2 spectrum, with however some oscillatory features due to the bounce. Modes with $\lambda < \lambda_*$ ($k > k_*$) cross the horizon again during the phase of inflation. For them, the spectrum agrees with the standard slow-roll inflation spectrum $\mathcal{P}_T \sim k^{-2\epsilon}$ where $\epsilon \ll 1$. The small tilt is due to slow increase of the Hubble radius. Contributions from different modes are then slightly different. At the end of inflation (at time t_4) the spectrum is therefore suppressed ($\mathcal{P}_T \sim k^2$) for $k < k_*$ and exhibits an inflationary shape ($\mathcal{P}_T \sim k^{-2\epsilon}$) for $k > k_*$. The spectrum is also modified by oscillations due to the bounce. This corresponds to the computations of this paper. The particular mode with wavelength λ_* (wave number k_*) should be studied into more details. The size of this mode overlaps with the size of the Hubble radius at the beginning of inflation: $k_* \simeq a(t_3)H(t_3)$. The physical length λ_* at the scale factor $a(t)$ is therefore equal to $\lambda_*(t) \simeq a(t)/[a(t_3)H(t_3)]$. This scale grows with cosmic expansion and it is crucial, from the observational point of view, to determine its present size (at time t_5). The case drawn in Fig. 6.9 corresponds to the present size of λ_* greater than the size of the horizon

(the Hubble radius). This is indeed rather unlikely that the present value of λ_* is below the size of the horizon just because the spectrum of scalar perturbations should then exhibit deviations from the nearly scale invariant inflationary prediction. Up to now, there is no observational evidence for such deviations. A remaining possibility would however be that the (slight) observed lack of power in the CMB spectrum of anisotropies could be due to the effects of the bounce. However, the present size of λ_* would then be comparable with the size of the horizon. This leads to the question: why should those two scales overlap right now? This is rather unnatural, and would lead to a new coincidence problem. However, as it was estimated in Ref. [23], these two scales can indeed overlap in the standard inflationary scenario for quite natural values of the parameters. There is therefore a glimpse of hope that the scale λ_* is at least not much bigger than the size of the horizon. This could allow us to see some UV features due to the bounce as the oscillations also affect sightly the inflationary part of the spectrum. These are however secondary effects and it is not clear whether they were not smoothed away during the radiation domination era. Moreover, in the region where those effects could be expected, errors due to the *cosmic variance* become significant. This is an unavoidable observational limitation which cannot be bettered, even by the improvement of resolution of the future CMB experiments.

6.5 Conclusions

In this chapter, we have investigated into the details by both analytical and numerical studies the primordial power spectrum of gravitational waves in LQC. It exhibits several characteristic features, namely a $\mathcal{P}_T \propto k^2$ IR power suppression, oscillations, and a bump at k_*. In the UV regime, the standard inflationary spectrum $\mathcal{P}_T \propto k^{-2\epsilon}$ is recovered. Therefore, in the UV limit the LQC results overlap with those obtained in the classical theory of gravity, as shown in Fig. 6.10.

The primordial tensor power spectrum transforms into B-type CMB polarization. The performed investigations therefore open the window for observational tests of the model, in particular through the amplification which occurs while approaching $k \to k_*$. The observed structures correspond to the UV region in the spectrum. If the present scale $\lambda_* \sim 1/k_*$ is not much larger than the size of horizon, then the effects of the bounce should be, in principle, observable. In particular, one should expect amplification, rather than suppression of the B-type polarization spectrum at low multipoles. The suppression for $k < k_*$ becomes dominant at much larger scale, probably far above the horizon. While the B-type polarization has not been detected yet, there are huge efforts in this direction. Experiments as PLANCK [55], BICEP [56] or QUaD [57] are (partly) devoted to the search of the B-mode. Even with the present observational constraints, one can already exclude some evolutionary scenarios and possible values of the parameters, in particular the inflaton mass m and the position of the bump k_* in the spectrum. This will be studied in Chapter 9.

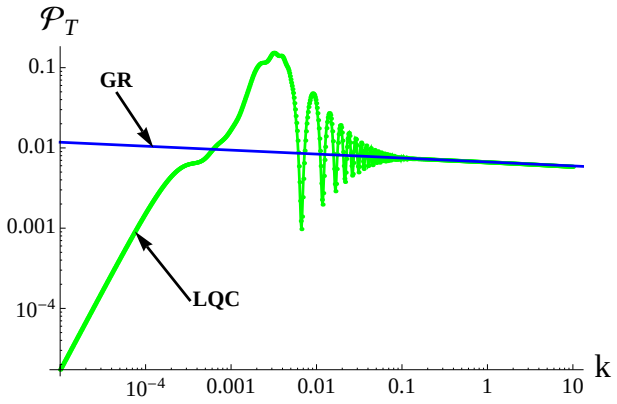

Figure 6.10: Comparison of the tensor power spectra from the slow-roll inflation obtained in loop quantum cosmology (LQC) and general relativity (GR) for $\mathfrak{m} = 10^{-2}\mathfrak{m}_{\mathrm{Pl}}$. Both spectra overlap in the UV limit while in the IR limit significant discrepancy due to the quantum gravitational effects is observed.

Chapter 7

Vector perturbations

In this chapter, we investigate vector perturbations with holonomy corrections. Conditions to achieve anomaly freedom for these perturbations are found at all orders. This requires an introduction of counter-terms in the Hamiltonian constraint. We also show that anomaly freedom requires the diffeomorphism constraint to hold its classical form when matter is added. The gauge-invariant variable and the corresponding equation of motion are derived. The propagation of vector modes through the bounce is finally discussed.

7.1 Holonomy-corrected constraints

Vector modes within the canonical formulation were studied in [33]. It was shown there that

$$\delta E^a_i = -\bar{p}(c_1 \partial^a F_i + c_2 \partial_i F^a), \tag{7.1}$$

where $c_1 + c_2 = 1$ and the divergence-free condition $\delta^i_a \delta E^a_i = 0$ is fulfilled. The values of c_1 and c_2 depend on the gauge choice. However, due to the Gauss constraint, only symmetric variables are invariant under internal rotations. This is the case for $\delta E^{(a}{}_{i)}$, which is consequently independent on the specific choice of c_1 and c_2, and should be preferred. Perturbation of the shift vector is parametrized as $\delta N^a = S^a$.

The quantum holonomy-corrected Hamiltonian constraint, corresponding to classical (4.70), is given by

$$S^Q[N] = \frac{1}{2\kappa} \int_\Sigma d^3x \left[\bar{N} (C^{(0)} + C^{(2)}) \right], \tag{7.2}$$

where

$$C^{(0)} = -6\sqrt{\bar{p}}\,(\mathbb{K}[1])^2\,, \tag{7.3}$$

$$C^{(2)} = -\frac{1}{2\bar{p}^{3/2}}\,(\mathbb{K}[1])^2\,(1+\alpha_1)(\delta E^c_j \delta E^d_k \delta^k_c \delta^j_d) + \sqrt{\bar{p}}(\delta K^j_c \delta K^k_d \delta^c_k \delta^d_j) - \frac{2}{\sqrt{\bar{p}}}\,(\mathbb{K}[\nu_1])\,(1+\alpha_2)(\delta E^c_j \delta K^j_c). \tag{7.4}$$

Holonomy corrections were introduced by replacing $\bar{k} \to \mathbb{K}[n]$. Two counter-term functions α_1 and α_2, whose interest will be made clear later, were also added. In the classical limit $\mathbb{K}[n] \to \bar{k}$, and $\alpha_i = \alpha_i(\bar{p}, \bar{k}) \to 0$, with $i = 1, 2$. We have assumed here that α_i are functions of the background variables only and that ν_1 is an integer to be fixed. The Hamiltonian constraint (7.2) corresponds to the one investigated in [33] while setting $\alpha_i = 0$. However, as we will show, it is necessary to introduce these additional factors, which vanish in the classical limit. These factors can, of course, also be viewed as contributions from the two counter-terms

$$S_{C1} = -\frac{\alpha_1}{2\kappa}\int_\Sigma d^3x \frac{\bar{N}}{2\bar{p}^{3/2}}\,(\mathbb{K}[1])^2\,(\delta E^c_j \delta E^d_k \delta^k_c \delta^j_d), \tag{7.5}$$

$$S_{C2} = -\frac{\alpha_2}{2\kappa}\int_\Sigma d^3x \frac{2\bar{N}}{\sqrt{\bar{p}}}\,(\mathbb{K}[\nu_1])\,(\delta E^c_j \delta K^j_c) \tag{7.6}$$

to the holonomy-corrected Hamiltonian constraint.

A similar method of counter-terms was successfully applied for perturbations with inverse-volume corrections. In that case, it was possible to fix the counter-terms so as to make the algebra anomaly free. In this article, we follow the same path so as to find explicit expressions for α_1 and α_2.

For the sake of completeness, we also introduce holonomy corrections to the diffeomorphism constraint, as follows:

$$D^Q[N^a] = \frac{1}{\kappa}\int_\Sigma d^3x \delta N^c \left[-\bar{p}(\partial_k \delta K^k_c) - (\mathbb{K}[\nu_2])\,\delta^k_c(\partial_d \delta E^d_k)\right], \tag{7.7}$$

where ν_2 is an unknown integer. It is worth emphasizing here that within LQG, the diffeomorphism constraint is fulfilled at the classical level while constructing the diffeomorphism invariant spin network states. If LQC was really derived from the full LQG theory, the classical form of the diffeomorphism constraint should therefore be used. However, at this early stage of the understanding of LQC, it might be safe to allow for some generalizations by introducing the holonomy correction also to the diffeomorphism constraint. This hypothesis was already studied in [39] in the case of holonomy-corrected scalar perturbations. It was assumed there that the holonomy correction function was given by $\mathbb{K}[2]$. In this work, we prefer to keep a more general expression $\mathbb{K}[\nu_2]$ with a free ν_2 parameter. We will investigate whether this additional modification can help to fulfill the anomaly freedom conditions.

7.2 Algebra of constraints

The algebra of constraints (7.2) and (7.7) shall now be investigated. Using the Poisson bracket (4.8), we find:

$$\begin{aligned}
\left\{S^Q[N_1], S^Q[N_1]\right\} &= 0, && (7.8)\\
\left\{D^Q[N_1^a], D^Q[N_2^a]\right\} &= 0, && (7.9)\\
\left\{S^Q[N], D^Q[N^a]\right\} &= \frac{\bar{N}}{\sqrt{\bar{p}}}\mathcal{B}D^Q[N^a] \\
&+ \frac{\bar{N}}{\kappa\sqrt{\bar{p}}}\int_\Sigma d^3x\delta N^c\delta_c^k(\partial_d\delta E_k^d)\delta E_k^d\mathcal{A}, && (7.10)
\end{aligned}$$

where $\mathcal{B} := (1+\alpha_2)\mathbb{K}[\nu_1]+\mathbb{K}[\nu_2]-2\mathbb{K}[2]$, and $\mathcal{A}$ is an anomaly function which, for reasons that shall be made clear later, is decomposed in two parts $\mathcal{A} = \mathcal{A}_1 + \mathcal{A}_2$, where

$$\begin{aligned}
\mathcal{A}_1 &= \mathcal{B}\mathbb{K}[\nu_2], && (7.11)\\
\mathcal{A}_2 &= 2\mathbb{K}[2]\bar{p}\frac{\partial\mathbb{K}[\nu_2]}{\partial\bar{p}} - \frac{1}{2}(\mathbb{K}[1])^2\cos(\nu_2\bar{\mu}\gamma\bar{k}) \\
&- 2\mathbb{K}[1]\bar{p}\frac{\partial\mathbb{K}[1]}{\partial\bar{p}}\cos(\nu_2\bar{\mu}\gamma\bar{k}) \\
&+ (1+\alpha_2)\mathbb{K}[\nu_1]\mathbb{K}[\nu_2] - \frac{1}{2}\mathbb{K}[1]^2(1+\alpha_1). && (7.12)
\end{aligned}$$

This decomposition was made so that in the classical limit ($\bar{\mu}\to 0$), both contributions to the anomaly vanish separately. Using the relation

$$\bar{p}\frac{\partial\mathbb{K}[n]}{\partial\bar{p}} = \left(\bar{k}\cos(n\bar{\mu}\gamma\bar{k}) - \mathbb{K}[n]\right)\beta, \tag{7.13}$$

the second contribution can be re-written as:

$$\begin{aligned}
\mathcal{A}_2 &= -2\beta\mathbb{K}[2]\mathbb{K}[\nu_2] + (1+\alpha_2)\mathbb{K}[\nu_1]\mathbb{K}[\nu_2] \\
&+ (2\beta - 1/2)(\mathbb{K}[1])^2\cos(\nu_2\bar{\mu}\gamma\bar{k}) \\
&- \frac{1}{2}(\mathbb{K}[1])^2(1+\alpha_1). && (7.14)
\end{aligned}$$

The full anomaly term is given by:

$$\begin{aligned}
\mathcal{A} &= 2(1+\alpha_2)\mathbb{K}[\nu_1]\mathbb{K}[\nu_2] - \frac{1}{2}(\mathbb{K}[1])^2(1+\alpha_1) \\
&- 2(1+\beta)\mathbb{K}[2]\mathbb{K}[\nu_2] + \mathbb{K}[\nu_2]^2 \\
&+ (2\beta - 1/2)(\mathbb{K}[1])^2\cos(\nu_2\bar{\mu}\gamma\bar{k}). && (7.15)
\end{aligned}$$

7.3 Anomaly freedom in the gravity sector

The requirement of the anomaly freedom for the gravity sector reads as $\mathcal{A} = 0$. Under this condition, the algebra of constraints becomes closed but deformed, in particular:

$$\left\{S^{Q}[N], D^{Q}[N^{a}]\right\} = D^{Q}\left[\frac{\bar{N}}{\sqrt{\bar{p}}}\mathcal{B}N^{a}\right]. \tag{7.16}$$

The structure of space-time is therefore also modified. This is illustrated in Fig. 7.1 where one can notice that the Hamiltonian and diffeomorphism constraints generate gauge transformations in directions respectively normal and parallel to the hypersurface. In the classical limit, $\mathcal{B} \to 0$ and both the transformations commute at the perturbative

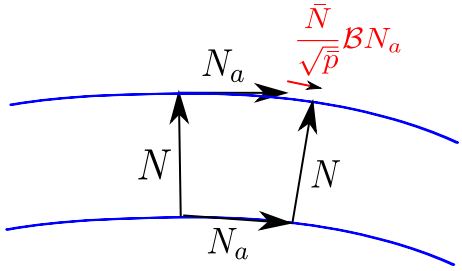

Figure 7.1: Pictorial representation of the hypersurface deformation algebra.

level.

7.3.1 The no counter-terms case

Let us start by analyzing the condition $\mathcal{A} = 0$ without any counter-term (*i.e.* with $\alpha_1 = \alpha_2 = 0$). This case corresponds to the one studied in [33] generalized by the contribution from the corrected diffeomorphism constraint. It was shown in that work that, if $\nu_2 = 0$, the anomaly-freedom condition can be satisfied up to the $\bar{k}^4$ order only. Here, we investigate whether this might be improved by the additional correction made to the diffeomorphism constraint.

By setting $\alpha_1 = \alpha_2 = 0$, the anomaly term given by (7.15) can be expanded in powers of the canonical variable $\bar{k}$ as follows:

$$\begin{aligned}\frac{\mathcal{A}}{(\bar{\mu}\gamma)^2} &= \frac{1}{12}\left(20 - 4\nu_1^2 - \nu_2^2 + 8\beta - 8\nu_2^2\beta\right)x^4 \\ &+ \frac{1}{720}\left(-224 + 12\nu_1^4 - 220\nu_2^2 + 40\nu_1^2\nu_2^2 + 17\nu_2^4\right. \\ &- \left. 128\beta + 80\nu_2^2\beta + 48\nu_2^4\beta\right)x^6 + \mathcal{O}(x^8),\end{aligned} \tag{7.17}$$

where we have defined $x := \bar{\mu}\gamma\bar{k}$ and $x \in [0, \pi]$. Clearly, in the classical limit $\bar{\mu} \to 0$, the anomaly tends to zero. Requiring the anomaly cancellation up to the fourth order leads

to the condition:

$$20 - 4\nu_1^2 - \nu_2^2 + 8\beta - 8\nu_2^2\beta = 0. \tag{7.18}$$

It can be shown that the condition of anomaly cancellation up to orders higher than four cannot be met. For $\beta = -1/2$ ($\bar{\mu}-$scheme), the above equation simplifies to the quadratic Diophantine equation:

$$16 - 4\nu_1^2 + 3\nu_2^2 = 0. \tag{7.19}$$

This equation can be reduced to a Pell-type equation and solved for an infinite number of pairs of integers (ν_1, ν_2). The first three solutions are $(2, 0)$, $(4, 4)$ and $(14, 16)$. The first one $(2, 0)$ corresponds to the case studied in [33], where the diffeomorphism constraint was kept at its classical form. The value $\nu_1 = 2$ obtained in this case was also used to fix the ambiguity for the holonomy-corrected tensor perturbations [34]. If the holonomy modified diffeomorphism constraint is used, the ambiguity cannot be fixed anymore due to the infinite number of solutions to Eq. (7.19).

As we have shown, the modification of the diffeomorphism constraint does not help satisfying the anomaly freedom conditions in the absence of counter-terms. In this case, the anomaly freedom can be fulfilled up to the fourth order in χ. In the semi-classical limit $\chi \ll 1$, the anomaly cancellation up to the fourth order might be a good approximation. However, when approaching the bounce, where $\chi = \frac{\pi}{2}$, contributions from higher order terms become significant and the effects of the anomaly cannot be neglected anymore. Studies of vector perturbations during the bounce phase cannot be performed in such a setup. In order to study vector perturbations through the bounce, the anomaly cancellation at all orders is required. This probably makes the introduction of counter-terms mandatory.

7.3.2 The general case

Let us consider the general case with non-vanishing counter-terms. In this case, the requirement $\mathcal{A} = 0$ can be translated into a relation between the two counter-terms α_1 and α_2:

$$\begin{aligned} \alpha_1 &= -1 + 4(1+\alpha_2)\frac{\mathbb{K}[\nu_1]\mathbb{K}[\nu_2]}{\mathbb{K}[1]^2} - 4(1+\beta)\frac{\mathbb{K}[2]\mathbb{K}[\nu_2]}{\mathbb{K}[1]^2} + 2\frac{\mathbb{K}[\nu_2]^2}{\mathbb{K}[1]^2} \\ &+ (4\beta - 1)\cos(\nu_2\bar{\mu}\gamma\bar{k}). \end{aligned} \tag{7.20}$$

With this choice for the α_1 function, the anomaly is removed. However a significant ambiguity remains. Namely, the function α_2 together with parameters ν_1 and ν_2 remain undetermined. A particularly interesting case corresponds to the choice $\alpha_2 = 0$. This determines α_1. Of course, this also works the other way round: one can set $\alpha_1 = 0$ and derive expression for α_2. Therefore, two special cases, heuristically motivated, where one

of the counter-terms is vanishing, are worth studying:

$$\begin{aligned}\alpha_1 &= -1 + 4\frac{\mathbb{K}[\nu_1]\mathbb{K}[\nu_2]}{\mathbb{K}[1]^2} - 4(1+\beta)\frac{\mathbb{K}[2]\mathbb{K}[\nu_2]}{\mathbb{K}[1]^2} + 2\frac{\mathbb{K}[\nu_2]^2}{\mathbb{K}[1]^2} \\ &+ (4\beta - 1)\cos(\nu_2\bar{\mu}\gamma\bar{k}), \qquad (7.21)\\ \alpha_2 &= 0, \qquad (7.22)\end{aligned}$$

and

$$\begin{aligned}\alpha_1 &= 0, \qquad (7.23)\\ \alpha_2 &= -1 + \frac{1}{4}\frac{(\mathbb{K}[1])^2}{\mathbb{K}[\nu_1]\mathbb{K}[\nu_2]} + (1+\beta)\frac{\mathbb{K}[2]}{\mathbb{K}[\nu_1]} - \frac{1}{2}\frac{\mathbb{K}[\nu_2]}{\mathbb{K}[\nu_1]} \\ &- (\beta - 1/4)\frac{(\mathbb{K}[1])^2\cos(\nu_2\bar{\mu}\gamma\bar{k})}{\mathbb{K}[\nu_1]\mathbb{K}[\nu_2]}. \qquad (7.24)\end{aligned}$$

To conclude, at least one counter-term is necessary to fulfill the anomaly freedom conditions for the gravity sector.

7.3.3 The $\mathcal{B} = 0$ case

Another possible way to fix the ambiguity in the choice of the α_1 and α_2 functions could be to set $\mathcal{B} = 0$. With this restriction, anomaly cancellation is fulfilled by imposing $\mathcal{A}_2 = 0$ as $\mathcal{A}_1 \propto \mathcal{B} = 0$. As mentioned earlier, both $\mathcal{A}_2$ and $\mathcal{A}_1$ separately tend to zero in the classical limit, making this decomposition meaningful.

In this case, the Poisson bracket between the hamiltonian and diffeomorphism constraints is just $\{S^Q[N], D^Q[N^a]\} = 0$. The conditions $\mathcal{B} = 0$ and $\mathcal{A}_2 = 0$ can be translated into expressions for the α_1 and α_2 functions:

$$\begin{aligned}\alpha_1 &= -1 + 4(1-\beta)\frac{\mathbb{K}[2]\mathbb{K}[\nu_2]}{\mathbb{K}[1]^2} - 2\frac{\mathbb{K}[\nu_2]^2}{\mathbb{K}[1]^2} + (4\beta - 1)\cos(\nu_2\bar{\mu}\gamma\bar{k}), \qquad (7.25)\\ \alpha_2 &= -1 + \frac{2\mathbb{K}[2] - \mathbb{K}[\nu_2]}{\mathbb{K}[\nu_1]}. \qquad (7.26)\end{aligned}$$

The expressions for α_1 and α_2 are parametrized by the integers ν_1 and ν_2 only. However, the dependence upon ν_1 vanishes when α_2 is used in the hamiltonian constraint.

7.4 Introducing matter

We have shown that the gravity sector of vector perturbations with holonomy corrections can be made anomaly free. We will now extend this result by introducing scalar matter. The matter Hamiltonian does not depend on the Ashtekar connection and therefore should not be a subject of the holonomy corrections[1]. Furthermore, for vector perturba-

[1]However, as we will see in case of the scalar perturbations, the quantum counter-terms to the matter Hamiltonian may be necessary to fulfill the requirement of the anomaly freedom

tions, $\delta N = 0$. The matter Hamiltonian constraint is perturbed up to the second order as follows:

$$S_\varphi[N] = \int_\Sigma d^3x \bar{N}(C_\varphi^{(0)} + C_\varphi^{(2)}), \tag{7.27}$$

where

$$C_\varphi^{(0)} = \bar{p}^{3/2}\left[\frac{1}{2}\frac{\bar{\pi}^2}{\bar{p}^3} + V(\bar{\varphi})\right]. \tag{7.28}$$

The value of $C_\varphi^{(2)}$ is given by

$$\begin{aligned} C_\varphi^{(2)} &= \frac{1}{2}\frac{\delta\pi^2}{\bar{p}^{3/2}} + \frac{1}{2}\sqrt{\bar{p}}\delta^{ab}\partial_a\delta\varphi\partial_b\delta\varphi + \frac{1}{2}\bar{p}^{3/2}V_{,\varphi\varphi}(\bar{\varphi})\delta\varphi^2 \\ &+ \left(\frac{1}{2}\frac{\bar{\pi}^2}{\bar{p}^{3/2}} - \bar{p}^{3/2}V(\bar{\varphi})\right)\frac{\delta_c^k\delta_d^j\delta E_j^c\delta E_k^d}{4\bar{p}^2}, \end{aligned} \tag{7.29}$$

where we have used the condition $\delta_a^i\delta E_i^a = 0$. The matter diffeomorphism constraint is given by:

$$D_\varphi[N^a] = \int_\Sigma d^3x\delta N^a\bar{\pi}(\partial_a\delta\varphi). \tag{7.30}$$

The total Hamiltonian and diffeomorphism constraints are

$$S_{tot}[N] = S^Q[N] + S_\varphi[N], \tag{7.31}$$

$$D_{tot}[N^a] = D^Q[N^a] + D_\varphi[N^a]. \tag{7.32}$$

The resulting Poisson brackets are the following:

$$\{S_{tot}[N_1], S_{tot}[N_1]\} = 0, \tag{7.33}$$

$$\{D_{tot}[N_1^a], D_{tot}[N_2^a]\} = 0, \tag{7.34}$$

$$\begin{aligned} \{S_{tot}[N], D_{tot}[N^a]\} &= \frac{\bar{N}}{\sqrt{\bar{p}}}\mathcal{B}D^Q[N^a] + \frac{\bar{N}}{\kappa\sqrt{\bar{p}}}\int_\Sigma d^3x\delta N^c\delta_c^k(\partial_d\delta E_k^d)\delta E_k^d\mathcal{A} \\ &+[\cos(\nu_2\bar{\mu}\gamma\bar{k}) - 1]\frac{\sqrt{\bar{p}}}{2}\left(\frac{\bar{\pi}^2}{2\bar{p}^3} - V(\bar{\varphi})\right)\int_\Sigma d^3x\bar{N}\partial_c(\delta N^a)\delta_a^j\delta E_j^c \\ &+\frac{\bar{\pi}}{\bar{p}^{3/2}}\int_\Sigma d^3x\bar{N}(\partial_a\delta N^a)\delta\pi - \bar{p}^{3/2}V_\varphi(\bar{\varphi})\int_\Sigma d^3x\bar{N}(\partial_a\delta N^a)\delta\varphi. \end{aligned} \tag{7.35}$$

Anomaly freedom requires $\mathcal{B} = 0$, $\mathcal{A} = 0$, $\nu_2 = 0$ (classical diffeomorphism constraint), and also $\delta\varphi = 0 = \delta\pi$. The latter conditions $\delta\varphi = 0 = \delta\pi$ are due to the fact that metric scalar perturbations are not considered. Consistently, scalar field perturbations are vanishing too. In fact, one could set $\delta\varphi = 0 = \delta\pi$ from the very beginning but, without assuming this, it can be shown that the condition $\delta\varphi = 0 = \delta\pi$ in fact resulting from the anomaly freedom.

The associated counter-terms are given by (7.25) and (7.26) with $\nu_2 = 0$. Two non-vanishing counter-terms are required in contrast to the gravity sector, where only one

counter-term was sufficient to fulfill anomaly freedom conditions. The integer ν_1 remains undetermined but the dependence upon this parameter cancels out in the hamiltonian constraint. Namely, applying the counter-terms (7.25) and (7.26) with $\nu_2 = 0$, we find that the anomaly free Hamiltonian constraint is given by:

$$S^{Q}_{free}[N] = \frac{1}{2\kappa}\int_{\Sigma} d^3x \left[\bar{N}(C^{(0)}_{free} + C^{(2)}_{free})\right], \tag{7.36}$$

where

$$\begin{aligned} C^{(0)}_{free} &= -6\sqrt{\bar{p}}\,(\mathbb{K}[1])^2, & (7.37)\\ C^{(2)}_{free} &= -\frac{1}{2\bar{p}^{3/2}}\left[4(1-\beta)\mathbb{K}[2]\bar{k} - 2\bar{k}^2 + (4\beta-1)\mathbb{K}[1]^2\right]\times \\ &\times\ (\delta E^c_j \delta E^d_k \delta^k_c \delta^j_d) + \sqrt{\bar{p}}(\delta K^j_c \delta K^k_d \delta^c_k \delta^d_j) \\ &-\ \frac{2}{\sqrt{\bar{p}}}\left(2\mathbb{K}[2] - \bar{k}\right)(\delta E^c_j \delta K^j_c).) & (7.38) \end{aligned}$$

The gravitational diffeomorphism constraint holds its classical form($\nu_2 = 0$). This is in agreement with LQG expectations. Interestingly, this can also be obtained here as a result of anomaly freedom.

The obtained anomaly-free Hamiltonian (7.36) is determined up to the choice of the $\bar{\mu}$ functions. There are no other remaining ambiguities. The $\bar{\mu}$ function appears in definition of the $\mathbb{K}[n]$ function. Because of this, there is also explicit appearance of the factor β in equation (7.38). The choice $\beta = -1/2$ is preferred by various considerations [43]. For this choice of the β parameter, the remaining freedom is a parameter of proportionality in relation $\bar{\mu} \propto \bar{p}^{-1/2}$. This parameter can be written as $\sqrt{\Delta}$, so $\bar{\mu} = \sqrt{\Delta/\bar{p}}$. The parameter Δ has the interpretation of a physical area, around which the elementary holonomy is defined. It is expected that $\Delta \sim l^2_{Pl}$, where l_{Pl} is the Planck length. However, determination of the accurate value of Δ is a subject to empirical verifications.

It is worth noticing about the Hamiltonian constraint (7.36) that the effective holonomy corrections, due to the counter-terms, are no longer *almost periodic functions*, defined as follows [18]

$$f(\bar{k}) = \sum_{n} \xi_n e^{i\bar{\mu}\gamma\bar{k}n}. \tag{7.39}$$

In this expression, n runs over a finite number of integers and $\xi_n \in \mathbb{C}$. This does not lead to any problem at the classical level. However, difficulties may appear when going to the quantum theory on lattice states. This is because the quantum operator corresponding to $\bar{k}$ does not exist in contrast to the $\mathbb{K}[n]$ functions, which are almost periodic functions. This problem does not exist if the gravitational sector, without any matter content, is considered alone. However, the diffeomorphism constraint then has to be holonomy corrected, as studied previously. In such a case, the background terms in the anomaly-free gravitational Hamiltonian are almost periodic functions. The loop quantization can therefore be directly performed.

7.5 Gauge invariant variable

The coordinate transformation $x^\mu \to x^\mu + \xi^\mu$ generates a tensor gauge transformation. In the case of vector modes, the coordinate transformation is parametrized by the shift vector $N^a = \xi^a$, where $\xi^a{}_{,a} = 0$, Therefore, the resulting gauge transformation is generated by the diffeomorphism constraint $\delta_\xi f = \{f, D^Q[\xi^a]\}$. The corresponding transformations for the canonical variables are:

$$\delta_\xi(\delta E^a_i) = \{\delta E^a_i, D^Q[\xi^a]\} = -\bar{p}\partial_i\xi^a, \tag{7.40}$$
$$\delta_\xi(\delta K^i_a) = \{\delta K^i_a, D^Q[\xi^a]\} = \mathbb{K}[\nu_2]\partial_a\xi^i. \tag{7.41}$$

Based on the equation of motion $\dot{E}^a_i = \{E^a_i, H_G\}$, and the definition (7.1), one finds the expression of δK^i_a. The dot means differentiation with respect to the conformal time since we have chosen $\bar{N} = \sqrt{\bar{p}}$. Using equations (7.40) and (7.41) one finds:

$$\delta_\xi F^a = \xi^a, \tag{7.42}$$
$$\delta_\xi S^a = \dot{\xi}^a + (2\mathbb{K}[2] - \mathbb{K}[\nu_1](1+\alpha_2) - \mathbb{K}[\nu_2])\xi^a. \tag{7.43}$$

Based on this, one can define a gauge invariant variable

$$\sigma^a := S^a - \dot{F}^a - \underbrace{(2\mathbb{K}[2] - \mathbb{K}[\nu_1](1+\alpha_2) - \mathbb{K}[\nu_2])}_{=-\mathcal{B}} F^a, \tag{7.44}$$

such that $\delta_\xi\sigma^a = 0$.

7.6 Equations of motion

In this section we derive an equation of motion for the gauge-invariant variable found in the previous section.

For the sake of completeness, we recall that equations of motion for the background part are:

$$\dot{\bar{p}} = \bar{N}2\sqrt{\bar{p}}(\mathbb{K}[2]), \tag{7.45}$$
$$\dot{\bar{k}} = -\frac{\bar{N}}{\sqrt{\bar{p}}}\left[\frac{1}{2}(\mathbb{K}[1])^2 + \bar{p}\frac{\partial}{\partial\bar{p}}(\mathbb{K}[1])^2\right] + \frac{\kappa}{3V_0}\left(\frac{\partial\bar{H}_\varphi}{\partial\bar{p}}\right), \tag{7.46}$$

where $\bar{H}_\varphi = V_0\bar{N}C^{(0)}_\varphi$ and $\bar{N} = \sqrt{\bar{p}}$. For a free scalar field, an analytical solution to these equations can be found [58]:

$$\bar{p} = \left(\frac{1}{6}\gamma^2\Delta\pi^2_\varphi\kappa + \frac{3}{2}\kappa\pi^2_\varphi t^2\right)^{1/3}. \tag{7.47}$$

This solution represents a symmetric bounce.

The diffeomorphism constraint $\frac{\delta}{\delta\delta N^a} D_{\rm tot}[N^a] = 0$ leads to the equation

$$\bar{p}(\partial_k \delta K^k_a) + (\mathbb{K}[\nu_2])\, \delta^k_a (\partial_d \delta E^d_k) = \kappa\bar{\pi}\partial_a(\delta\varphi). \tag{7.48}$$

Using the symmetrized variables

$$\begin{aligned}
\delta K^{(i}{}_{a)} &= \frac{1}{2}\left[(2\mathbb{K}[2] - \mathbb{K}[\nu_1](1+\alpha_2))\left(F_{a,}{}^{i} + F^{i}{}_{,a}\right)\right. \\
&+ \left.\left(F_{a,}{}^{i} + F^{i}{}_{,a}\right)^{\cdot} - \left(S_{a,}{}^{i} + S^{i}{}_{,a}\right)\right] \\
&= -\frac{1}{2}\left(\sigma_{a,}{}^{i} + \sigma^{i}{}_{,a}\right) + \frac{1}{2}\mathbb{K}[\nu_2]\left(F_{a,}{}^{i} + F^{i}{}_{,a}\right),
\end{aligned} \tag{7.49}$$

and

$$\delta E^{(i}{}_{a)} = -\bar{p}\frac{1}{2}\left(F_{a,}{}^{i} + F^{i}{}_{,a}\right), \tag{7.50}$$

equation (8.3) can be rewritten as

$$-\frac{\bar{p}}{2}\nabla^2\sigma_a = \kappa\bar{\pi}\partial_a(\delta\varphi). \tag{7.51}$$

Because $\delta\varphi = 0$ (from the anomaly-free condition), the symmetric diffeomorphism constraint simplifies to the Laplace equation $\nabla^2\sigma_a = 0$. Since, the spatial slice is flat ($\Sigma = \mathbb{R}^3$) there are no boundary conditions on σ_a. This restricts the possible solutions of the Laplace equation to $\sigma_a = b_a + d^c_a x_c$, where b_a and d^c_a are sets of constants. However, because σ_a is a perturbation (there is no contribution from the zero mode),

$$\int_\Sigma d^3x\sigma_a = 0, \tag{7.52}$$

as required from the consistency of the perturbative expansion. Additionally, this is the reason why the first order perturbation of the Hamiltonian is vanishing, $\int_\Sigma C^{(1)} d^3x = 0$. Condition (7.52) implies $b_a = 0$ and $d^c_a = 0$, which leads to $\sigma_a = 0$. This shows that our gauge invariant variable σ_a is identically equal to zero in absence of vector matter, in agreement with earlier studies [59]. This can also be proved by expanding σ_a into Fourier modes.

In order to have non-vanishing (physical) vector modes σ_a, a source term in equation (7.51) therefore has to be present. With "vector matter", this reads as [33]:

$$-\frac{1}{2\bar{p}}\nabla^2\sigma_a = 8\pi G(\rho + P)V_a, \tag{7.53}$$

where ρ and P are the energy density and pressure of the vector matter and V_a is a matter perturbation vector. If $(\rho + P)V_a \neq 0$ then $\sigma_a \neq 0$ so physical vector perturbations are expected. However, it should be pointed out that proving that the formulation remains anomaly-free in presence of the vector matter remains an open issue. This could

be checked, *e.g.*, by introducing an electromagnetic field in the Hamiltonian formulation [60]. We leave this problem to be analyzed elsewhere.

Due to the Gauss constraint, we introduce the symmetrized variable

$$\mathfrak{S}^i_a := \sigma^i{}_{,a} + \sigma_{a,}{}^i. \tag{7.54}$$

The equation of motion for this variable reads as:

$$-\frac{1}{2}\frac{d}{d\eta}\mathfrak{S}^i_a - \frac{1}{2}(2\mathbb{K}[2] + \mathcal{B})\mathfrak{S}^i_a + \mathcal{A}F^{(i}{}_{,a)} = \kappa\bar{p}\delta T^{(i}_{a)}, \tag{7.55}$$

where

$$\delta T^i_a = \frac{1}{\bar{p}}\left[\left(\frac{1}{3V_0}\frac{\partial\bar{H}_\varphi}{\partial\bar{p}}\right)\left(\frac{\delta E^c_j\delta^j_a\delta^i_c}{\bar{p}}\right) + \frac{\delta H_\varphi}{\delta\delta E^a_i}\right]. \tag{7.56}$$

For scalar matter $\delta T^i_a = 0$. The same holds for tensor modes [51] (the reasons are the same because $\delta^i_a\delta E^a_i = 0$ and $\delta N = 0$). When imposing the anomaly freedom conditions $\mathcal{A} = 0$ and $\mathcal{B} = 0$, equation (7.55) simplifies to

$$-\frac{1}{2}\frac{d}{d\eta}\mathfrak{S}^i_a - \frac{1}{2}\underbrace{(2\mathbb{K}[2])}_{=\frac{1}{\bar{p}}\frac{d\bar{p}}{d\eta}}\mathfrak{S}^i_a = 0, \tag{7.57}$$

with fully determined coefficients. Of course without vector matter, as discussed above, the variable $\mathfrak{S}^i_a$ is equal to zero and the equation (7.57) is trivially satisfied. However, the presence on a non-vanishing contribution from V_a allows for non-trivial solutions of equation (7.57). In such a case, equation (7.57) leads to:

$$\mathfrak{S}^i_a = \frac{\text{const}}{\bar{p}} = \frac{\text{const}}{a^2}. \tag{7.58}$$

For a symmetric bounce driven by a free scalar field:

$$\mathfrak{S}^i_a \propto \frac{1}{\left(\frac{2\pi}{3\sqrt{3}}\gamma^3 l^2_{Pl} + t^2\right)^{1/3}}. \tag{7.59}$$

This evolution is smooth through the bounce. The amplitude of the perturbations grows during the contraction and decreases in the expanding phase. The maximum amplitude is reached at the transition point (bounce). Moreover, this evolution is independent on the length of the considered mode, as can be seen by performing a Fourier transform of the function σ_a. Because of this, there is significant difference with respect to tensor and scalar perturbations. For the scalar and tensor perturbations, the evolution is different depending on whether the mode length is shorter or longer that the Hubble horizon. In particular, on super-horizon scales, the amplitude of the scalar and tensor perturbations

is *frozen*. In contrast, for vector modes there is no such effect. Therefore, in an expanding universe, the amplitude of vector modes decreases with respect to the super-horizon tensor and scalar perturbations. The contribution from vector modes becomes negligible during the expansion phase. However, the situation reverses in the contracting phase, before the bounce. Then, the amplitude of the vector perturbations grows with respect to the super-horizon tensor and scalar perturbations. Therefore, on very large scales vector perturbations can play an important role, *e.g.* leading to the generation of large scale magnetic fields [61]. This could lead to a new tool to explore physics of the (very) early universe.

7.7 Conclusions

In this chapter we have studied the issue of anomaly cancellation for vector modes with holonomy corrections in LQC. Our strategy is based on the introduction of counter-terms in the holonomy-corrected Hamiltonian constraint. In our study, we have also introduced possible holonomy corrections to the diffeomorphism constraint. We have shown, first, that the anomaly cancellation cannot be achieved without counter-terms. Holonomy corrections to the diffeomorphism constraint do not help significantly to fulfill the anomaly freedom conditions, that are anyway satisfied up to the fourth order in the canonical variable $\bar{k}$. Then, we have studied the anomaly issue for the gravitational sector with two counter-terms. We have shown that the conditions of anomaly freedom can be met with at least one non-vanishing counter-term. The resulting effective holonomy corrections are almost periodic functions only if the diffeomorphism constraint is holonomy corrected. Subsequently, we have investigated the issue of anomaly cancellation when a matter scalar field is added. In this case, closure conditions are more restrictive and fully determine the form of the resulting Hamiltonian constraint. Moreover, this requires that the diffeomorphism constraint holds its classical form, in agreement with LQG expectations. Because of this, the effective holonomy corrections, which take into account contributions from the counter-terms, are no more almost periodic functions. We have found the gauge invariant variable and the corresponding equation of motion. The solution to this equation were also given. We have analyzed this solution for the symmetric bounce model to point out that the vector perturbations smoothly pass through the bounce, where their amplitude reaches its maximum but finite value.

Chapter 8

Scalar perturbations

Scalar perturbations are the most complicated type of cosmological perturbations. This is because they are coupled with the perturbations of the scalar field. In this section we will introduce anomaly free formulation of the scalar perturbations with the holonomy corrections. We will determine the gauge invariant variables and derive the corresponding equations of motion.

8.1 Scalar perturbations with holonomy corrections

For scalar perturbations, the holonomy-modified version of the Hamiltonian constraint (4.79) can be written as:

$$S^{Q}[N] = \frac{1}{2\kappa}\int_{\Sigma} d^3x \left[\bar{N}(C^{(0)} + C^{(2)}) + \delta N C^{(1)}\right], \tag{8.1}$$

where

$$\begin{aligned}
C^{(0)} &= -6\sqrt{\bar{p}}(\mathbb{K}[1])^2, \\
C^{(1)} &= -4\sqrt{\bar{p}}\left(\mathbb{K}[s_1] + \alpha_1\right)\delta_j^c \delta K_c^j - \frac{1}{\sqrt{\bar{p}}}\left(\mathbb{K}[1]^2 + \alpha_2\right)\delta_c^j \delta E_j^c \\
&+ \frac{2}{\sqrt{\bar{p}}}(1+\alpha_3)\partial_c \partial^j \delta E_j^c, \\
C^{(2)} &= \sqrt{\bar{p}}(1+\alpha_4)\delta K_c^j \delta K_d^k \delta_k^c \delta_j^d - \sqrt{\bar{p}}(1+\alpha_5)(\delta K_c^j \delta_j^c)^2 \\
&- \frac{2}{\sqrt{\bar{p}}}\left(\mathbb{K}[s_2] + \alpha_6\right)\delta E_j^c \delta K_c^j - \frac{1}{2\bar{p}^{3/2}}\left(\mathbb{K}[1]^2 + \alpha_7\right)\delta E_j^c \delta E_k^d \delta_c^k \delta_d^j \\
&+ \frac{1}{4\bar{p}^{3/2}}\left(\mathbb{K}[1]^2 + \alpha_8\right)(\delta E_j^c \delta_c^j)^2 - \frac{1}{2\bar{p}^{3/2}}(1+\alpha_9)\delta^{jk}(\partial_c \delta E_j^c)(\partial_d \delta E_k^d).
\end{aligned} \tag{8.2}$$

The standard holonomy corrections are parametrized by two integers s_1 and s_2. The α_i are counter-terms, which are introduced to remove anomalies. Those factors are defined

so that they vanish in the classical limit ($\bar{\mu} \to 0$). The counter-terms could be, in general, functions of all the canonical variables. We however assume here that they are functions of the gravitational background variables only.

In our approach, the diffeomorphism constraint holds the classical form

$$D[N^a] = \frac{1}{\kappa}\int_\Sigma d^3x \delta N^c \left[\bar{p}\partial_c(\delta^d_k \delta K^k_d) - \bar{p}(\partial_k \delta K^k_c) - \bar{k}\delta^k_c(\partial_d \delta E^d_k)\right]. \tag{8.3}$$

In general, the diffeomorphism constraint could also be holonomy corrected. this possibility was studied, *e.g.*, in [39]. However, in LQG the diffeomorphism constraint is satisfied at the classical level. Therefore, if LQC is to be considered as a specific model of LQG, the diffeomorphism constraint should naturally hold its classical form. Because of this, in this paper, the diffeomorphism constraint is not modified by the holonomies. It is worth stressing, that the classicality of the diffeomorphism constraint is also imposed by the requirement of anomaly cancelation. Namely, if one replaces $\bar{k} \to \mathbb{K}[n]$ in (8.3), the condition $n = 0$ would anyway be required by the introduction of scalar matter. In the previous chapter, the same condition was obtained for vector modes with holonomy corrections.

Let us now calculate the possible Poisson brackets for the constraints $S^Q[N]$ and $D[N^a]$.

8.1.1 The $\{S^Q, D\}$ bracket

Using the definition of the Poisson bracket (4.8), we derive:

$$\begin{aligned}\left\{S^Q[N], D[N^a]\right\} &= -S^Q\left[\delta N^a \partial_a \delta N\right] + \mathcal{B}\, D[N^a] \\ &+\frac{\sqrt{\bar{p}}}{\kappa}\int_\Sigma d^3x \delta N^a(\partial_a \delta N)\mathcal{A}_1 + \frac{\bar{N}\sqrt{\bar{p}}\bar{k}}{\kappa}\int_\Sigma d^3x \delta N^a(\partial_i \delta K^i_a)\mathcal{A}_2 \\ &+\frac{\bar{N}}{\kappa\sqrt{\bar{p}}}\int_\Sigma d^3x \delta N^i(\partial_a \delta E^a_i)\mathcal{A}_3 + \frac{\bar{N}}{2\kappa\sqrt{\bar{p}}}\int_\Sigma d^3x (\partial_a \delta N^a)(\delta E^b_i \delta^i_b)\mathcal{A}_4,\end{aligned} \tag{8.4}$$

where

$$\mathcal{B} = \frac{\bar{N}}{\sqrt{\bar{p}}}\left[-2\mathbb{K}[2] + \bar{k}(1+\alpha_5) + \mathbb{K}[s_2] + \alpha_6\right], \tag{8.5}$$

and

$$\mathcal{A}_1 = 2\bar{k}(\mathbb{K}[s_1] + \alpha_1) + \alpha_2 - 2\mathbb{K}[1]^2, \tag{8.6}$$

$$\mathcal{A}_2 = \alpha_5 - \alpha_4, \tag{8.7}$$

$$\begin{aligned}\mathcal{A}_3 &= -\mathbb{K}[1]^2 - \bar{p}\frac{\partial}{\partial\bar{p}}\mathbb{K}[1]^2 - \frac{1}{2}\alpha_7 \\ &+ \bar{k}(-2\mathbb{K}[2] + \bar{k}(1+\alpha_5) + 2\mathbb{K}[s_2] + 2\alpha_6),\end{aligned} \tag{8.8}$$

$$\mathcal{A}_4 = \alpha_8 - \alpha_7. \tag{8.9}$$

The functions $\mathcal{A}_1, \ldots, \mathcal{A}_4$ are the first anomalies coming from effective nature of the Hamiltonian constraint. Later, we will set them to zero so as to fulfill the requirement of anomaly freedom. This will lead to constraints on the form of the counter-terms.

Beside the anomalies, the $\left\{S^Q, D\right\}$ bracket contains the $-S^Q\left[\delta N^a \partial_a \delta N\right]$ term, which is expected classically. There is also additional contribution from the diffeomorphism constraint $\mathcal{B}\ D[N^a]$. This term is absent in the classical theory. This is however consistent as, for $\bar{\mu} \to 0$, the $\mathcal{B}$ function tends to zero.

8.1.2 The $\left\{S^Q, S^Q\right\}$ bracket

The next bracket is:

$$\begin{aligned}
\left\{S^Q[N_1], S^Q[N_2]\right\} &= (1+\alpha_3)(1+\alpha_5) D\left[\frac{\bar{N}}{\bar{p}} \partial^a (\delta N_2 - \delta N_1)\right] \\
&+ \frac{\bar{N}}{\kappa} \int_\Sigma d^3x \partial^a (\delta N_2 - \delta N_1)(\partial_i \delta K_a^i)(1+\alpha_3)\mathcal{A}_5 \\
&+ \frac{\bar{N}}{\kappa \bar{p}} \int_\Sigma d^3x (\delta N_2 - \delta N_1)(\partial^i \partial_a \delta E_i^a)\mathcal{A}_6 \\
&+ \frac{\bar{N}}{\kappa} \int_\Sigma d^3x (\delta N_2 - \delta N_1)(\delta_i^a \delta K_a^i)\mathcal{A}_7 \\
&+ \frac{\bar{N}}{\kappa \bar{p}} \int_\Sigma d^3x (\delta N_2 - \delta N_1)(\delta_a^i \delta E_i^a)\mathcal{A}_8, \qquad (8.10)
\end{aligned}$$

where

$$\begin{aligned}
\mathcal{A}_5 &= \alpha_5 - \alpha_4, \qquad (8.11) \\
\mathcal{A}_6 &= (1+\alpha_9)(\mathbb{K}[s_1]+\alpha_1) - (1+\alpha_3)(\mathbb{K}[s_2]+\alpha_6) + \mathbb{K}[2](1+\alpha_3) \\
&- 2\mathbb{K}[2]\bar{p}\frac{\partial \alpha_3}{\partial \bar{p}} + \frac{1}{2}\left(\mathbb{K}[1]^2 + 2\bar{p}\frac{\partial}{\partial \bar{p}}\mathbb{K}[1]^2\right)\frac{\partial \alpha_3}{\partial \bar{k}} - \bar{k}(1+\alpha_3)(1+\alpha_5), \qquad (8.12) \\
\mathcal{A}_7 &= 4\mathbb{K}[2]\bar{p}\frac{\partial}{\partial \bar{p}}(\mathbb{K}[s_1]+\alpha_1) - \left(\mathbb{K}[1]^2 + 2\bar{p}\frac{\partial}{\partial \bar{p}}\mathbb{K}[1]^2\right)\frac{\partial}{\partial \bar{k}}(\mathbb{K}[s_1]+\alpha_1) \\
&+ \left(1 + \frac{3}{2}\alpha_5 - \frac{1}{2}\alpha_4\right)(\mathbb{K}[1]^2+\alpha_2) - 2(\mathbb{K}[s_2]+\alpha_6)(\mathbb{K}[s_1]+\alpha_1) \\
&+ 2\mathbb{K}[2](\mathbb{K}[s_1]+\alpha_1), \qquad (8.13) \\
\mathcal{A}_8 &= \frac{1}{2}(\mathbb{K}[s_2]+\alpha_6)(\mathbb{K}[1]^2+\alpha_2) - (\mathbb{K}[s_1]+\alpha_1)(\mathbb{K}[1]^2+\alpha_7) \\
&+ \frac{3}{2}(\mathbb{K}[s_1]+\alpha_1)(\mathbb{K}[1]^2+\alpha_8) - \frac{1}{2}\mathbb{K}[2](\mathbb{K}[1]^2+\alpha_2) \\
&+ \mathbb{K}[2]\bar{p}\frac{\partial}{\partial \bar{p}}(\mathbb{K}[1]^2+\alpha_2) - \frac{1}{4}\left(\mathbb{K}[1]^2 + 2\bar{p}\frac{\partial}{\partial \bar{p}}\mathbb{K}[1]^2\right)\frac{\partial}{\partial \bar{k}}(\mathbb{K}[1]^2+\alpha_2). \qquad (8.14)
\end{aligned}$$

The $\mathcal{A}_5, \ldots, \mathcal{A}_8$ are the next four anomalies. Moreover, the diffeomorphism constraint is multiplied by the factor $(1+\alpha_3)(1+\alpha_5)$.

8.1.3 The $\{D, D\}$ bracket

The Poisson bracket between the diffeomorphism constraints is:

$$\{D[N_1^a], D[N_2^a]\} = 0. \tag{8.15}$$

8.2 Scalar matter

In this section, we introduce scalar matter. The scalar matter diffeomorphism constraint is

$$D_\varphi[N^a] = \int_\Sigma \delta N^a \bar{\pi}(\partial_a \delta\varphi). \tag{8.16}$$

The scalar matter Hamiltonian can be expressed as:

$$S_\varphi^Q[N] = S_\varphi[\bar{N}] + S_\varphi[\delta N],$$

where

$$S_\varphi[\bar{N}] = \int_\Sigma d^3x \bar{N} \left[\left(C_\pi^{(0)} + C_\varphi^{(0)} \right) + \left(C_\pi^{(2)} + C_\nabla^{(2)} + C_\varphi^{(2)} \right) \right], \tag{8.17}$$

$$S_\varphi[\delta N] = \int_\Sigma d^3\delta N \left[C_\pi^{(1)} + C_\varphi^{(1)} \right]. \tag{8.18}$$

The factors in equations (8.17) and (8.18) are

$$
\begin{aligned}
C_\pi^{(0)} &= \frac{\bar{\pi}^2}{2\bar{p}^{3/2}}, \\
C_\varphi^{(0)} &= \bar{p}^{3/2} V(\bar{\varphi}), \\
C_\pi^{(1)} &= \frac{\bar{\pi}\delta\pi}{\bar{p}^{3/2}} - \frac{\bar{\pi}^2}{2\bar{p}^{3/2}} \frac{\delta_c^j \delta E_j^c}{2\bar{p}}, \\
C_\varphi^{(1)} &= \bar{p}^{3/2} \left[V_{,\varphi}(\bar{\varphi})\delta\varphi + V(\bar{\varphi}) \frac{\delta_c^j \delta E_j^c}{2\bar{p}} \right], \\
C_\pi^{(2)} &= \frac{1}{2}\frac{\delta\pi^2}{\bar{p}^{3/2}} - \frac{\bar{\pi}\delta\pi}{\bar{p}^{3/2}} \frac{\delta_c^j \delta E_j^c}{2\bar{p}} + \frac{1}{2}\frac{\bar{\pi}^2}{\bar{p}^{3/2}} \left[\frac{(\delta_c^j \delta E_j^c)^2}{8\bar{p}^2} + \frac{\delta_c^k \delta_d^j \delta E_j^c \delta E_k^d}{4\bar{p}^2} \right], \qquad (8.19) \\
C_\nabla^{(2)} &= \frac{1}{2}\sqrt{\bar{p}}(1+\alpha_{10})\delta^{ab}\partial_a\delta\varphi\partial_b\delta\varphi, \\
C_\varphi^{(2)} &= \frac{1}{2}\bar{p}^{3/2} V_{,\varphi\varphi}(\bar{\varphi})\delta\varphi^2 + \bar{p}^{3/2} V_{,\varphi}(\bar{\varphi})\delta\varphi \frac{\delta_c^j \delta E_j^c}{2\bar{p}} \qquad (8.20) \\
&+ \bar{p}^{3/2} V(\bar{\varphi}) \left[\frac{(\delta_c^j \delta E_j^c)^2}{8\bar{p}^2} - \frac{\delta_c^k \delta_d^j \delta E_j^c \delta E_k^d}{4\bar{p}^2} \right]. \qquad (8.21)
\end{aligned}
$$

Here, we have introduced the counter-term α_{10} in the factor $C_\nabla^{(2)}$. Thanks to this, the Poisson bracket between two matter Hamiltonians takes the following form:

$$
\left\{ S_\varphi^Q[N_1], S_\varphi^Q[N_2] \right\} = (1+\alpha_{10}) D_\varphi \left[\frac{\bar{N}}{\bar{p}} \partial^a (\delta N_2 - \delta N_1) \right]. \qquad (8.22)
$$

As will be explained later, the appearance of the front-factor $(1+\alpha_{10})$ will allow us to close the algebra of total constraints. In principle, other prefactors could have been expected, however they do not help removing anomalies.

8.2.1 Total constraints

Total Hamiltonian and diffeomorphism constraints are the following:

$$
\begin{aligned}
S_{tot}[N] &= S^Q[N] + S_\varphi^Q[N], \qquad (8.23) \\
D_{tot}[N^a] &= D[N^a] + D_\varphi[N^a]. \qquad (8.24)
\end{aligned}
$$

The Poisson bracket between two total diffeomorphism constraints is vanishing:

$$
\{ D_{tot}[N_1^a], D_{tot}[N_2^a] \} = 0. \qquad (8.25)
$$

A bracket between the total Hamiltonian and diffeomorphism constraints can be decomposed as follows:

$$\begin{aligned}\{S_{tot}[N], D_{tot}[N^a]\} &= \left\{S^Q_\varphi[N], D_{tot}[N^a]\right\} + \left\{S^Q[N], D[N^a]\right\} \\ &+ \left\{S^Q[N], D_\varphi[N^a]\right\}. \end{aligned} \tag{8.26}$$

The first bracket in the sum (8.26) is given by

$$\left\{S^Q_\varphi[N], D_{tot}[N^a]\right\} = -S^Q_\varphi[\delta N^a \partial_a \delta N]. \tag{8.27}$$

The second contribution to Eq. (8.26) is given by (8.4), while the last contribution is vanishing:

$$\left\{S^Q[N], D_\varphi[N^a]\right\} = 0. \tag{8.28}$$

The Poisson bracket between the two total Hamiltonian constraints can be decomposed in the following way:

$$\begin{aligned}\{S_{tot}[N_1], S_{tot}[N_2]\} &= \left\{S^Q[N_1], S^Q[N_2]\right\} + \left\{S^Q_\varphi[N_1], S^Q_\varphi[N_2]\right\} \\ &+ \left[\left\{S^Q[N_1], S^Q_\varphi[N_2]\right\} - (N_1 \leftrightarrow N_2)\right]. \end{aligned} \tag{8.29}$$

The contribution from the last brackets can be expressed as

$$\begin{aligned}&\left\{S^Q[N_1], S^Q_\varphi[N_2]\right\} - (N_1 \leftrightarrow N_2) = \\ &= \frac{1}{2}\int_\Sigma d^3x \bar{N}(\delta N_2 - \delta N_1)\left(\frac{\bar{\pi}^2}{2\bar{p}^3} - V(\bar{\varphi})\right)(\partial_c \partial^j \delta E^c_j)\mathcal{A}_9 \\ &+3\int_\Sigma d^3x \bar{N}(\delta N_2 - \delta N_1)\left(\frac{\bar{\pi}\delta\pi}{\bar{p}^2} - \bar{p}V_\varphi(\bar{\varphi})\delta\varphi\right)\mathcal{A}_{10} \\ &+\int_\Sigma d^3x \bar{N}(\delta N_2 - \delta N_1)(\delta^c_j \delta K^c_j)\left(\frac{\bar{\pi}^2}{2\bar{p}^3} - V(\bar{\varphi})\right)\bar{p}\mathcal{A}_{11} \\ &+\frac{1}{2}\int_\Sigma d^3x \bar{N}(\delta N_2 - \delta N_1)(\delta^j_c \delta E^c_j)\left(\frac{\bar{\pi}^2}{2\bar{p}^3}\right)\mathcal{A}_{12} \\ &+\frac{1}{2}\int_\Sigma d^3x \bar{N}(\delta N_2 - \delta N_1)(\delta^j_c \delta E^c_j)V(\bar{\varphi})\mathcal{A}_{13}, \end{aligned} \tag{8.30}$$

where

$$\mathcal{A}_9 = \frac{\partial \alpha_3}{\partial \bar{k}}, \tag{8.31}$$

$$\mathcal{A}_{10} = \mathbb{K}[2] - \mathbb{K}[s_1] - \alpha_1, \tag{8.32}$$

$$\mathcal{A}_{11} = -\frac{\partial}{\partial \bar{k}}(\mathbb{K}[s_1] + \alpha_1) + \frac{3}{2}(1 + \alpha_5) - \frac{1}{2}(1 + \alpha_4), \tag{8.33}$$

$$\mathcal{A}_{12} = -\frac{1}{2}\frac{\partial}{\partial \bar{k}}(\mathbb{K}[1]^2 + \alpha_2) + 5(\mathbb{K}[s_1] + \alpha_1) - 5\mathbb{K}[2] + \mathbb{K}[s_2] + \alpha_6, \tag{8.34}$$

$$\mathcal{A}_{13} = \frac{1}{2}\frac{\partial}{\partial \bar{k}}(\mathbb{K}[1]^2 + \alpha_2) + \mathbb{K}[s_1] + \alpha_1 - \mathbb{K}[2] - \mathbb{K}[s_2] - \alpha_6. \tag{8.35}$$

The functions $\mathcal{A}_9, \ldots, \mathcal{A}_{13}$ are the last five anomalies.

8.3 Anomaly freedom

The requirement of anomaly freedom is equivalent to the conditions $\mathcal{A}_i = 0$ for $i = 1, \ldots, 13$.

Let us start from the condition $\mathcal{A}_9 = 0$. Since α_3 cannot be a constant, this condition implies $\alpha_3 = 0$. The condition $\mathcal{A}_{10} = 0$ gives $\alpha_1 = \mathbb{K}[2] - \mathbb{K}[s_1]$. Using this, the condition $\mathcal{A}_1 = 0$, can be written as $\alpha_2 = 2\mathbb{K}[1]^2 - 2\bar{k}\mathbb{K}[2]$. The conditions $\mathcal{A}_2 = 0$ and $\mathcal{A}_5 = 0$ are equivalent and lead to $\alpha_4 = \alpha_5$. Based on this, the requirement $\mathcal{A}_{11} = 0$, leads to:

$$1 + \alpha_4 = \frac{\partial \mathbb{K}[2]}{\bar{k}} = \cos(2\bar{\mu}\gamma\bar{k}) =: \Omega. \tag{8.36}$$

For the sake of simplicity we have defined here the Ω-function. With use of this, the condition $\mathcal{A}_6 = 0$ leads to

$$\alpha_6 = \mathbb{K}[2](2 + \alpha_9) - \mathbb{K}[s_2] - \bar{k}\Omega. \tag{8.37}$$

So, equation (8.34) simplifies to

$$\mathcal{A}_{12} = \alpha_9 \mathbb{K}[2]. \tag{8.38}$$

Therefore, requiring $\mathcal{A}_{12} = 0$ is equivalent to the condition $\alpha_9 = 0$. Furthermore, $\mathcal{A}_4 = 0$ gives $\alpha_7 = \alpha_8$. The expression for α_7 can be derived from the condition $\mathcal{A}_3 = 0$. Namely, using Eq. (8.48) one obtains:

$$\alpha_7 = 2(2\beta - 1)\mathbb{K}[1]^2 + 4(1 - \beta)\bar{k}\mathbb{K}[2] - 2\bar{k}^2\Omega. \tag{8.39}$$

The condition $\mathcal{A}_{13} = 0$ is fulfilled by using the expressions derived for α_1, α_2 and α_6. The last two anomalies (8.13) and (8.14) can be simplified to:

$$\mathcal{A}_7 = 2(1 + 2\beta)(\Omega\mathbb{K}[1]^2 - \mathbb{K}[2]^2), \tag{8.40}$$

$$\mathcal{A}_8 = \bar{k}(1 + 2\beta)(\mathbb{K}[2]^2 - \Omega\mathbb{K}[1]^2). \tag{8.41}$$

The anomaly freedom conditions for those last terms, $\mathcal{A}_7 = 0$ and $\mathcal{A}_8 = 0$, are fulfilled if and only if $\beta = -1/2$.

It is also worth noticing that the function $\mathcal{B}$ given by Eq. (8.5) is equal to zero when the expression obtained for α_6 is used. There is finally no contribution from the diffeomorphism constraint in the $\{S^Q, D\}$ bracket.

Using the anomaly freedom conditions given above, the bracket between the total Hamiltonian constraints simplifies to

$$\begin{aligned}\{S_{tot}[N_1], S_{tot}[N_2]\} &= \Omega D_{tot}\left[\frac{\bar{N}}{\bar{p}}\partial^a(\delta N_2 - \delta N_1)\right] \\ &+ (\alpha_{10} - \alpha_4) D_\varphi\left[\frac{\bar{N}}{\bar{p}}\partial^a(\delta N_2 - \delta N_1)\right].\end{aligned} \tag{8.42}$$

The closure of the algebra of total constraints implies the last condition $\alpha_{10} = \alpha_4 = \Omega - 1$.

To summarize, the counter-terms allowing the algebra to be anomaly-free are uniquely determined, and are given by:

$$\begin{aligned}
\alpha_1 &= \mathbb{K}[2] - \mathbb{K}[s_1], && (8.43)\\
\alpha_2 &= 2\mathbb{K}[1]^2 - 2\bar{k}\mathbb{K}[2], && (8.44)\\
\alpha_3 &= 0, && (8.45)\\
\alpha_4 &= \Omega - 1, && (8.46)\\
\alpha_5 &= \Omega - 1, && (8.47)\\
\alpha_6 &= 2\mathbb{K}[2] - \mathbb{K}[s_2] - \bar{k}\Omega, && (8.48)\\
\alpha_7 &= -4\mathbb{K}[1]^2 + 6\bar{k}\mathbb{K}[2] - 2\bar{k}^2\Omega, && (8.49)\\
\alpha_8 &= -4\mathbb{K}[1]^2 + 6\bar{k}\mathbb{K}[2] - 2\bar{k}^2\Omega, && (8.50)\\
\alpha_9 &= 0, && (8.51)\\
\alpha_{10} &= \Omega - 1. && (8.52)
\end{aligned}$$

It is straightforward to check that the counter-terms $\alpha_1, \ldots, \alpha_{10}$ are vanishing in the classical limit ($\bar{\mu} \to 0$), as expected.

Those counter-terms are defined up to the two integers s_1 and s_2, which appear in (8.43) and (8.48). However, in the Hamiltonian (8.1), the factor α_1 appears with $\mathbb{K}[s_1]$ and the factor α_6 appears with $\mathbb{K}[s_2]$. Namely, we have $\mathbb{K}[s_1] + \alpha_1 = \mathbb{K}[2]$ and $\mathbb{K}[s_2] + \alpha_6 = 2\mathbb{K}[2] - \bar{k}\Omega$. Therefore, the final Hamiltonian will not depend on the parameters s_1 and s_2. No ambiguity remains to be fixed.

Moreover, the anomaly cancellation requires

$$\beta = -\frac{1}{2}, \tag{8.53}$$

which fixes the functional form of the $\bar{\mu}$ factor. The fact that anomaly freedom requires $\beta = -1/2$ is a quite surprising result. The exact value of β is highly debated in LQC. The only *a priori* obvious statement is that $\beta \in [-1/2, 0]$. The choice $\beta = -1/2$ is called the $\bar{\mu}-$scheme (new quantization scheme) and is preferred by some authors for physical reasons [43]. Our result seems to show that the $\bar{\mu}-$scheme is embedded in the structure of the theory and this gives a new motivation for this particular choice of quantization scheme. The quantity $\bar{\mu}^2\bar{p}$ can be interpreted as the physical area of an elementary loop along which the holonomy is calculated. Because, in the $\bar{\mu}-$scheme, $\bar{\mu}^2 \propto \bar{p}^{-1}$, the physical area of the loop remains constant. This elementary area is usually set to be the area gap Δ derived in LQG. Therefore, in the $\bar{\mu}-$scheme,

$$\bar{\mu} = \sqrt{\frac{\Delta}{\bar{p}}}. \tag{8.54}$$

8.3.1 Algebra of constraints

Taking into account the previous conditions of anomaly-freedom, the non-vanishing Poisson brackets for the gravity sector are:

$$\left\{S^{Q}[N], D[N^a]\right\} = -S^{Q}[\delta N^a \partial_a \delta N], \tag{8.55}$$

$$\left\{S^{Q}[N_1], S^{Q}[N_2]\right\} = \Omega D\left[\frac{\bar{N}}{\bar{p}}\partial^a(\delta N_2 - \delta N_1)\right]. \tag{8.56}$$

This clearly shows that the *gravity sector is anomaly free*. The remaining non-vanishing brackets are:

$$\left\{S^{Q}_{\varphi}[N], D_{tot}[N^a]\right\} = -S^{Q}_{\varphi}[\delta N^a \partial_a \delta N], \tag{8.57}$$

$$\left\{S^{Q}_{\varphi}[N_1], S^{Q}_{\varphi}[N_2]\right\} = \Omega D_{\varphi}\left[\frac{\bar{N}}{\bar{p}}\partial^c(\delta N_2 - \delta N_1)\right]. \tag{8.58}$$

The algebra of total constraints therefore takes the following form:

$$\{D_{tot}[N_1^a], D_{tot}[N_2^a]\} = 0, \tag{8.59}$$

$$\{S_{tot}[N], D_{tot}[N^a]\} = -S_{tot}[\delta N^a \partial_a \delta N], \tag{8.60}$$

$$\{S_{tot}[N_1], S_{tot}[N_2]\} = \Omega D_{tot}\left[\frac{\bar{N}}{\bar{p}}\partial^a(\delta N_2 - \delta N_1)\right]. \tag{8.61}$$

Although the algebra is closed, there are however modifications with respect to the classical case, due to the presence of the factor Ω in Eq. (8.61). Therefore, not only the dynamics, as a result of the modification of the Hamiltonian constraint, is modified but also the very structure of the space-time itself is *deformed*. This is embedded in the form of the algebra of constraints. The hypersurface deformation algebra generated by (8.61) is pictorially represented in Fig. 8.3.1.

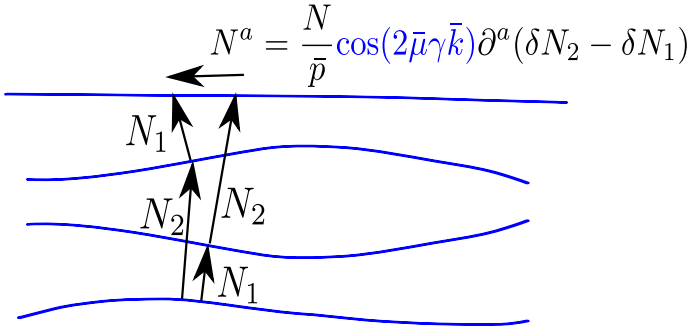

Figure 8.1: Pictorial representation of the hypersurface deformation algebra (8.61).

The $\Omega \in [-1, 1]$, appearing in (8.61) can change its sign in time. In order to see when this might happen let us express the parameter Ω as:

$$\Omega = \cos(2\bar{\mu}\gamma\bar{k}) = 1 - 2\frac{\rho}{\rho_c}, \tag{8.62}$$

where ρ is the energy density of the matter field and

$$\rho_c = \frac{3}{\kappa\gamma\bar{\mu}^2\bar{p}} = \frac{3}{\kappa\gamma\Delta}. \tag{8.63}$$

In low energy limit, $\rho \to 0$, the classical case ($\Omega \to 1$) is correctly recovered. However, while approaching high energy domain the situation drastically changes. Namely, for $\rho = \rho_c/2$ the $\Omega = 0$. At this point, the maximum value of the Hubble parameter is also reached. At the maximum allowed energy density is $\rho = \rho_c$, corresponding to the bounce, we have $\Omega = -1$.

In order to understand what can be the physical meaning of this new feature of the sign change in the algebra of constraints, let us recall expression for the classical algebra of constraints [41]

$$\{S[N_1], S[N_2]\} = sD\left[\frac{\bar{N}}{\bar{p}}\partial^a(\delta N_2 - \delta N_1)\right], \tag{8.64}$$

derived for the general type of a metric signature s. Namely, $s = 1$ corresponds to the Lorentzian signature and $s = -1$ to the Euclidean one. Based on this, one can interpret the peculiar behavior of the sign change in algebra (8.61) in terms of geometry change. Namely, *the effective algebra of constraints shows that the space is Euclidian for* $\rho > \rho_c/2$. At the particular value $\rho = \frac{\rho_c}{2}$, the geometry switches to the Minkowski one. This will become more transparent while analyzing the Mukhanov equation in Sec. 8.4. Consequences have not yet been fully understood, but it is interesting to notice that this model naturally have properties of the Hartle-Hawking no-boundary proposal [62].

8.4 Equations of motion

Once the anomaly-free theory of scalar perturbations with holonomy corrections is constructed, the equations of motion for the canonical variables can be derived. This can be achieved through the Hamilton equation

$$\dot{f} = \{f, H[N, N^a]\}, \tag{8.65}$$

where the Hamiltonian $H[N, N^a]$ is the sum of all constraints

$$H[N, N^a] = S^Q[N] + S^Q_\varphi[N] + D[N^a] + D_\varphi[N^a]. \tag{8.66}$$

8.4.1 Background equations

Based on the Hamilton equation (8.65), equations for the canonical background variables are the following:

$$\dot{\bar{k}} = -\frac{\bar{N}}{2\sqrt{\bar{p}}}\mathbb{K}[1]^2 - \bar{N}\sqrt{\bar{p}}\frac{\partial}{\partial\bar{p}}\mathbb{K}[1]^2 + \frac{\kappa}{2}\sqrt{\bar{p}}\bar{N}\left[-\frac{\bar{\pi}^2}{2\bar{p}^3} + V(\bar{\varphi})\right], \tag{8.67}$$

$$\dot{\bar{p}} = 2\bar{N}\sqrt{\bar{p}}\mathbb{K}[2], \tag{8.68}$$

$$\dot{\bar{\varphi}} = \bar{N}\frac{\bar{\pi}}{\bar{p}^{3/2}}, \tag{8.69}$$

$$\dot{\bar{\pi}} = -\bar{N}\bar{p}^{3/2}V_{,\varphi}(\bar{\varphi}). \tag{8.70}$$

In the following, we choose time to be conformal by setting $\bar{N} = \sqrt{\bar{p}}$. The " $\cdot$ " then means differentiation with respect to conformal time η.

Eqs. (8.69) and (8.70) can be now combined into the Klein-Gordon equation

$$\ddot{\bar{\varphi}} + 2\mathbb{K}[2]\dot{\bar{\varphi}} + \bar{p}V_{,\varphi}(\bar{\varphi}) = 0. \tag{8.71}$$

Eq. (8.68), together with the background part of the Hamiltonian constraint

$$\frac{1}{V_0}\frac{\partial H}{\partial\bar{N}} = \frac{1}{2\kappa}\left[-6\sqrt{\bar{p}}(\mathbb{K}[1])^2\right] + \bar{p}^{3/2}\left[\frac{\bar{\pi}^2}{2\bar{p}^3} + V(\bar{\varphi})\right] = 0, \tag{8.72}$$

lead to the modified Friedmann equation

$$\mathcal{H}^2 = \bar{p}\frac{\kappa}{3}\rho\left(1 - \frac{\rho}{\rho_c}\right). \tag{8.73}$$

Another useful expression is:

$$3\mathbb{K}[1]^2 = \frac{\bar{\pi}^2}{2\bar{p}^2} + \bar{p}V(\bar{\varphi}). \tag{8.74}$$

Here $\mathcal{H}$ stands for the conformal Hubble factor

$$\mathcal{H} := \frac{\dot{\bar{p}}}{2\bar{p}} = \mathbb{K}[2]. \tag{8.75}$$

The energy density and pressure of the scalar field are given by:

$$\rho = \frac{\bar{\pi}^2}{2\bar{p}^3} + V(\varphi), \tag{8.76}$$

$$P = \frac{\bar{\pi}^2}{2\bar{p}^3} - V(\varphi). \tag{8.77}$$

For the purpose of further considerations, we also derive the relation

$$\kappa\left(\frac{\bar{\pi}^2}{2\bar{p}^2}\right) = \bar{k}\mathbb{K}[2] - \dot{\bar{k}}, \tag{8.78}$$

which comes from Eq. (8.67) combined with (8.72).

8.4.2 Equations for the perturbed variables

Equations for the perturbed parts of the canonical variables are:

$$\begin{aligned}
\delta\dot{E}^a_i &= -\bar{N}\left[\sqrt{\bar{p}}\Omega\delta K^j_c\delta^c_i\delta^a_j - \sqrt{\bar{p}}\Omega(\delta K^j_c\delta^c_j)\delta^a_i - \frac{1}{\sqrt{\bar{p}}}(2\mathbb{K}[2]-\bar{k}\Omega)\delta E^a_i\right] + \\
&+ \delta N\left(2\mathbb{K}[2]\sqrt{\bar{p}}\delta^a_i\right) - \bar{p}(\partial_i\delta N^a - (\partial_c\delta N^c)\delta^a_i), \qquad (8.79)\\
\delta\dot{K}^i_a &= \bar{N}\left[-\frac{1}{\sqrt{\bar{p}}}(2\mathbb{K}[2]-\bar{k}\Omega)\delta K^i_a\right.\\
&- \frac{1}{2\bar{p}^{3/2}}(-3\mathbb{K}[1]^2+6\bar{k}\mathbb{K}[2]-2\bar{k}^2\Omega)\delta E^c_j\delta^j_a\delta^i_c\\
&+ \left.\frac{1}{4\bar{p}^{\frac{3}{2}}}(-3\mathbb{K}[1]^2+6\bar{k}\mathbb{K}[2]-2\bar{k}^2\Omega)(\delta E^c_j\delta^j_c)\delta^i_a + \frac{\delta^{ik}}{2\bar{p}^{\frac{3}{2}}}\partial_a\partial_d\delta E^d_k\right]\\
&+ \frac{1}{2}\left[-\frac{1}{\sqrt{\bar{p}}}(3\mathbb{K}[1]^2-2\bar{k}\mathbb{K}[2])\delta^i_a\delta N + \frac{2}{\sqrt{\bar{p}}}(\partial_a\partial^i\delta N)\right]\\
&+ \delta^i_c(\partial_a\delta N^c) + \kappa\delta N\frac{\sqrt{\bar{p}}}{2}\left[-\frac{\bar{\pi}^2}{2\bar{p}^3}+V(\bar{\varphi})\right]\delta^i_a\\
&+ \kappa\bar{N}\left[-\frac{\bar{\pi}\delta\pi}{2\bar{p}^{5/2}}\delta^i_a + \frac{\sqrt{\bar{p}}}{2}\delta\varphi\frac{\partial V(\bar{\varphi})}{\partial\bar{\varphi}}\delta^i_a + \left(\frac{\bar{\pi}^2}{2\bar{p}^{3/2}}+\bar{p}^{3/2}V(\bar{\varphi})\right)\frac{\delta^j_c\delta E^c_j}{4\bar{p}^2}\delta^i_a\right.\\
&+ \left.\left(\frac{\bar{\pi}^2}{2\bar{p}^{3/2}}-\bar{p}^{3/2}V(\bar{\varphi})\right)\frac{\delta^i_c\delta^j_a\delta E^c_j}{2\bar{p}^2}\right], \qquad (8.80)\\
\delta\dot{\varphi} &= \delta N\left(\frac{\bar{\pi}}{\bar{p}^{3/2}}\right) + \bar{N}\left(\frac{\delta\pi}{\bar{p}^{3/2}} - \frac{\bar{\pi}}{\bar{p}^{3/2}}\frac{\delta^j_c\delta E^c_j}{2\bar{p}}\right), \qquad (8.81)\\
\delta\dot{\pi} &= -\delta N\left(\bar{p}^{3/2}V_{,\varphi}(\bar{\varphi})\right) + \bar{\pi}(\partial_a\delta N^a)\\
&- \bar{N}\left[-\sqrt{\bar{p}}\Omega\delta^{ab}\partial_a\partial_b\delta\varphi + \bar{p}^{3/2}V_{,\varphi\varphi}(\bar{\varphi})\delta\varphi + \bar{p}^{3/2}V_{,\varphi}(\bar{\varphi})\frac{\delta^j_c\delta E^c_j}{2\bar{p}}\right]. \qquad (8.82)
\end{aligned}$$

8.4.3 Longitudinal gauge

As an example of application we will now derive equations in the longitudinal gauge. In this case, the E and B perturbations are set to zero. The line element therefore simplifies to

$$ds^2 = a^2\left[-(1+2\phi)d\eta^2 + (1-2\psi)\delta_{ab}dx^a dx^b\right], \qquad (8.83)$$

where ϕ and ψ are two remaining perturbation functions and a is the scale factor. From the metric above, one can derive the lapse function, the shift vector and the spatial metric:

$$N = a\sqrt{1+2\phi}, \tag{8.84}$$
$$N^a = 0, \tag{8.85}$$
$$q_{ab} = a^2(1-2\psi)\delta_{ab}. \tag{8.86}$$

The lapse function can be expanded for the background and perturbation part as $N = \bar{N} + \delta N$, where

$$\bar{N} = \sqrt{\bar{p}} = a, \tag{8.87}$$
$$\delta N = \bar{N}\phi. \tag{8.88}$$

Using Eq. (8.86), the perturbation of the densitized triad is expressed as:

$$\delta E^a_i = -2\bar{p}\psi\delta^a_i. \tag{8.89}$$

Time derivative of this expression will also be useful and can be written as:

$$\delta\dot{E}^a_i = -2\bar{p}(2\mathbb{K}[2]\psi + \dot{\psi})\delta^a_i. \tag{8.90}$$

Let us now find the expression for the perturbation of the extrinsic curvature δK^i_a in terms of metric perturbations ϕ and ψ. For this purpose, one can apply the expression (8.89) to the left hand side of (8.79). The resulting equation can be solved for δK^i_a, leading to:

$$\delta K^i_a = -\delta^i_a \frac{1}{\Omega}\left(\dot{\psi} + \bar{k}\Omega\psi + \mathbb{K}[2]\phi\right). \tag{8.91}$$

The time derivative of this variable is given by

$$\delta\dot{K}^i_a = \delta^i_a \frac{1}{\Omega}\left[-\ddot{\psi} - \dot{\bar{k}}\Omega\psi + \dot{\psi}\left(\frac{\dot{\Omega}}{\Omega} - \bar{k}\Omega\right) + \phi\mathbb{K}[2]\frac{\dot{\Omega}}{\Omega} - \phi\dot{\mathbb{K}}[2] - \mathbb{K}[2]\dot{\phi}\right]. \tag{8.92}$$

Applying (8.92) to the left hand side of (8.80), the equation containing the diagonal part as well as the off-diagonal contribution is easily obtained. The off-diagonal part leads to

$$\partial_a\partial^i(\phi - \psi) = 0. \tag{8.93}$$

This translates into $\psi = \phi$. In what follows, we will therefore consider ϕ only. The diagonal part of the discussed equation can be expressed as:

$$\ddot{\phi} + \dot{\phi}\left[3\mathbb{K}[2] - \frac{\dot{\Omega}}{\Omega}\right] + \phi\left[\dot{\mathbb{K}}[2] + 2\mathbb{K}[2]^2 - \mathbb{K}[2]\frac{\dot{\Omega}}{\Omega}\right] = 4\pi G\Omega\left[\dot{\bar{\varphi}}\delta\dot{\varphi} - \bar{p}\delta\varphi V_{,\varphi}(\bar{\varphi})\right]. \tag{8.94}$$

One can now use the diffeomorphism constraint

$$\kappa\frac{\delta H[N,N^a]}{\delta(\delta N^c)} = \bar{p}\partial_c(\delta^d_k\delta K^k_d) - \bar{p}(\partial_k\delta K^k_c) - \bar{k}\delta^k_c(\partial_d\delta E^d_k) + \kappa\bar{\pi}(\partial_c\delta\varphi) = 0. \tag{8.95}$$

With the expressions for δK^i_a and δE^a_i, it can be derived that

$$\partial_c\left[\dot{\phi} + \phi\mathbb{K}[2]\right] = 4\pi G\Omega\dot{\bar{\varphi}}\partial_c\delta\varphi. \tag{8.96}$$

Next equation comes from the perturbed part of the Hamiltonian constraint:

$$\begin{aligned}\frac{\delta H[N,N^a]}{\delta(\delta N)} &= \frac{1}{2\kappa}\left[-4\sqrt{\bar{p}}\mathbb{K}[2]\delta^c_j\delta K^j_c - \frac{1}{\sqrt{\bar{p}}}\left(3\mathbb{K}[1]^2 - 2\bar{k}\mathbb{K}[2]\right)\delta^j_c\delta E^c_j\right.\\ &+ \left.\frac{2}{\sqrt{\bar{p}}}\partial_c\partial^j\delta E^c_j\right] + \frac{\bar{\pi}\delta\pi}{\bar{p}^{3/2}} - \frac{\bar{\pi}^2}{2\bar{p}^{3/2}}\frac{\delta^j_c\delta E^c_j}{2\bar{p}}\\ &+ \bar{p}^{3/2}\left[V_{,\varphi}(\bar{\varphi})\delta\varphi + V(\bar{\varphi})\frac{\delta^j_c\delta E^c_j}{2\bar{p}}\right] = 0.\end{aligned} \tag{8.97}$$

Using the expressions for δK^i_a and δE^a_i, this can be rewritten as:

$$\Omega\nabla^2\phi - 3\mathbb{K}[2]\dot{\phi} - \left[\dot{\mathbb{K}}[2] + 2\mathbb{K}[2]^2\right]\phi = 4\pi G\Omega\left[\dot{\bar{\varphi}}\delta\dot{\varphi} + \bar{p}\delta\varphi V_{,\varphi}(\bar{\varphi})\right]. \tag{8.98}$$

The last equality comes from (8.81) and (8.82):

$$\delta\ddot{\varphi} + 2\mathbb{K}[2]\delta\dot{\varphi} - \Omega\nabla^2\delta\varphi + \bar{p}V_{,\varphi\varphi}(\bar{\varphi})\delta\varphi + 2\bar{p}V_{,\varphi}(\bar{\varphi})\phi - 4\dot{\bar{\varphi}}\dot{\phi} = 0. \tag{8.99}$$

Equations (8.94), (8.96) and (8.98) can be now combined into:

$$\ddot{\phi} + 2\left[\mathcal{H} - \left(\frac{\ddot{\bar{\varphi}}}{\dot{\bar{\varphi}}} + \varepsilon\right)\right]\dot{\phi} + 2\left[\dot{\mathcal{H}} - \mathcal{H}\left(\frac{\ddot{\bar{\varphi}}}{\dot{\bar{\varphi}}} + \varepsilon\right)\right]\phi - c_s^2\nabla^2\phi = 0, \tag{8.100}$$

with the quantum correction

$$\varepsilon = \frac{1}{2}\frac{\dot{\Omega}}{\Omega} = 3\mathbb{K}[2]\left(\frac{\rho + P}{\rho_c - 2\rho}\right), \tag{8.101}$$

and the squared velocity

$$c_s^2 = \Omega. \tag{8.102}$$

The squared velocity of the perturbation field ϕ is equal to Ω. Because $-1 \leqslant \Omega \leqslant 1$, the speed of perturbations is never super-luminal. However, for $\Omega < 0$ perturbations become unstable ($c_s^2 < 0$). This corresponds to the energy density regime $\rho > \frac{\rho_c}{2}$, where the phase of super-inflation is expected.

At the point $\rho = \frac{\rho_c}{2}$, velocity of the perturbation field ϕ is equal to zero. Therefore, perturbations don't propagate anymore when approaching $\rho = \frac{\rho_c}{2}$, where the Hubble

factor reaches its maximal value. Moreover, at this point, the quantum correction $\epsilon \to \infty$. Because of this, Eq. (8.100) becomes divergent and cannot be used to determine the propagation of the perturbations. However, as shown in the next section, the equation for the gauge-invariant Mukhanov variable does not exhibit such a pathology.

It is interesting to notice that the equations of motion derived in this subsection are the same as those found in [40]. This is quite surprising, because the same equations were derived in two independent ways. In our approach, we introduced most general form of the holonomy corrections to the Hamiltonian. Then, by applying the method of counter-terms, anomalies in algebra of constraint were removed. The method proposed in [40] utilizes diagonal form of metric in the longitudinal gauge. This enables to introduce holonomy corrections almost the same way like in case of the homogeneous models. It was shown that a system, defined this way, stays on-shell, therefore is free from anomalies. The non-trivial equivalence of both approaches may suggest uniqueness in defining theory of scalar perturbations with holonomy corrections in anomaly-free manner.

8.4.4 Gauge invariant variables and Mukhanov equation

Considering the scalar perturbations, there is only one physical degree of freedom. As it was shown in [27], this physical variable combines both the perturbation of the metric and the perturbation of matter. The classical expression on this gauge-invariant quantity is:

$$\nu = a(\eta)\left(\delta\varphi^{GI} + \frac{\dot{\bar{\varphi}}}{\mathcal{H}}\Psi\right), \tag{8.103}$$

and its equation of motion is given by

$$\ddot{\nu} - \nabla^2\nu - \frac{\ddot{z}}{z}\nu = 0, \tag{8.104}$$

where

$$z = a(\eta)\frac{\dot{\bar{\varphi}}}{\mathcal{H}}. \tag{8.105}$$

In the canonical formalism with scalar perturbations, the gauge transformation of a variable X under a small coordinate transformation

$$x^\mu \to x^\mu + \xi^\mu \quad ; \quad \xi^\mu = (\xi^0, \partial^a\xi), \tag{8.106}$$

is given by (see [32] for details):

$$\delta_{[\xi^0,\xi]}X \doteq \{X, S^{(2)}[\bar{N}\xi^0] + D^{(2)}[\partial^a\xi]\}, \tag{8.107}$$

and it is straightforward to see that, classically,

$$\delta_{[\xi^0,\xi]}\nu = 0. \tag{8.108}$$

This means that ν is diffeomorphism-invariant and can be taken as an observable.

Taking into account the holonomy corrections introduced in this paper, the Ω function will modify the gauge transformations of the time derivative of a variable X, so that

$$\delta_{[\xi^0,\xi]}\dot{X} - (\delta_{[\xi^0,\xi]}X)^{\cdot} = \Omega \cdot \delta_{[0,\xi^0]}X. \tag{8.109}$$

Using this relation and gauge transformations of the metric perturbations

$$\begin{aligned}
\delta_{[\xi^0,\xi]}\psi &= -\mathbb{K}[2]\xi^0, && (8.110)\\
\delta_{[\xi^0,\xi]}\phi &= \dot{\xi}^0 + \mathbb{K}[2]\xi^0, && (8.111)\\
\delta_{[\xi^0,\xi]}E &= \xi, && (8.112)\\
\delta_{[\xi^0,\xi]}B &= \dot{\xi}, && (8.113)
\end{aligned}$$

one can define the gauge-invariant variables (Bardeen potentials) as:

$$\begin{aligned}
\Phi &= \phi + \frac{1}{\Omega}(\dot{B} - \ddot{E}) + \left(\frac{\mathbb{K}[2]}{\Omega} - \frac{\dot{\Omega}}{\Omega}\right)(B - \dot{E}), && (8.114)\\
\Psi &= \psi - \frac{\mathbb{K}[2]}{\Omega}(B - \dot{E}), && (8.115)\\
\delta\varphi^{GI} &= \delta\varphi + \frac{\dot{\bar{\varphi}}}{\Omega}(B - \dot{E}). && (8.116)
\end{aligned}$$

The normalization of these variables was set such that, in the longitudinal gauge ($B = 0 = E$), we have $\Phi = \phi$, $\Psi = \psi$ and $\delta\varphi^{GI} = \delta\varphi$. It is possible to define the analogous of the Mukhanov variable (8.103):

$$\nu := \sqrt{\bar{p}}\left(\delta\varphi^{GI} + \frac{\dot{\bar{\varphi}}}{\mathbb{K}[2]}\Psi\right). \tag{8.117}$$

Writing the equations for Ψ and $\delta\varphi^{GI}$, which are

$$\ddot{\Psi} + 2\left[\mathcal{H} - \left(\frac{\ddot{\bar{\varphi}}}{\dot{\bar{\varphi}}} + \varepsilon\right)\right]\dot{\Psi} + 2\left[\dot{\mathcal{H}} - \mathcal{H}\left(\frac{\ddot{\bar{\varphi}}}{\dot{\bar{\varphi}}} + \varepsilon\right)\right]\Psi - c_s^2\nabla^2\Psi = 0 \tag{8.118}$$

and

$$\delta\ddot{\varphi}^{GI} + 2\mathbb{K}[2]\delta\dot{\varphi}^{GI} - \Omega\nabla^2\delta\varphi^{GI} + \bar{p}V_{,\varphi\varphi}(\bar{\varphi})\delta\varphi^{GI} + 2\bar{p}V_{,\varphi}(\bar{\varphi})\Psi - 4\dot{\bar{\varphi}}^{GI}\dot{\Psi} = 0, \tag{8.119}$$

one obtains equation for the variable (8.117):

$$\begin{aligned}
\ddot{\nu} - \Omega\nabla^2\nu - \frac{\ddot{z}}{z}\nu &= 0, && (8.120)\\
z &= \sqrt{\bar{p}}\frac{\dot{\bar{\varphi}}}{\mathbb{K}[2]}, && (8.121)
\end{aligned}$$

which corresponds to the Mukhanov equation for our model. As we see, the difference between the classical and the holonomy-corrected case is the factor Ω in front of the Laplacian. This quantum contribution leads to a variation of the propagation velocity of the perturbation v. This is similar to the case of the perturbation ϕ considered in the previous subsection. The main difference is that there is no divergence for $\rho = \rho_c/2$ and the evolution of perturbations can be investigated in the regime of high energy densities. It is worth noticing that for $\rho > \rho_c/2$, the Ω becomes negative and equation (8.120) changes its form from the hyperbolic to elliptic-type partial differential equation. In this sense, time part becomes indistinguishable from the spatial one. This can be interpreted in thrms of transition between Minkowski and Euclidean geometry, as mentioned earlier.

Finally, it is also possible to define the perturbation of a curvature $\mathcal{R}$ such that

$$\mathcal{R} = \frac{v}{z}. \tag{8.122}$$

Based on this, one can now calculate the power spectrum of scalar perturbations. This opens new possible ways to study quantum gravity effects in the very early universe. Promising applications of the derived equations will be investigated elsewhere.

8.5 Conclusions

In this chapter, we have investigated theory of scalar perturbations in the presence of holonomy corrections. Such corrections are expected due to the quantum gravity effects predicted by LQG. The holonomy corrections originate from regularization of the curvature of connection at the Planck scale. Because of this, the holonomy corrections become dominant in the high curvature regime. The introduction of general type holonomy corrections leads to anomalous algebra of constraint. The conditions of anomaly freedom impose certain constraints on the form of the holonomy corrections. However, it appears that the holonomy corrections, in the standard form, cannot fully satisfy the anomaly-free condition. In order to solve this difficulty, the additional counter-terms were introduced. Such counter-terms tend to zero in the classical limit, however play the role of regularizator of anomalies in the quantum (high curvature) regime. The method of counter-terms was earlier successfully applied in case of the cosmological perturbations with the inverse-triad type corrections [31].

We have shown that, thanks to the counter-terms, the theory of cosmological perturbations with holonomy corrections can be formulated in the anomaly-free manner. The anomaly freedom was shown to be fulfilled not only for the gravity sector but also by taking into account the scalar matter. The requirements of the anomaly freedom were used to determine the form of the counter-terms. Furthermore, conditions for the anomaly free algebra of constraints were shown to be fulfilled only for a particular choice of the $\bar{\mu}$ function. Namely, for the $\bar{\mu}$—scheme (new quantization scheme). This quantization scheme was shown earlier to be favored from the requirements of the consistency of the background dynamics. Our result supports these earlier claims.

In our formulation, the diffeomorphism constraint holds the classical form, in agreement with the LQG expectations. The obtained anomaly-free gravitational Hamiltonian contains seven holonomy modifications. It was also necessary to introduce one counterterm into the matter Hamiltonian in order to ensure closure of the algebra of total constraints. There is no ambiguity, of defining the holonomy corrections, left after imposing the anomaly-free conditions. The only remaining free parameter of the theory is the area gap Δ used in defining the $\bar{\mu}$ function. This quantity can be however possibly fixed based on the spectrum of the area operator in LQG. Based on the equations derived in this paper it will be also possible to put an observational constraint on the value of Δ and hence on the critical energy density ρ_c.

Based on the studied anomaly-free formulation, equations of motion were derived. As an example of application, we applied the equations to the case of longitudinal gauge. Thereafter, we have also found gauge invariant variables, which are the holonomy-corrected version of the Bardeen potentials. Based on this, we have found equation on the Mukhanov variable. This equation can be directly applied to compute power spectrum of the scalar perturbations, in presence of the quantum gravitational holonomy corrections.

Chapter 9

Confrontation with the astronomical data

Theoretical considerations performed so far carried us to the point where confrontation with astronomical observations becomes possible. A variety of applications emerge from the theory of cosmological perturbations developed in the previous chapters. In particular, based on the obtained equations of motion for the scalar and tensor perturbations, quantum corrections to the inflationary power spectrum can be studied. Such corrections can be then confronted with spectra of anisotropy and polarization of the CMB.

In this chapter, we will focus on two applications. Firstly, based on the obtained spectrum of primordial gravitational waves, we will perform predictions regarding the B-type polarization of the CMB. We will confront the predictions with available observational constraints. Thanks to this, we will derive observational constraint on the value of the parameter F_B. Secondly, we will investigate the possibility of testing the effect of suppression of the spectrum of primordial perturbations. As it was shown, such effect is a general feature of loop quantum cosmology. Considering some phenomenological form of the scalar power spectrum, we will study whether it is possible to discriminate between the Big Bounce and Big Bang scenarios. Further issues, as quantum holonomy corrections to the inflationary phase, will be studied elsewhere.

9.1 B-type polarization of the CMB

The cosmic microwave background radiation is polarized due to the Thomson scattering of the CMB photons. The polarization pattern of the CMB can be decomposed for two types, depending on the symmetry. The first, E-type polarization pattern was already observed and is due to both scalar and tensor perturbations. The second, B-type polarization has not been detected yet. However, there are huge efforts in this direction. The B-type of polarization is related to the tensor perturbations only. Therefore, detection of this type of polarization would give us a possibility of investigating the primordial gravitational waves. At present, observational constraints on the B-type polarization spectrum C_l^{BB} are available from the experiments as WMAP [8], BICEP [56] or QUaD [57]. These

constraints are shown in Fig. 9.1. The data points should be understood as the lower

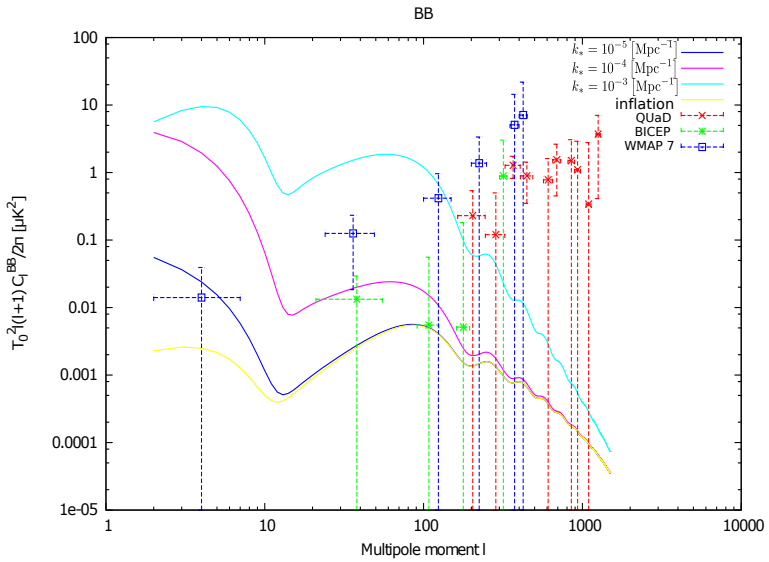

Figure 9.1: The B-type polarization spectrum (continuous lines) predicted in LQC compared with the available current observational constraints. The predicted spectra are shown for the different values of the parameter k_*. It was assumed that inflation mass $m = 10^{-6} m_{Pl}$.

observational limits on the value of C_l^{BB}. In Fig. 9.1, the observational constraints were confronted with predictions made based on the tensor power spectrum (6.48):

$$\mathcal{P}_T(k) = \frac{16}{\pi}\left(\frac{H}{m_{Pl}}\right)^2 \frac{1}{1+(k_*/k)^2}\left[1+\frac{4R-2}{1+(k/k_*)^2}\right]. \tag{9.1}$$

For simplicity we have neglected here the small inflationary slope $k^{-2\epsilon}$. The predictions were obtained with use of publicly available CAMB code [63]. In Fig. 9.1, the value of parameter $R = 8000$ was fixed by assuming that $m = 10^{-6} m_{Pl}$ in equation (6.46). The employed value of the inflaton mass is predicted based on confrontation of the scalar perturbations with the CMB data. This value of the Hubble factor H in equation (9.1) was determined based on the Friedmann equation

$$H^2 \approx \frac{8\pi G}{3} V(\varphi_{obs}) = \frac{8\pi G}{3}\frac{1}{2} m^2 \varphi_{obs}^2. \tag{9.2}$$

The value of φ_{obs} can be determined from the WMAP 7 observations, based on a relation

$$\varphi_{obs} = \frac{m_{Pl}}{\sqrt{\pi(1-n_s)}} = 2.9 \pm 0.5\ m_{Pl}.$$

As we see in In Fig. 9.1, the predicted amplitude of the B-type polarization can exceed or not the observational constraints, depending on the value of k_*. The model of standard inflation (yellow line) corresponds to the limit $k_* \to 0$ in spectrum (9.1). In this case,

predicted amplitude of the B-type polarization is below the current observational constraint. However, if k_* is non-vanishing, the B-type polarization is amplified by the bump in the power spectrum (9.1). The amplification in the C_l^{BB} spectrum is maximal at some multipole l_*, which corresponds to the wavelength k_*. While the value of k_* is growing, amplification of the C_l^{BB} spectrum is shifting into the region of higher multipoles. Power excess due to the bump in the spectrum (9.1) is so significant that the value of C_l^{BB} can exceed the observational limits for some value of k_*. Thanks to this, the following observational constraint of the value of the k_* parameter can be obtained [64]:

$$k_* < 2.43 \cdot 10^{-4} \mathrm{Mpc}^{-1}. \tag{9.3}$$

The value of k_* can be related with φ_{obs} and φ_{max} by the following formula:

$$k_* \approx k_0 \left(\frac{\varphi_{max}}{m_{Pl}}\right) \left(\frac{m_{Pl}}{\varphi_{obs}}\right) \exp\left\{2\pi \frac{(\varphi_{obs}^2 - \varphi_{max}^2)}{m_{Pl}^2}\right\}, \tag{9.4}$$

where k_0 is a pivot number, for WMAP $k_0 = 0.002\ \mathrm{Mpc}^{-1}$. From the constraint on k_* (9.3) applied to (9.4) one can find that $\varphi_{max} > 2.94 m_{Pl}$. In Chapter 3, we derived relation (3.8), based on which we have

$$\varphi_{max} = (2.33 + 1.28 \cdot 10^6 \sqrt{F_B}) m_{Pl} > 2.94 m_{Pl}. \tag{9.5}$$

This translates into the constraint on the parameter F_B, which describes contribution from the potential energy at the bounce:

$$F_B > 2.3 \cdot 10^{-13}.$$

This constraint means that, at least some small contribution from the potential energy is required at the bounce. The case with $F_B = 0$ would correspond to the perfectly symmetric model of the bounce. However, the observational data support the *asymmetric* bounce model! This result is of course very preliminary and is based on some particular values of m and ρ_c. However, it gives general idea of constraining F_B based on the astronomical observations. More accurate analysis will be possible to perform after the spectrum of the scalar perturbation with the holonomy corrections will be derived. This will be done elsewhere based on the results of Chapter 8.

9.2 Modified inflationary spectrum and the CMB

A spectrum of the scalar perturbations with the holonomy corrections has not been computed yet. However, this can be done by solving the modified Mukhanov equation (8.120) numerically. Before this analysis will be done it is worth to investigate what kind of modifications of the scalar power spectrum are possible to investigate with use of the cosmic microwave background radiation. As we have already learned, by investigating tensor

modes and the scalar field fluctuations, the power spectrum of both exhibit two new features. Firstly, the standard inflationary spectrum is suppressed at the large scales. Secondly, the spectrum is modified by oscillations converging in the UV limit. It is expected that the same features will be present in the spectrum of scalar perturbations in LQC. In order to investigate if such effects are observationally accessible we will consider the following phenomenological form of the scalar spectrum:

$$\mathcal{P}_S(k) \;=\; \Delta(k, k_*) A_s \left(\frac{k}{k_0}\right)^{n_s - 1}. \tag{9.6}$$

This is, in fact, the standard inflationary spectrum modified by the additional prefactor $\Delta(k, k_*)$. The LQC factor $\Delta(k, k_*)$ is assumed to be

$$\Delta(k, k_*) = 1 - \frac{\sin\left(\frac{3k}{2k_*}\right)}{\left(\frac{3k}{2k_*}\right)}, \tag{9.7}$$

which is the simplified form of the expression (5.41), found for the scalar field perturbations. The k_* is a parameter of the model and its interpretation will be discussed later. The factor $\Delta(k, k_*)$ reflects typical modifications which appear in the bouncing cosmology. In the UV limit, $\lim_{k\to\infty} \Delta(k, k_*) = 1$, therefore the standard inflationary spectrum

$$\mathcal{P}_S^{inf}(k) = A_s \left(\frac{k}{k_0}\right)^{n_s - 1}, \tag{9.8}$$

is recovered. In turn, in the IR limit, $\lim_{k\to 0} \Delta(k, k_*) = 0$, and the spectrum is suppressed. This behavior of the power spectrum is typical for the bouncing cosmologies. The two effects of the bounce are transparent: suppression on the low k and additional oscillations. In Fig. 9.2 we show function $\Delta(k, k_*)$ defined by equation (9.7). Instead of using the wavenumber k we have translated it to the corresponding length $\lambda = \frac{2\pi}{k}$, respectively $\lambda_* = \frac{2\pi}{k_*}$. In Fig. 9.2 we also show the function

$$\Delta(\lambda, \lambda_*) \approx 1 + \frac{2}{3}\frac{\lambda}{\lambda_*}. \tag{9.9}$$

This function measures the modification due to the oscillations for $\lambda/\lambda_* \ll 1$. At $\lambda/\lambda_* \approx 1$ the spectrum becomes suppressed. In the bouncing cosmology the length scale λ_* can be related with the scale of horizon at the beginning of inflation. This issue was discussed while considering tensor modes in Chapter 6. Therefore, if the present value of the scale factor is equal $a_0 = 1$, we have $k_* \simeq a_i H_i$ where a_i is the value of the scale factor at the beginning of inflation and H_i is the value of the Hubble factor at the same time. Therefore if k_* and H_i could be measured, the total increase of the scale factor, from the beginning of inflation till present, can be found. The value of k_* and respectively λ_* ,which is a scale

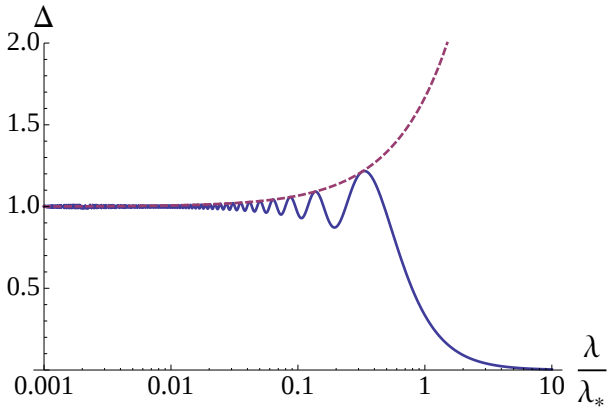

Figure 9.2: Plot of function $\Delta(k, k_*)$ defined by equation (9.7) (solid line). The dashed line represents approximation (9.9).

of suppression in the spectrum is the crucial observational parameter of the bounce. In what follows, we make an attempt of determining this value based on the observations of the CMB.

As mentioned earlier, beside the effect of suppression, also oscillations of the spectrum are predicted within the bouncing cosmologies. This effect is much weaker than suppression, however is present also on the much smaller scales. This is important from the observational point of view. Namely, the length scale $\lambda_* = \frac{2\pi}{k_*}$ can be much larger than the present size of the horizon ($k/k_* \ll 1$). Then, the effect of suppression would be inaccessible observationally. However, some oscillations are still present on the sub-horizontal scales. Of course the amplitude of these oscillations decreases while $k/k_* \gg 1$. If the scale λ_* is however not much higher than the size of the horizon, the effect of sub-horizontal oscillations could be quite significant. The oscillations in the primordial power spectrum translate into the additional oscillation in the spectrum of the CMB anisotropies (see e.g. [65]). For the small multipoles, this subtle effect can be dominated by the contribution from the cosmic variance. However, for the larger multipoles this effect can dominate. At these scales, improvement of the instrumental resolution are still possible, what gives the chance to, at least, put a stronger constrain on these effects.

Let us now confront the spectrum (9.6) with observed anisotropies of the cosmic microwave background radiation. We use the seven years of observations made by the WMAP satellite [8]. In the numerical calculations we use the publicly available CAMB code [63] and Markov Chain Monte Carlo (MCMC) package CosmoMC [66] together with the CosmoClust code [67] for computing the Bayesian evidence. The codes were suitably modified to investigate the spectrum (9.6). In computations, we take the standard cosmological parameters as follows

$$(H_0, \Omega_b h^2, \Omega_c h^2, \tau) = (70, 0.0226, 0.112, 0.09) \tag{9.10}$$

and the pivot scale $k_0 = 0.05\,\mathrm{Mpc}^{-1}$.

In Fig. 9.3 we show spectrum of the CMB temperature anisotropies obtained based on power spectrum (9.6). The case $\Delta(k, k_*) = 1$ $(k \to 0)$ corresponds to the classical case

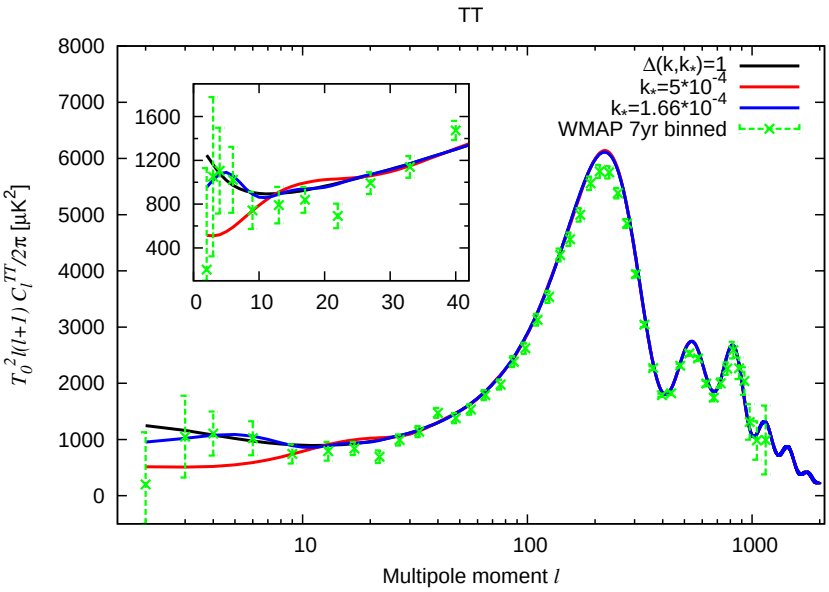

Figure 9.3: Spectrum of the CMB anisotropy.

with no contribution due to the bounce. The blue line corresponds to the best fit case. In this case, the modulations on the low multipoles are well reproduced. This is due to the oscillations in the primordial power spectrum (9.6). This suggests that the effects of oscillations in the primordial power spectrum can be indeed studied basing on the CMB data. Perhaps the anomalous behavior of the CMB spectrum at $l \approx 20$ and $l \approx 40$ could be also explained by the oscillations within the bouncing scenario. However, not basing on the parametrization employed here. The amplitude of oscillations on lower scales must be higher than predicted by our model.

We also find confidence intervals for the parameters of the model, namely on A_s, n_s and k_*. In these computations we take into account the temperature anisotropy data (TT spectrum) as well as the polarization data (TE and EE spectra). We neglect a contribution from the tensor modes, putting $\mathcal{P}_T = 0$. We show the obtained confidence intervals in Fig. 9.4. As it can be seen from Fig. 9.4, the parameters A_s are n_s are constrained from both sides. Based on the fit to the WMAP data we find

$$\begin{aligned} n_s &= 0.97 \pm 0.07, \\ A_s &= 2.1 \cdot 10^{-9} \pm 0.1 \cdot 10^{-9}. \end{aligned}$$

These results are in agreement with WMAP 7 results [8]. However, it must be pointed out that they were computed at the different pivot scales.

The parameter k_* has the upper constraint, however it is unbounded from below (large scales). It could be expected, since there is no observational data on the super-

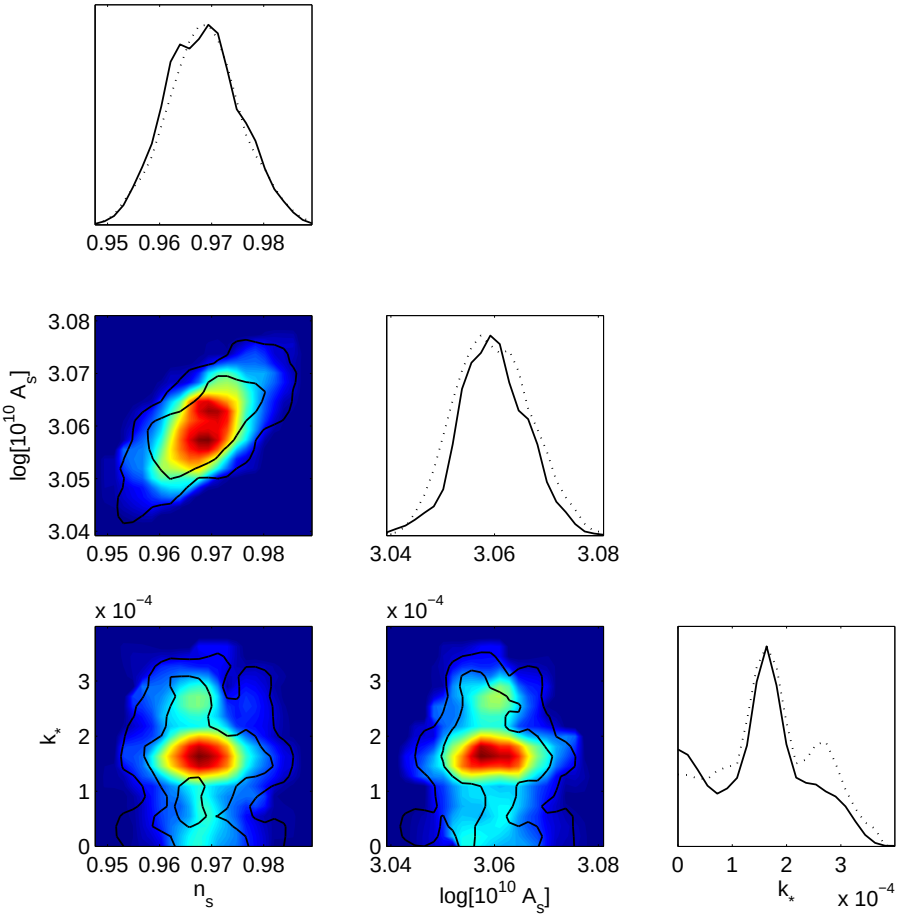

Figure 9.4: Constraints for the parameters A_s, n_s and k_*. 2D plots: solid lines show the 68% and 95% confidence intervals. 1D plots: dotted lines are mean likelihoods of samples, solid lines are marginalized probabilities.

horizontal scales. Nevertheless some particular value of k_* is privileged what leads to the peak in the probability distribution. Based on the fit to the WMAP data we have obtained following values of this parameter:

$$k_* = 1.7 \cdot 10^{-4} \pm 0.8 \cdot 10^{-4}\ [\mathrm{Mpc}^{-1}].$$

The length scale corresponding to k_* is equal to

$$\lambda_* = \frac{2\pi}{k_*} \approx 4 \cdot 10^4\ \mathrm{Mpc}. \tag{9.11}$$

9.3 Big Bang vs. Big Bounce

In this section we compare the model with suppression with the standard inflationary model. Suppression appears generically within the Big Bounce cosmology. In turn, slow-roll inflation in the standard Big Bang scenario does not lead to any suppression. While the suppression introduces a new length scale, the model with suppression has one more parameter in comparison with the standard case. The considered models are:

H_1 – The slow-roll inflation within the Big Bang cosmology (spectrum given by Eq. 9.8). This model has two parameters A_s and n_s.

H_2 – The slow-roll inflation within the Big Bounce cosmology (spectrum given by Eq. 9.6). This model has three parameters A_s, n_s and k_*.

In the Bayesian approach to a model comparison the best model has the largest value of the so-called posterior probability in the light of data, which is defined in the following way [68]:

$$P(H_i|D) = \frac{P(D|H_i)P(H_i)}{P(D)}. \tag{9.12}$$

The H_i stands for considered model and D denotes data used in analysis. $P(H_i)$ is a prior probability for the model under investigation, which should reflect all information which we have about it before the analysis with the data D, that comes from theoretical investigations, or from analysis with other data sets. In particular, if we have no foundation to favor one model over another one, which is usually the case, we take equal values of $P(H_i)$ for all considered models. $P(D|H_i)$ is the marginalized likelihood function over the allowed parameters range, which we called evidence and is given by

$$E_i \equiv P(D|H_i) = \int d\hat{\theta} L(\hat{\theta}) P(\hat{\theta}|H_i). \tag{9.13}$$

The $\hat{\theta}$ denotes vector of model parameters, $L(\hat{\theta})$ is the likelihood function for considered model and $P(\hat{\theta}|H_i)$ is the prior probability distribution function for model parameters.

It is convenient to consider the ratio of posterior probabilities, which is reduced to the evidence ratio (so called Bayes factor) when all considered models have equal prior probabilities:

$$B_{ij} = \frac{E_i}{E_j}. \tag{9.14}$$

Their values give us information about the strength of evidence in favor of a better model [69]: if $0 < \ln B < 1$ we could not give conclusive answer, if $1 < \ln B < 2.5$ there is weak evidence, if $2.5 < \ln B < 5$ evidence is moderate, and for $\ln B > 5$ evidence is strong.

Values of evidence for two alternative models of primordial perturbation spectrum was calculated with the help of CosmoClust code, which was introduced by [67] as a part of CosmoMC code. We have based on anisotropy (TT) and polarization (TE, EE) data from

the WMAP satellite. In computations, the contribution from the tensor power spectrum was neglected.

We assume that models are equally probable ($P(H_1) = P(H_2) = 1/2$). We consider flat prior probability distribution functions for unknown parameters in the following ranges: $A_s \in [1.5 \cdot 10^{-9}, 5.5 \cdot 10^{-9}]$, $n_s \in [0.5, 1.5]$, $k_* \in [10^{-6}, 10^{-3}]$. The value of logarithm of the Bayes factor which was obtained in the analysis, i.e.

$$\ln(E_1/E_2) = \ln B_{12} = 0.2 \pm 0.6, \tag{9.15}$$

does not give a conclusive answer. The data was not informative enough to distinguish these models. Therefore, in the light of the recent WMAP data the Big Bang and Big Bounce cosmologies are indistinguishable. The Big Bounce predictions are not in conflict with the observational data. Moreover, beside the fact that the Big Bounce model has one more parameter k_*, the obtained evidence is comparable with the Big Bang case.

The above result was obtained with use of the CosmoClust code which bases on the nested sampling method [70]. This method was applied also in the CosmoNest code [71]. The computations with use of CosmoNest gives $\ln B_{12} = 1.1 \pm 0.2$. Therefore a weak evidence for Big Bang model is obtained. However, the CosmoNest was designed only for the case of unimodal likelihood functions. In turn, the CosmoClust code extends to the case of multi-modal likelihood functions. As it is clear from the bottom right panel in Fig. 9.4, the considered likelihood function (dotted line) is bimodal in the subspace k_*. The first peak is located at $k_* \sim 1.5 \cdot 10^{-4}\mathrm{Mpc}^{-1}$ while the second at $k_* \sim 2.5 \cdot 10^{-4}\mathrm{Mpc}^{-1}$. Therefore the results from CosmoClust are more relevant for our model. The CosmoNest samples only around the highest peak, neglecting the contribution from the smaller one. Because of this, the observed discrepancy between the CosmoClust and CosmoNest results appears. It is worth to note that, a similar model with suppression on the large scales was shown as an example of use of the CosmoClust code [67]. Bimodality of the likelihood functions was also observed and applicability of the CosmoClust code to that cases was emphasized.

The issue of constraining the bouncing cosmology with the observational data was raised before in literature. In particular, studies based on SNIa data, location of acoustic peaks in the CMB and constraints from primordial nucleosynthesis (BBN) were performed in Ref. [72, 73]. However, these cosmographic methods are inefficient in searching for the effects of the bounce. It is due to the fact that the factor $\frac{\rho}{\rho_c}$ is extremely low at the energy scales covered with this method. Even during the BBN, where $T_{BBN} \sim 1$ MeV, we have $\rho_{BBN} \approx 10^{-90}\rho_{Pl}$. Therefore, if $\rho_c \approx \rho_{Pl}$, we have $\frac{\rho}{\rho_c} \approx 10^{-90}$ and the holonomy corrections in the Friedmann equation (3.1) are vanishingly small [1]. Based on the method developed in the present paper, we reach $\rho_{obs} = \frac{m^2\varphi_{obs}^2}{2} \approx 10^{-11}\rho_{Pl}$, what gives $\frac{\rho}{\rho_c} \approx 10^{-11}$ for $\rho_c \approx \rho_{Pl}$. Therefore, sensitivity on the holonomy corrections was increased around 10^{80} times with respect to the BBN constraint.

[1] The constraint from the BBN can be however more significant in case of the inverse volume effects in LQC [74]

Based on the results presented in this section one can conclude that the Big Bounce is consistent with the observations up to energy scales $\approx 10^{-11}\rho_{\rm Pl}$. In this region the Big Bounce and Big Bang cosmologies are indistinguishable in the light of the available observational data. The advantage of the Big Bounce model is however that the initial singularity problem is resolved and the initial conditions for the phase of inflation are naturally generated.

9.4 Can we see the Big Bounce?

The present value of scale λ_* is crucial from the point of possible observational investigations of the Big Bounce cosmology. As it was discussed before, this scale overlaps with the size of the Hubble radius at the beginning of inflation. Therefore, it corresponds to the point of maximal displacement of the inflaton field, namely $\varphi_{\rm max}$. In this section we investigate how $\varphi_{\rm max}$ influences the present value of λ_*. Based on this, we will formulate conditions on the possibility of observing the Big Bounce effects.

In Fig. 9.5, schematic illustration of the scalar field evolution near the place of its maximal displacement was shown. In this figure we have marked the discussed $\varphi_{\rm max}$

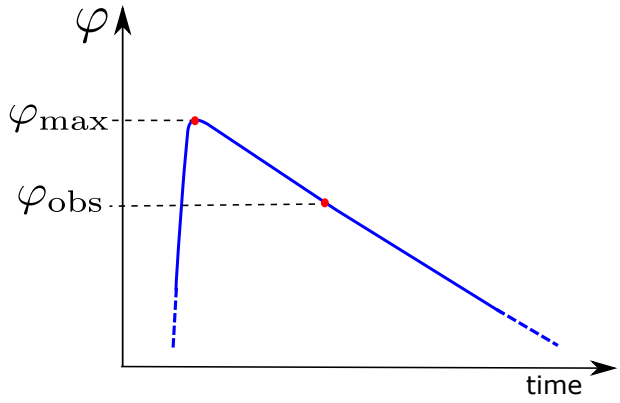

Figure 9.5: Schematic illustration of the scalar field evolution near the place of the maximal displacement. The $\varphi_{\rm max}$ is the maximal displacement of the field. The $\varphi_{\rm obs}$ is the value of the scalar field that corresponds to the powers spectrum measured at the pivot scale $\lambda_0 = 3.14$ Gpc.

value as well as the observed value $\varphi_{\rm obs} = 2.9 m_{\rm Pl}$. While $\varphi = \varphi_{\rm obs}$, the modes of the present size $\lambda_0 = 3.14$ Gpc (pivot scale) were formed. Based on this, we can determine what is the present size of the mode, which was equal to the Hubble radius at $\varphi = \varphi_{\rm max}$. The transition from $\varphi = \varphi_{\rm max}$ to $\varphi \approx 0$ corresponding to the total amount of e-folds from inflation, which can be decomposed as follows $N_{\rm tot} = \Delta N + N_{\rm obs}$. Here $N_{\rm obs}$ is the observed value, which corresponds to the transition from $\varphi = \varphi_{\rm obs}$ to $\varphi \approx 0$. The number

of e-foldings during the transition from φ_{max} to φ_{obs} can be expressed as follows

$$\Delta N = -\frac{4\pi}{m_{Pl}^2}\int_{\varphi_{max}}^{\varphi_{obs}} \frac{V}{V'} d\phi = \frac{2\pi}{m_{Pl}^2}\left(\varphi_{max}^2 - \varphi_{obs}^2\right). \tag{9.16}$$

Employing this expression together with the Friedmann equation, the present value of λ_* can be expressed as follows

$$\lambda_* \approx \lambda_0 \left(\frac{\varphi_{obs}}{m_{Pl}}\right)\left(\frac{m_{Pl}}{\varphi_{max}}\right) \exp\left\{2\pi\left(\frac{\varphi_{max}}{m_{Pl}}\right)^2 - 2\pi\left(\frac{\varphi_{obs}}{m_{Pl}}\right)^2\right\}, \tag{9.17}$$

where $\lambda_0 = 3.14$ Gpc and $\varphi_{obs} = 2.9 m_{Pl}$. In Fig. 9.6 we plot function $\lambda_*(\varphi_{max})$ given by (9.17). For comparison, we also show some relevant length scales. The first one is the

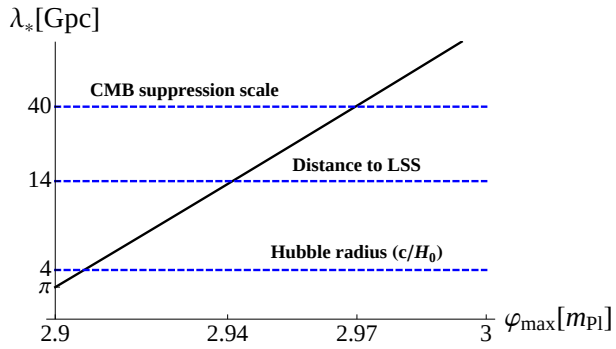

Figure 9.6: The present value of the scale λ_* as a function of φ_{max}.

Hubble radius $H_0/c \approx 4$ Gpc. The second is the distance to the last scattering shell (LSS), $D_{LSS} \approx 14$ Gpc. The last scale is the scale of suppression $\lambda_* \approx 40$ Gpc obtained in Sec. 9.3. If $\varphi_{max} > 2.94 m_{Pl}$ then the scale λ_* is placed behind the scale of LSS. In such a case there is no chance to see the effect of suppression directly. It is because, the scale of suppression is higher than the physical horizon of photons, released during the recombination. Therefore only if $\varphi_{max} < 2.94 m_{Pl}$, there is a possibility to study the effects of suppression on the CMB. From the fit performed in Sec. 9.3 we got $\lambda_* \approx 40$ Gpc, which corresponds to $\varphi_{max} \approx 2.97 m_{Pl}$. Based on this, one particular evolutionary trajectory can be distinguished. However, one have to keep in mind that the probability distribution on the parameter k_* was unbounded from below. Therefore the obtained value $\varphi_{max} \approx 2.97 m_{Pl}$ could be seen rather as a lower constraint on φ_{max}. As mentioned, in order to make the direct observations of the suppression possible, the value of φ_{max} should be smaller than $2.94 m_{Pl}$. The observations suggest that this value is higher, what unfortunately exclude this possibility. Based on this one can however exclude some models, where the predicted value of φ_{max} is not higher than $2.94 m_{Pl}$. This is in fact a case for the *symmetric* inflation as studied in Ref. [46]. The issue of constraining this model was preliminary discussed in Chapter 3. This also is still possible that the effect of oscillations can be observed. Perhaps

it is even the reason why the particular value of k_* was distinguished from the WMAP observations. Namely, it was possible because the structure of modulations at the low multipoles was reconstructed, not because the scale of suppression was detected.

We finish this section with the discussion of the observational constraint on the the parameters ρ_c and γ. In loop quantum cosmology, total energy density is constrained by $\rho \leqslant \rho_c$. At the stage of inflation when the present pivot scale crossed the Hubble radius, the energy density was equal to

$$\rho_{obs} = \frac{m^2\varphi_{obs}^2}{2} \approx 8 \cdot 10^{-12} m_{Pl}^4.$$

Based on this, we infer that $\rho_c > \rho_{obs}$. Because $\rho_{obs} \ll \rho_{Pl}$, the observed constraint on the energy scale of the bounce is very weak. However, since $\rho_c \sim 1/\gamma^3$, the constraint on the parameter γ can be much stronger. Indeed, based on (3.2) we find

$$\gamma < 1100. \tag{9.18}$$

The value obtained from the consideration of black hole entropy $\gamma = 0.239$ places within this observational bound. It must be kept in mind that constraint (9.18) is based on relation (3.2), which validity can be questioned.

To conclude, some models of the bouncing cosmology can be excluded based on the observations of CMB. It is based on the observational constraint on φ_{max}. Direct observations of the bounce effects are however much harder to detect. As we have indicated, the effect of suppression cannot be used. It is because the scale of suppression was shown to be higher than the scale of the horizon. The effect of oscillations gives a chance of observing some footprints of the Planck epoch. However this effect is, in general, weaker than suppression and can be undetectable due to the *cosmic variance*. It must be also pointed out that the discussed effects can be also predicted from different models as some string cosmologies. Therefore, an important task is to find some observables which enable to distinguish between LQC and those other models of the Planck epoch. It is a challenge for future research.

Chapter 10

Summary

The aim of this thesis was to relate physics at the Planck epoch with observational cosmology. It is expected that, in the Planck epoch, dynamics of the Universe is governed by the quantum gravity effects. In our considerations, we applied loop quantum cosmology to describe this phase. The effects of quantum gravity were introduced through the quantum holonomies. These effects may be seen as a kind of discretization of the continuous space. Here, discretization has a form of a regular lattice with the elementary lattice spacing λ. The volume of elementary cubic cell is equal to λ^3. Based on various indications, as renormalization of the perturbative quantum gravity, one may expect that $\lambda \sim l_{\mathrm{Pl}}$. The quantity λ^2 can be fixed also based on the area gap in LQG. In our considerations, λ was kept as a free parameter to be determined observationally, wherever possible.

We have constructed anomaly-free theory of cosmological perturbations with the effects of quantum holonomies. This was achieved by introducing counter-terms into the holonomy-corrected constraints. Such a method was previously successfully applied in case of perturbations with inverse-volume corrections [31]. We investigated all three possible types of perturbations: tensor, vector and scalar modes.

For the tensor perturbations, we derived equations of motion by taking into account the holonomy corrections. In this case, the algebra of constraints was shown to automatically fulfill the conditions of anomaly freedom. Based on this, we performed canonical quantization of these perturbations, by applying methods of the quantum field theory on curved spacetimes. We computed power spectrum of the tensor modes for the model with a massive scalar field. Thanks to this, we determined spectrum of gravitational waves for the joined bounce with inflation cosmological evolution. The obtained spectrum converges to the classical inflationary spectrum in the UV limit. However, in the IR limit, we observed significant modifications due to the quantum bounce. In particular, one can distinguish suppression of power in the IR limit and a bump in the intermediate energy range. The power excess at the bump was shown to depend mainly on the mass of the inflaton field. The obtained tensor power spectra allowed us to perform predictions regarding the spectrum of the B-type polarization of the CMB radiation. Based on the obtained spectrum of primordial tensor modes, predictions regarding the present stochastic

background of gravitational waves can be performed.

In case of vector perturbations, the requirement of anomaly freedom is not as trivial as for the tensor perturbations. The algebra of the holonomy-corrected constraint suffers on anomalies. However, we have shown that it is possible to introduce some suitable counter-terms which remove the anomalies. Based on this method, we found the anomaly-free constraints for the vector modes with the holonomy corrections. We determined the gauge-invariant variable and the corresponding equations of motion. We showed that evolution of the vector modes is continuous through the phase of the bounce. We indicated some possible observational consequences.

The case of scalar perturbations is the most laborious one. However, at the same time, it is the most interesting from the observational viewpoint. We have shown that the anomaly-free theory of scalar perturbations with holonomy corrections can be formulated. This goal was achieved by introducing counter-terms into the Hamiltonian constraint. The anomaly freedom was shown to be fulfilled not only for the gravity sector but also by taking into account the scalar matter. Furthermore, conditions for the anomaly free algebra of constraints were shown to be fulfilled only for the particular choice of the $\bar{\mu}$ function. Namely, for the $\bar{\mu}-$scheme ("new quantization scheme").

We have shown that not only constraints but also the algebra of constraint itself is modified due to the holonomies. This deformation of the algebra of constraints indicates that the structure of space-time is quantum modified. This means that initial general covariance is broken at the quantum level. The possible interpretation which emerges from the performed analysis is that for the energy densities $\rho > \rho_c/2$, the space-time becomes Euclidean. This suggests that the non-boundary proposal by Hartle and Hawking [62] can have physical realization in loop quantum cosmology. Here transition, between the Lorentzian and Euclidean geometries, occurs at the energy density $\rho = \rho_c/2$. Better understanding of this intriguing possibility requires further investigations.

For the scalar perturbations, we have also derived the resulting equations of motion. Furthermore, we have found expressions for the gauge invariant variables. These variables are analogues of the classical Bardeen potentials. Finally, we have found the analogue of the Mukhanov equation, which takes into account the effects of holonomies. This equation can be directly applied to study generation of the cosmological perturbations in the early universe. In particular, one can study generation of the scalar perturbations during the phase of quantum bounce. Quantum gravity corrections to the inflationary power spectrum can be also derived, based on this new equation. This opens new possibilities of studying observational effects of LQC. The only new parameter which appears in the derived equations is critical energy density ρ_c. Therefore, by deriving quantum-modified versions of the inflationary scalar power-spectrum it will be possible to put a robust constraint on the energy scale of the Big Bounce (ρ_c). This can be achieved by comparison with the current as well as with the forthcoming CMB data. This analysis will be continued in the immediate future.

In order to verify whether the current CMB data are adequate to study the effects of quantum holonomies we have investigated a scalar power spectrum typical for the Big

Bounce cosmologies. We have computed the corresponding spectrum of the temperature anisotropies in the CMB. The obtained spectrum was compared with the CMB data for the WMAP satellite. By applying the Bayesian analysis, we compared the quantum Big Bounce and the classical Big Bang cosmologies. We have found that, the available data was not informative enough to distinguish these models. The Big Bounce predictions are not in conflict with the observational data. Moreover, beside the fact that the Big Bounce model has one more parameter, the obtained evidence is comparable with the Big Bang case.

Furthermore, we have investigated necessary conditions allowing to detect footprints of the Big Bounce in the spectrum of the CMB anisotropies. We have focussed here on the effect of suppression of the power spectrum at large scales. Such effect was shown to be generically predicted for the bouncing cosmologies. We found that only if the total number of $e-$folds during inflation is sufficiently small, the effect of suppression can be directly seen in the CMB spectrum. It means that, inflation cannot be much longer than the observed value for the pivot scale to see those effects. Otherwise only some small oscillations of the spectrum, due to the bounce, can be available in the observational window. However, they are much harder to detect due to the presence of cosmic variance.

Based on the performed analysis we have found the current observational constraint on the value of the Barbero-Immirzi parameter. In order to find this constraint we have made the usual assumption that $\lambda^2 = \Delta$ is equal to area gap in LQG, $A_0 = 2\sqrt{3}\pi\gamma^2 l_{\rm Pl}^2$. With use of the CMB data, we found that $\gamma < 1100$. The obtained bound is quite weak if compared with the value of γ derived from considerations of the black hole entropies ($\gamma = 0.239$). This result reflects the position we are right now in approaching the Planck scale by observations of the early universe.

To conclude, we have developed a method of deriving observational predictions from the Planck epoch, within the framework of loop quantum cosmology. The observational quantities, as power spectra of primordial perturbations, can be found based on the derived equations. This enables comparison with observations of the cosmic microwave background radiation. However, as we have shown, the effects due to the quantum gravity can be directly observed only if certain conditions are fulfilled. If this is the case, physics at the Planck epoch can be directly probed. However, if not, what seems to be suggested by the available CMB data, one can only constrain this physics. In particular, on can put constrains on the parameters as γ, ρ_c or F_B, as discussed in this dissertation. Such constraints give us certain knowledge about possible conditions at the Planck epoch. We hope that this empirical factor will bring us closer to understanding the nature of quantum gravity.

Chapter 11

Appendixes

11.1 Useful formulas

In this appendix we derive some useful relations between the phase space variables.

11.1.1 Two expressions on densitized triad variable E^a_i

Let us show that the denistitized triad variable, defined as follows:

$$E^a_i := \mathrm{sgn}(\det e)\frac{1}{2}\epsilon^{abc}\epsilon_{ijk}e^j_b e^k_c, \tag{11.1}$$

where $\det e := \det(e^i_a)$ can be expressed as

$$E^a_i = |\det e| e^a_i. \tag{11.2}$$

For this purpose, let us prove that the following equality holds

$$\mathrm{sgn}(\det e)\frac{1}{2}\epsilon^{abc}\epsilon_{ijk}e^j_b e^k_c = |\det e| e^a_i. \tag{11.3}$$

Contracting both sides of the above equality with $\mathrm{sgn}(\det e)e^i_a$ we obtain

$$\frac{1}{2}\underbrace{\epsilon^{abc}\epsilon_{ijk}e^i_a e^j_b e^k_c}_{=3!\det e} = (\det e)\underbrace{e^a_i e^i_a}_{=3}, \tag{11.4}$$

therefore

$$3\det e = 3\det e, \tag{11.5}$$

which completes the proof.

11.1.2 Relating co-triad e^i_a with densitized triad E^a_i

Let us prove that co-triad e^i_a can be expressed in terms of densitized triad E^a_i variable as follows:

$$e^i_a = \frac{1}{2}\frac{\mathrm{sgn}(\det E)\epsilon_{abc}\epsilon^{ijk}E^b_j E^c_k}{\sqrt{|\det E|}}. \tag{11.6}$$

Applying definition of the densitized triad, we calculate

$$\begin{aligned}
\epsilon_{abc}\epsilon^{ijk}E^b_j E^c_k &= \frac{1}{4}\epsilon_{abc}\epsilon^{ijk}\epsilon^{bde}\epsilon_{jlm}e^l_d e^m_e \epsilon^{cfg}\epsilon_{kns}e^n_f e^s_g \\
&= \frac{1}{4}(\delta^f_a\delta^g_b - \delta^f_b\delta^g_a)(\delta^i_n\delta^j_s - \delta^i_s\delta^j_n)\epsilon^{bde}\epsilon_{jlm}e^l_d e^m_e e^n_f e^s_g \\
&= \frac{1}{2}\left(e^a_i \underbrace{\epsilon^{bde}\epsilon_{jlm}e^j_b e^l_d e^m_e}_{=3!\det e} - \underbrace{\epsilon^{bde}\epsilon_{jlm}e^l_d e^m_e}_{=2\mathrm{sgn}(\det e)E^b_j} e^i_b e^j_a\right) \\
&= \frac{1}{2}\left(6e^a_i \det e - 2\underbrace{\mathrm{sgn}(\det e)|\det e|}_{=\det e}\underbrace{e^b_j e^i_b}_{\delta^i_j} e^j_a\right) \\
&= 2(\det e)e^i_a,
\end{aligned} \tag{11.7}$$

which leads to

$$e^i_a = \frac{1}{2}\frac{\epsilon_{abc}\epsilon^{ijk}E^b_j E^c_k}{\det e}. \tag{11.8}$$

Because $\det e = \sqrt{|\det E|}\mathrm{sgn}(\det E)$, the above equation can be rewritten to the form

$$e^i_a = \frac{1}{2}\frac{\mathrm{sgn}(\det E)\epsilon_{abc}\epsilon^{ijk}E^b_j E^c_k}{\sqrt{|\det E|}}, \tag{11.9}$$

completing the proof.

11.1.3 Relating co-triad e^i_a with volume V

The volume of subspace $B \subseteq \Sigma$ can be expressed as follows:

$$V = \int_B d^3y \sqrt{|\det E(\mathbf{y})|}, \tag{11.10}$$

where, for the later purpose, one can express

$$\det E = \frac{1}{3!}\epsilon_{abc}E^a_i E^b_j E^c_k \epsilon^{ijk}. \tag{11.11}$$

Let us vary volume V with respect to densitized triad E^a_i:

$$\begin{aligned}\frac{\delta V}{\delta E^a_i(\mathbf{x})} &= \frac{1}{2}\int_B d^3y \frac{1}{\sqrt{|\det E|}}\frac{\delta|\det E|}{\delta E^a_i(\mathbf{x})} \\ &= \frac{1}{2}\int_B d^3y \frac{\mathrm{sgn}(\det E)}{\sqrt{|\det E|}}\frac{\delta \det E}{\delta E^a_i(\mathbf{x})} \\ &= \frac{1}{4}\mathrm{sgn}(\det E)\frac{1}{\sqrt{\det E}}\epsilon_{abc}\epsilon^{ijk}E^b_j E^c_k, \end{aligned} \tag{11.12}$$

where we have used the fact that

$$\frac{\delta E^b_j(\mathbf{y})}{\delta E^a_i(\mathbf{x})} = \delta^b_a \delta^i_j \delta^{(3)}(\mathbf{x}-\mathbf{y}), \tag{11.13}$$

together with equation (11.11). Let us now calculate the following Poisson bracket

$$\begin{aligned}\{A^i_a(\mathbf{x}), V\} &= 8\pi G\gamma \int_\Sigma d^3z \left[\frac{\delta A^i_a(\mathbf{x})}{\delta A^j_b(\mathbf{z})}\frac{\delta V}{\delta E^b_j(\mathbf{z})} - 0\right] \\ &= 8\pi G\gamma \int_\Sigma d^3z \delta^i_j \delta^b_a \delta^{(3)}(\mathbf{x}-\mathbf{z})\frac{\delta V}{\delta E^b_j(\mathbf{z})} \\ &= 8\pi G\gamma \frac{\delta V}{\delta E^a_i(\mathbf{x})} = 2\pi G\gamma \frac{\mathrm{sgn}(\det E)}{\sqrt{|\det E|}}\epsilon_{abc}\epsilon^{ijk}E^b_j E^c_k, \end{aligned} \tag{11.14}$$

where in the last equality we have used relation (11.12). By applying obtained relation (11.14) to

$$e^i_a = \frac{1}{2}\frac{\mathrm{sgn}(\det E)\epsilon_{abc}\epsilon^{ijk}E^b_j E^c_k}{\sqrt{|\det E|}}, \tag{11.15}$$

we find the following formula:

$$e^i_a = \frac{1}{4\pi G\gamma}\{A^i_a(\mathbf{x}), V\}. \tag{11.16}$$

11.2 Perturbative expansion of $\sqrt{\det E}$ and $1/\sqrt{\det E}$

In this appendix we perform perturbative expansions of $\sqrt{\det E}$ and $1/\sqrt{\det E}$ up to the second order. We consider the following decompozition of the desitized triad

$$E^a_i = \bar{E}^a_i + \delta E^a_i = \bar{p}\delta^a_i + \delta E^a_i, \tag{11.17}$$

which holds for the flat FRW background. Moreover, for the consistency of the perturbative expansions we require that $|\delta E^a_i/\bar{E}^a_i| \ll 1$.

By applying the formula

$$\det M = e^{\mathrm{tr}\log M}, \tag{11.18}$$

where M is a matrix, one can write

$$(\det E_i^a)^{\pm\frac{1}{2}} = \exp\left\{\pm\frac{1}{2}\mathrm{tr}\log E_i^a\right\}. \tag{11.19}$$

With use of decomposition $E_i^a = \bar{p}\left(\delta_i^a + \frac{1}{\bar{p}}\delta E_i^a\right)$, we obtain

$$(\det E_i^a)^{\pm\frac{1}{2}} = \bar{p}^{\pm\frac{3}{2}}\exp\left\{\pm\frac{1}{2}\mathrm{tr}\log\left(\delta_i^a + \frac{1}{\bar{p}}\delta E_i^a\right)\right\}. \tag{11.20}$$

Based on the Taylor expansion

$$\log(1+x) = x - \frac{x^2}{2} + \frac{x^3}{3} + \ldots \tag{11.21}$$

we obtain

$$\log\left(\delta_i^a + \frac{1}{\bar{p}}\delta E_i^a\right) = \frac{\delta E_i^a}{\bar{p}} - \frac{1}{2\bar{p}^2}\delta E_j^a\delta_b^j\delta E_i^b + \frac{1}{3\bar{p}^3}\delta E_j^a\delta_b^j\delta E_k^b\delta_c^k\delta E_i^c + \ldots, \tag{11.22}$$

what leads to

$$\pm\frac{1}{2}\mathrm{tr}\log\left(\delta_i^a + \frac{1}{\bar{p}}\delta E_i^a\right) = \pm\frac{1}{2\bar{p}}\delta_a^i\delta E_i^a \mp \frac{1}{4\bar{p}^2}\delta_a^i\delta E_j^a\delta_b^j\delta E_i^b \pm \frac{1}{6\bar{p}^3}\delta_a^i\delta E_j^a\delta_b^j\delta E_k^b\delta_c^k\delta E_i^c + \ldots. \tag{11.23}$$

With use of the following expansion

$$e^x = \sum_{n=0}^{\infty}\frac{x^n}{n!} = 1 + x + \frac{x^2}{2} + \ldots, \tag{11.24}$$

we obtain the final expression

$$(\det E_i^a)^{\pm\frac{1}{2}} = \bar{p}^{\pm\frac{3}{2}}\left[1 \pm \frac{1}{2\bar{p}}\delta_a^i\delta E_i^a \mp \frac{1}{4\bar{p}^2}\delta_a^i\delta E_j^a\delta_b^j\delta E_i^b + \frac{1}{8\bar{p}^2}\delta_a^i\delta E_i^a\delta_b^j\delta E_j^b + \mathcal{O}(E^3)\right]. \tag{11.25}$$

Bibliography

[1] M. Heller, G. V. Coyne, "A COMPREHENSIBLE UNIVERSE. A Natural History of Knowing in Science", 2007.

[2] C. Rovelli, "Quantum Gravity", Cambridge, Cambridge University Press, 2004.

[3] S. Hossenfelder, "Experimental Search for Quantum Gravity," [arXiv:1010.3420 [gr-qc]].

[4] G. Amelino-Camelia, J. R. Ellis, N. E. Mavromatos, D. V. Nanopoulos and S. Sarkar, "Tests of quantum gravity from observations of gamma-ray bursts," Nature **393** (1998) 763 [arXiv:astro-ph/9712103].

[5] M. Ackermann *et al.* [Fermi GBM/LAT Collaborations], "A limit on the variation of the speed of light arising from quantum gravity effects," Nature **462** (2009) 331 [arXiv:0908.1832 [astro-ph.HE]].

[6] A. H. Guth, "The Inflationary Universe: A Possible Solution to the Horizon and Flatness Problems," Phys. Rev. D **23** (1981) 347.

[7] A. D. Linde, "Inflationary Cosmology," Lect. Notes Phys. **738** (2008) 1 [arXiv:0705.0164 [hep-th]].

[8] E. Komatsu *et al.* [WMAP Collaboration], "Seven-Year Wilkinson Microwave Anisotropy Probe (WMAP) Observations: Cosmological Interpretation," Astrophys. J. Suppl. **192** (2011) 18 [arXiv:1001.4538 [astro-ph.CO]].

[9] J. Ambjorn, J. Jurkiewicz and R. Loll, "Quantum Gravity, or The Art of Building Spacetime," In *Oriti, D. (ed.): Approaches to quantum gravity* 341-359 [hep-th/0604212].

[10] L. Bombelli, J. Lee, D. Meyer and R. Sorkin, "Space-Time as a Causal Set," Phys. Rev. Lett. **59** (1987) 521.

[11] A. Ashtekar and J. Lewandowski, "Background independent quantum gravity: A status report," Class. Quant. Grav. **21** (2004) R53 [arXiv:gr-qc/0404018].

[12] S. Weinberg, "The Quantum Theory of Fields II: Modern Applications". Cambridge University Press 2000.

[13] Clifford M. Will, "The Confrontation between General Relativity and Experiment", Living Rev. Relativity **9**, (2006), http://www.livingreviews.org/lrr-2006-3.

[14] C. Rovelli and L. Smolin, "Spin networks and quantum gravity," Phys. Rev. D **52** (1995) 5743 [gr-qc/9505006].

[15] A. Ashtekar and J. Lewandowski, "Quantum theory of geometry. 1: Area operators," Class. Quant. Grav. **14** (1997) A55 [gr-qc/9602046].

[16] M. Bojowald, "Loop quantum cosmology," Living Rev. Rel. **11** (2008) 4.

[17] A. Ashtekar and P. Singh, "Loop Quantum Cosmology: A Status Report," Class. Quant. Grav. **28** (2011) 213001 [arXiv:1108.0893 [gr-qc]].

[18] A. Ashtekar, M. Bojowald and J. Lewandowski, "Mathematical structure of loop quantum cosmology," Adv. Theor. Math. Phys. **7** (2003) 233 [gr-qc/0304074].

[19] M. Bojowald, "Absence of singularity in loop quantum cosmology," Phys. Rev. Lett. **86** (2001) 5227 [gr-qc/0102069].

[20] A. Ashtekar, T. Pawlowski and P. Singh, "Quantum nature of the big bang," Phys. Rev. Lett. **96** (2006) 141301 [gr-qc/0602086].

[21] M. Bojowald, "Inflation from quantum geometry," Phys. Rev. Lett. **89** (2002) 261301 [gr-qc/0206054].

[22] A. Ashtekar, T. Pawlowski and P. Singh, "Quantum Nature of the Big Bang: Improved dynamics," Phys. Rev. D **74** (2006) 084003 [gr-qc/0607039].

[23] J. Mielczarek, "Possible observational effects of loop quantum cosmology," Phys. Rev. D **81** (2010) 063503 [arXiv:0908.4329 [gr-qc]].

[24] A. Ashtekar and D. Sloan, "Loop quantum cosmology and slow roll inflation," Phys. Lett. B **694** (2010) 108 [arXiv:0912.4093 [gr-qc]].

[25] A. Ashtekar and D. Sloan, "Probability of Inflation in Loop Quantum Cosmology," Gen. Rel. Grav. **43** (2011) 3619 [arXiv:1103.2475 [gr-qc]].

[26] G. W. Gibbons and N. Turok, "The Measure Problem in Cosmology," Phys. Rev. D **77** (2008) 063516 [arXiv:hep-th/0609095].

[27] V. F. Mukhanov, H. A. Feldman, R. H. Brandenberger, "Theory of cosmological perturbations. Part 1. Classical perturbations. Part 2. Quantum theory of perturbations. Part 3. Extensions," Phys. Rept. **215** (1992) 203-333.

[28] S. Weinberg, “Cosmology", Oxford University Press 2008.

[29] A. Ashtekar, “New Variables for Classical and Quantum Gravity,” Phys. Rev. Lett. **57** (1986) 2244.

[30] M. Bojowald, H. H. Hernandez, M. Kagan, P. Singh and A. Skirzewski, “Hamiltonian cosmological perturbation theory with loop quantum gravity corrections,” Phys. Rev. D **74** (2006) 123512 [arXiv:gr-qc/0609057].

[31] M. Bojowald, G. M. Hossain, M. Kagan and S. Shankaranarayanan, “Anomaly freedom in perturbative loop quantum gravity,” Phys. Rev. D **78** (2008) 063547 [arXiv:0806.3929 [gr-qc]].

[32] M. Bojowald, G. M. Hossain, M. Kagan and S. Shankaranarayanan, “Gauge invariant cosmological perturbation equations with corrections from loop quantum gravity,” Phys. Rev. D **79** (2009) 043505 [Erratum-ibid. D **82** (2010) 109903] [arXiv:0811.1572 [gr-qc]].

[33] M. Bojowald and G. M. Hossain, “Cosmological vector modes and quantum gravity effects,” Class. Quant. Grav. **24** (2007) 4801 [arXiv:0709.0872 [gr-qc]].

[34] M. Bojowald and G. M. Hossain, “Loop quantum gravity corrections to gravitational wave dispersion,” Phys. Rev. D **77** (2008) 023508 [arXiv:0709.2365 [gr-qc]].

[35] M. Bojowald and G. Calcagni, “Inflationary observables in loop quantum cosmology,” JCAP **1103** (2011) 032 [arXiv:1011.2779 [gr-qc]].

[36] M. Bojowald, G. Calcagni and S. Tsujikawa, “Observational constraints on loop quantum cosmology,” Phys. Rev. Lett. **107** (2011) 211302 [arXiv:1101.5391 [astro-ph.CO]].

[37] M. Bojowald, G. Calcagni and S. Tsujikawa, “Observational test of inflation in loop quantum cosmology,” JCAP **1111** (2011) 046 [arXiv:1107.1540 [gr-qc]].

[38] Y. Li and J. Y. Zhu, “Application of higher order holonomy corrections to the perturbation theory of cosmology,” Class. Quant. Grav. **28** (2011) 045007 [arXiv:1102.2720 [gr-qc]].

[39] J. P. Wu and Y. Ling, “The cosmological perturbation theory in loop cosmology with holonomy corrections,” arXiv:1001.1227 [hep-th].

[40] E. Wilson-Ewing, “Holonomy Corrections in the Effective Equations for Scalar Mode Perturbations in Loop Quantum Cosmology,” arXiv:1108.6265 [gr-qc].

[41] T. Thiemann, “Modern Canonical Quantum General Relativity”,Cambridge University Press, 2007;

[42] H. Nicolai, K. Peeters and M. Zamaklar, "Loop quantum gravity: An outside view," Class. Quant. Grav. **22** (2005) R193 [arXiv:hep-th/0501114].

[43] W. Nelson and M. Sakellariadou, Phys. Rev. D **76** (2007) 104003 [arXiv:0707.0588 [gr-qc]]. W. Nelson, M. Sakellariadou, "Lattice Refining Loop Quantum Cosmology and Inflation," Phys. Rev. **D76** (2007) 044015. [arXiv:0706.0179 [gr-qc]]. A. Corichi, P. Singh, "Is loop quantization in cosmology unique?," Phys. Rev. **D78** (2008) 024034. [arXiv:0805.0136 [gr-qc]]. M. Sakellariadou, "Lattice refinement in loop quantum cosmology," J. Phys. Conf. Ser. **189** (2009) 012035 [arXiv:0810.5356 [gr-qc]].

[44] K. A. Meissner, "Black hole entropy in loop quantum gravity," Class. Quant. Grav. **21** (2004) 5245 [arXiv:gr-qc/0407052].

[45] P. Singh, K. Vandersloot and G. V. Vereshchagin, "Non-singular bouncing universes in loop quantum cosmology," Phys. Rev. D **74** (2006) 043510 [arXiv:gr-qc/0606032].

[46] D. W. Chiou and K. Liu, "Cosmological inflation driven by holonomy corrections of loop quantum cosmology," arXiv:1002.2035 [gr-qc].

[47] M. Bojowald, "Quantum nature of cosmological bounces," Gen. Rel. Grav. **40** (2008) 2659 [arXiv:0801.4001 [gr-qc]].

[48] M. Bojowald, "How quantum is the big bang?," Phys. Rev. Lett. **100** (2008) 221301 [arXiv:0805.1192 [gr-qc]].

[49] N. D. Birrell, P. C. W. Davies, "Quantum field in curved space," Cambridge University Press 1982.

[50] J. Mielczarek and M. Kamionka, "Smoothed quantum fluctuations and CMB observations," arXiv:0909.4411 [hep-th].

[51] J. Mielczarek, "Tensor power spectrum with holonomy corrections in LQC," Phys. Rev. D **79** (2009) 123520 [arXiv:0902.2490 [gr-qc]].

[52] J. Mielczarek and M. Szydlowski, "Relic gravitons as the observable for loop quantum cosmology," Phys. Lett. B **657** (2007) 20 [arXiv:0705.4449 [gr-qc]].

[53] J. Grain, A. Barrau and A. Gorecki, "Inverse volume corrections from loop quantum gravity and the primordial tensor power spectrum in slow-roll inflation," Phys. Rev. D **79** (2009) 084015 [arXiv:0902.3605 [gr-qc]].

[54] J. Grain and A. Barrau, "Cosmological footprints of loop quantum gravity," Phys. Rev. Lett. **102**, 081301 (2009) [arXiv:0902.0145 [gr-qc]].

[55] [Planck Collaboration], "Planck: The scientific programme," arXiv:astro-ph/0604069.

[56] H. C. Chiang *et al.*, "Measurement of CMB Polarization Power Spectra from Two Years of BICEP Data," arXiv:0906.1181 [astro-ph.CO].

[57] S. Gupta *et al.* [QUaD Collaboration], "Parameter Estimation from Improved Measurements of the CMB from QUaD," Astrophys. J. **716** (2010) 1040 [arXiv:0909.1621 [astro-ph.CO]].

[58] J. Mielczarek, T. Stachowiak and M. Szydlowski, "Exact solutions for Big Bounce in loop quantum cosmology," Phys. Rev. D **77** (2008) 123506 [arXiv:0801.0502 [gr-qc]].

[59] D. Langlois, "Hamiltonian formalism and gauge invariance for linear perturbations in inflation," Class. Quant. Grav. **11** (1994) 389-407.

[60] M. Bojowald, R. Das, "Radiation equation of state and loop quantum gravity corrections," Phys. Rev. **D75** (2007) 123521. [arXiv:0710.5721 [gr-qc]].

[61] T. J. Battefeld and R. Brandenberger, "Vector perturbations in a contracting universe," Phys. Rev. D **70** (2004) 121302 [arXiv:hep-th/0406180].

[62] J. B. Hartle, S. W. Hawking, "Wave Function of the Universe," Phys. Rev. **D28** (1983) 2960-2975.

[63] A. Lewis, A. Challinor and A. Lasenby, "Efficient Computation of CMB anisotropies in closed FRW models," Astrophys. J. **538** (2000) 473 [arXiv:astro-ph/9911177].

[64] Y. Z. Ma, W. Zhao and M. L. Brown, "Constraints on standard and non-standard early Universe models from CMB B-mode polarization," JCAP **1010** (2010) 007 [arXiv:1007.2396 [astro-ph.CO]].

[65] F. T. Falciano, M. Lilley and P. Peter, "A classical bounce: constraints and consequences," Phys. Rev. D **77** (2008) 083513 [arXiv:0802.1196 [gr-qc]].

[66] A. Lewis and S. Bridle, "Cosmological parameters from CMB and other data: a Monte-Carlo approach," Phys. Rev. D **66** (2002) 103511 [arXiv:astro-ph/0205436].

[67] R. Shaw, M. Bridges and M. P. Hobson, "Clustered nested sampling: efficient Bayesian inference for cosmology," Mon. Not. Roy. Astron. Soc. **378** (2007) 1365 [arXiv:astro-ph/0701867].

[68] H. Jeffreys, *Theory of Probability* (Oxford University Press, Oxford, 1961).

[69] R. Trotta, Contemporary Physics **49**, 71 (2008).

[70] P. Mukherjee, D. Parkinson and A. R. Liddle, "A Nested Sampling Algorithm for Cosmological Model Selection," Astrophys. J. **638** (2006) L51 [arXiv:astro-ph/0508461].

[71] D. Parkinson, P. Mukherjee and A. R. Liddle, "A Bayesian model selection analysis of WMAP3," Phys. Rev. D **73** (2006) 123523 [arXiv:astro-ph/0605003].

[72] M. Szydlowski, W. Godlowski, A. Krawiec and J. Golbiak, "Can the initial singularity be detected by cosmological tests?," Phys. Rev. D **72** (2005) 063504 [arXiv:astro-ph/0504464].

[73] M. Szydlowski, W. Godlowski and T. Stachowiak, "Testing and selection of cosmological models with $(1+z)^6$ corrections," Phys. Rev. D **77** (2008) 043530 [arXiv:0706.0283 [gr-qc]].

[74] M. Bojowald, R. Das and R. J. Scherrer, "Dirac Fields in Loop Quantum Gravity and Big Bang Nucleosynthesis," Phys. Rev. D **77** (2008) 084003 [arXiv:0710.5734 [astro-ph]].